

# Heavy lepton quintuplet and TeV scale seesaw mechanism

---

**Radovčić, Branimir**

**Doctoral thesis / Disertacija**

**2013**

*Degree Grantor / Ustanova koja je dodijelila akademski / stručni stupanj:* **University of Zagreb, Faculty of Science / Sveučilište u Zagrebu, Prirodoslovno-matematički fakultet**

*Permanent link / Trajna poveznica:* <https://um.nsk.hr/um:nbn:hr:217:416821>

*Rights / Prava:* [In copyright](#)/[Zaštićeno autorskim pravom.](#)

*Download date / Datum preuzimanja:* **2024-10-14**



*Repository / Repozitorij:*

[Repository of the Faculty of Science - University of Zagreb](#)



UNIVERSITY OF ZAGREB  
FACULTY OF SCIENCE  
PHYSICS DEPARTMENT

Branimir Radovčić

# Heavy lepton quintuplet and TeV scale seesaw mechanism

Doctoral Thesis submitted to the Physics Department  
Faculty of Science, University of Zagreb  
for the academic degree of  
Doctor of Natural Sciences (Physics)

Zagreb, 2013.



SVEUČILIŠTE U ZAGREBU  
PRIRODOSLOVNO-MATEMATIČKI FAKULTET  
FIZIČKI ODSJEK

Branimir Radovčić

# **Kvintuplet teških leptona i mehanizam njihalice na skali TeV-a**

Doktorska disertacija  
predložena Fizičkom odsjeku  
Prirodoslovno-matematičkog fakulteta Sveučilišta u Zagrebu  
radi stjecanja akademskog stupnja  
doktora prirodnih znanosti fizike

Zagreb, 2013.



This thesis was made under the mentorship of Prof. Ivica Picek, within University post-graduate studies at Physics Department of Faculty of Science of University of Zagreb.

Ova disertacija izrađena je pod vodstvom prof. dr. sc. Ivice Piceka, u sklopu Sveučilišnog poslijediplomskog studija pri Fizičkom odsjeku Prirodoslovno-matematičkoga fakulteta Sveučilišta u Zagrebu.



# Acknowledgments

I would like to thank my supervisor, Prof. Ivica Picek, for the patient guidance and the friendly support he has provided throughout my research.

I would also like to thank Prof. Krešimir Kumerički for helping me solve many problems and providing me with insightful suggestions. Without his involvement, this work would not have been possible.

My sincere gratitude goes to Prof. Walter Grimus for sharing his knowledge and for the hospitality during my research stay at the University of Vienna.

Completing this work would have been all the more difficult were it not for the illuminating discussions, support and friendship provided by my colleagues Mirko, Ivica, Sanjin and Luka. I am indebted to them for their help.

I would like to thank my family, who experienced all of the ups and downs of my research, for their love and support. I would like to express my heartfelt thanks to my girlfriend Zorana. Thanks for your love and encouragement.

In particular I would like to thank all my friends who provided a much needed form of escape from my studies and helped me keep things in perspective.





# BASIC DOCUMENTATION CARD

University of Zagreb  
Faculty of Science  
Physics Department

Doctoral Thesis

## Heavy lepton quintuplet and TeV scale seesaw mechanism

BRANIMIR RADOVČIĆ  
Faculty of Science, Zagreb

Two novel seesaw models based on weak-isospin quintuplet leptons are presented. In the first one, the zero hypercharge Majorana quintuplet lepton is accompanied by a scalar weak-isospin quadruplet, and in the second one, a non-zero hypercharge Dirac quintuplet lepton is accompanied by two scalar weak-isospin quadruplets. In both models scalar quadruplets attain the induced vacuum expectation values. This leads to neutrino mass contribution  $\sim v_H^6/M^5$  arising at the tree level from a dimension-nine operator. Additional neutrino mass contribution  $\sim (1/16\pi^2) \cdot v_H^2/M$  comes from a loop suppressed dimension-five operator. The empirical masses  $m_\nu \sim 0.1$  eV can be achieved with the new states being within the reach of the Large Hadron Collider and the origin of the neutrino masses could be directly tested. The Drell-Yan production of the new fermions is abundant due to nontrivial electroweak gauge charges and their decays lead to interesting multilepton and same sign dilepton events. The charged components of new scalar multiplets contribute to loop-mediated Higgs decays  $h \rightarrow \gamma\gamma$  and  $h \rightarrow Z\gamma$ . The neutral component of the Majorana quintuplet, previously identified as a minimal dark matter candidate, becomes unstable in the proposed seesaw setup. The stability can be restored by introducing a  $Z_2$  symmetry, in which case neutrinos get mass only from radiative contributions.

(112 pages, 111 references, original in English)

Keywords: Neutrino mass, Beyond Standard Model, Quintuplet leptons, Exotic leptons, Non-standard scalar fields, Dark matter

Supervisor: - Prof. Ivica Picek, University of Zagreb

Committee: 1. Prof. Krešimir Kumerički, University of Zagreb  
2. Prof. Walter Grimus, University of Vienna  
3. Dr. sc. Vuko Brigljević, Senior research associate, Ruđer Bošković Institute, Zagreb  
4. Prof. Ivica Picek, University of Zagreb  
5. Prof. Mirko Planinić, University of Zagreb

Replacements: 1. Prof. Dubravko Klabučar, University of Zagreb  
2. Dr. sc. Krešo Kadija, Senior research scientist, Ruđer Bošković Institute, Zagreb

Thesis accepted: 2013.

# TEMELJNA DOKUMENTACIJSKA KARTICA

Sveučilište u Zagrebu  
Prirodoslovno-matematički fakultet  
Fizički odsjek

Doktorska disertacija

## Kvintuplet teških leptona i mehanizam njihalice na skali TeV-a

BRANIMIR RADOVČIĆ

Prirodoslovno-matematički fakultet, Zagreb

Prezentirana su dva nova mehanizma njihalice bazirana na kvintupletu leptona slabog izospina. U prvom je modelu Majoranin kvintuplet leptona isčezavajućeg hipernaboja u sprezi sa skalarnim kvadrupletom slabog izospina, a u drugom modelu je Diracov kvintuplet leptona neisčezavajućeg hipernaboja u sprezi s dva skalarna kvadrupleta slabog izospina. U oba modela skalarni kvadrupleti poprimaju induciranu vakuumsku očekivanu vrijednost. To vodi na doprinos masama neutrina  $\sim v_H^6/M^5$  koji dolazi od operatora dimenzije devet na granastom nivou. Dodatni doprinos masama neutrina  $\sim (1/16\pi^2) \cdot v_H^2/M$  dolazi od operatora dimenzije pet potisnutog na razini petlje. Eksperimentalne vrijednosti masa neutrina  $m_\nu \sim 0.1$  eV se mogu ostvariti s novim stanjima u doseg velikog hadronskog sudarivača i mogućnošću direktnog testiranja porijekla masa neutrina. Drell-Yanova produkcija novih fermiona je obilna zbog netrivialnih elektroslabih naboja, a njihovi raspadni vode na interesantne događaje s više leptona u konačnom stanju i narušenjem leptonskog broja. Ispitana je uloga novih skalara u raspadima Higgsovog bozona na razini petlje,  $h \rightarrow \gamma\gamma$  i  $h \rightarrow Z\gamma$ . Neutralna komponenta Majoraninog kvintupleta, prijašnji kandidat za minimalnu tamnu tvar, postaje nestabilna u predloženom modelu njihalice. Uvođenjem  $Z_2$  simetrije može se osigurati njezina stabilnost, a u tom slučaju neutriini dobivaju masu samo od doprinosa na razini petlje.

(112 stranice, 111 literaturnih navoda, jezik izvornika engleski)

Ključne riječi: mase neutrina, fizika izvan standardnog modela, kvintuplet leptona, egzotični leptoni, nestandardna skalarna polja, tamna tvar

Mentor: - Prof. dr. sc. Ivica Picek, Sveučilište u Zagrebu

Ocjenjivači: 1. Prof. dr. sc. Krešimir Kumerički,  
Sveučilište u Zagrebu  
2. Prof. dr. sc. Walter Grimus, Sveučilište u Beču  
3. Dr. sc. Vuko Brigljević, v. zn. sur., IRB, Zagreb  
4. Prof. dr. sc. Ivica Picek, Sveučilište u Zagrebu  
5. Prof. dr. sc. Mirko Planinić, Sveučilište u Zagrebu

Zamjene: 1. Prof. dr. sc. Dubravko Klabučar,  
Sveučilište u Zagrebu  
2. Dr. sc. Krešo Kadija, zn. savj., IRB, Zagreb

Rad prihvaćen: 2013.

# Contents

|  |           |
|--|-----------|
| Contents   | xiii      |
| <b>Introduction</b>  | <b>1</b>  |
| <b>1 Overture</b>  | <b>3</b>  |
| 1.1 Neutrino oscillations, masses and mixing . . . . .             | 3         |
| 1.2 Seesaw mechanisms . . . . .                                    | 5         |
| 1.3 Low scale seesaw mechanisms . . . . .                          | 6         |
| 1.4 Higher dimensional representations . . . . .                   | 7         |
| <b>2 Model with Majorana lepton quintuplet</b>                     | <b>9</b>  |
| 2.1 The model . . . . .  | 10        |
| 2.2 Scalar potential . . . . .                                     | 11        |
| 2.3 Neutrino masses . . . . .                                      | 12        |
| 2.4 Production of Majorana quintuplet leptons at the LHC . . . . . | 16        |
| 2.5 Decays of Majorana quintuplet leptons . . . . .                | 20        |
| 2.6 Possible role as dark matter . . . . .                         | 25        |
| 2.7 Loop induced Higgs decays . . . . .                            | 25        |
| 2.7.1 Exotic scalar couplings to Higgs boson . . . . .             | 26        |
| 2.7.2 Higgs diphoton-decay width . . . . .                         | 27        |
| 2.7.3 Higgs to Z-photon decay width . . . . .                      | 29        |
| 2.8 Direct and indirect bounds on new scalars . . . . .            | 31        |
| 2.9 Testability at the LHC . . . . .                               | 32        |
| <b>3 Model with Dirac lepton quintuplet</b>                        | <b>35</b> |
| 3.1 Dirac vectorlike multiplets in seesaw mechanism . . . . .      | 36        |
| 3.2 The model . . . . .  | 37        |
| 3.3 Neutrino masses . . . . .                                      | 39        |
| 3.4 Production of Dirac quintuplet leptons at the LHC . . . . .    | 42        |
| 3.5 Decays of Dirac quintuplet leptons . . . . .                   | 45        |
| 3.5.1 Pointlike decays . . . . .                                   | 45        |

|          |  |            |
|----------|--|------------|
| 3.5.2    | Cascade decays . . . . .   | 49         |
| 3.5.3    | Golden $\Sigma^{+++} \rightarrow W^+W^+l^+$ decay . . . . .                              | 50         |
| <b>4</b> | <b>Concluding remarks</b>  | <b>53</b>  |
|          | <b>Appendices</b>  | <b>55</b>  |
| <b>A</b> | <b>Scalar potential</b>  | <b>57</b>  |
| <b>B</b> | <b>Majorana quintuplet interactions in the mass basis</b>                                | <b>63</b>  |
| <b>C</b> | <b>Dirac quintuplet interactions in the mass basis</b>                                   | <b>69</b>  |
| <b>5</b> | <b>Prošireni sažetak: Kvintuplet teških leptona i mehanizam njihalice na skali TeV-a</b> | <b>77</b>  |
| 5.1      | Oscilacije, mase i miješanja neutrina . . . . .  | 77         |
| 5.1.1    | Mehanizmi njihalice . . . . .  | 79         |
| 5.1.2    | Mehanizmi njihalice na niskoj skali . . . . .  | 80         |
| 5.1.3    | Reprezentacije viših dimenzija . . . . .   | 80         |
| 5.2      | Model s Majoraninim leptonskim kvintupletom . . . . .                                    | 81         |
| 5.2.1    | Skalarni potencijal . . . . .  | 82         |
| 5.2.2    | Mase neutrina . . . . .  | 83         |
| 5.2.3    | Produkcija stanja Majoraninog kvintupleta na LHC-u . . . . .                             | 85         |
| 5.2.4    | Raspadi leptona iz Majoraninog kvintupleta . . . . .                                     | 87         |
| 5.2.5    | Kvintuplet kao tamna tvar . . . . .  | 89         |
| 5.2.6    | Raspadi higgasa inducirani kvantnom petljom . . . . .                                    | 90         |
| 5.2.7    | Mogućnost provjere na LHC-u . . . . .  | 91         |
| 5.3      | Model s Diracovim leptonskim kvintupletom . . . . .                                      | 92         |
| 5.3.1    | Mase neutrina . . . . .  | 94         |
| 5.3.2    | Produkcija stanja Diracovog kvintupleta na LHC-u . . . . .                               | 96         |
| 5.3.3    | Raspadi leptona iz Diracovog kvintupleta . . . . .                                       | 97         |
| 5.4      | Zaključak . . . . .  | 101        |
|          | <b>Bibliography</b>  | <b>103</b> |

# Introduction

This doctoral thesis presents two novel seesaw models based on weak-isospin quintuplet leptons. In the first one, a hypercharge-zero Majorana quintuplet lepton is accompanied by a scalar weak-isospin quadruplet, and in the second one a non-zero hypercharge Dirac quintuplet lepton is accompanied by two scalar weak-isospin quadruplets. In both models neutrino masses arise at the tree level from dimension-nine operator and from loop-suppressed dimension-five operator. This allows the new states to be within reach of the Large Hadron Collider (LHC) where they can be produced and these models for neutrino masses can be directly tested.

The thesis is organized as follows:

- The first chapter gives a brief overview of experimental evidence for small neutrino masses and seesaw mechanisms as an explanation of their smallness.
- The second chapter presents a model with hypercharge-zero Majorana quintuplet leptons accompanied by a scalar weak-isospin quadruplet. This model predicts neutrino masses, phenomenology of new leptons at the LHC, effects of the new scalars on loop Higgs decays and possible dark matter (DM) candidates.
- The third chapter presents a model with non-zero hypercharge Dirac quintuplet leptons accompanied by two scalar weak-isospin quadruplets. This model predicts neutrino masses and phenomenology of new leptons the LHC.



- Concluding remarks are given in the final, fourth chapter.

The main results of the thesis are the following:

- By employing the fermion and scalar higher weak-isospin multiplets in a seesaw mechanism the neutrino masses arise at the tree level from higher dimension operators and from loop suppressed dimension-five operator and thus lower the seesaw scale.
- The quintuplet leptons can be within the reach of the LHC so that the origin of the neutrino masses can be directly tested.

# Chapter 1

## Overture

In the Standard Model (SM) the neutrinos are electrically neutral fermions that participate only in the weak interactions, both in charged currents mediated by  $W^\pm$  boson and neutral currents mediated by  $Z^0$  boson. There are three different neutrino flavours: electron neutrino  $\nu_e$  and electron antineutrino  $\bar{\nu}_e$ , muon neutrino  $\nu_\mu$  and muon antineutrino  $\bar{\nu}_\mu$ , tau neutrino  $\nu_\tau$  and tau antineutrino  $\bar{\nu}_\tau$ . Together with their accompanying charged leptons they form weak-isospin doublets. The definition of neutrino flavour is dynamical, determined by associated charged lepton. For example, the electron antineutrino  $\bar{\nu}_e$  is produced with an electron  $e^-$  or produces a positron  $e^+$  in charge current interactions, the muon neutrino  $\nu_\mu$  is produced with a muon  $\mu^-$  or produces an antimuon  $\mu^+$  in charge current interactions, *ect.*

### § 1.1 Neutrino oscillations, masses and mixing

It is established that neutrinos change flavour after propagating a finite distance. For a neutrino of a given flavour produced with energy  $E$  in some weak interaction process, at a sufficiently large distance  $L$  from the source there is a non-zero probability to find a neutrino of a different flavour. A change of neutrino flavour in propagation is known as neutrino oscillation [1, 2, 3], because the probability of neutrino flavour change depends oscillatory on the neutrino energy and a distance of the propagation.

In many neutrino experiments the disappearance or the appearance of a particular neutrino flavour due to oscillations has been observed:

- A disappearance of solar electron neutrinos  $\nu_e$  in solar neutrino experiments [4, 5, 6, 7, 8, 9, 10, 11, 12].
- A disappearance of atmospheric muon neutrinos  $\nu_\mu$  and antineutrinos  $\bar{\nu}_\mu$  in Super-Kamiokande [13, 14] experiment.
- A disappearance of reactor electron antineutrinos  $\bar{\nu}_e$  in reactor KamLAND [15, 16] experiment.
- A disappearance of muon neutrinos  $\nu_\mu$  in long-baseline accelerator neutrino experiments K2K [17] and MINOS [18, 19].
- An appearance of electron neutrino  $\nu_e$  in a beam of muon neutrinos  $\nu_\mu$  in long-baseline accelerator neutrino experiments T2K [20] and MINOS [21].
- A disappearance of reactor electron antineutrinos  $\bar{\nu}_e$  in short-baseline reactor experiments Daya Bay [22] and RENO [23].

The experiments with solar, atmospheric, reactor and accelerator neutrinos have provided compelling evidences for oscillations of neutrinos caused by non-zero neutrino masses and neutrino mixing. This means that the neutrino flavour eigenstate fields ( $\nu_e, \nu_\mu, \nu_\tau$ ) which enter into the lepton charged current in weak interactions are linear combinations of the neutrino mass eigenstate fields ( $\nu_1, \nu_2, \nu_3$ )

$$\nu_l(x) = \sum_{i=1}^3 U_{li} \nu_i(x), \quad l = e, \mu, \tau. \quad (1.1)$$

$U$  is unitary neutrino mixing matrix [1, 2, 3], often called the Pontecorvo-Maki-Nakagawa-Sakata ( $U_{PMNS}$ ) mixing matrix parameterized as

$$U_{PMNS} = \begin{pmatrix} c_{12}c_{13} & s_{12}c_{13} & s_{13}e^{-i\delta} \\ -s_{12}c_{23} - c_{12}s_{23}s_{13}e^{i\delta} & c_{12}c_{23} - s_{12}s_{23}s_{13}e^{i\delta} & s_{23}c_{13} \\ s_{12}s_{23} - c_{12}c_{23}s_{13}e^{i\delta} & -c_{12}s_{23} - s_{12}c_{23}s_{13}e^{i\delta} & c_{23}c_{13} \end{pmatrix} \times P, \quad (1.2)$$

where  $P = \text{diag}(1, e^{i\alpha}, e^{i\beta})$ . Here  $c_{ij} = \cos \theta_{ij}$  and  $s_{ij} = \sin \theta_{ij}$  with  $\theta_{12}$ ,  $\theta_{23}$  and  $\theta_{13}$  being the solar mixing angle, atmospheric mixing angle and the

reactor mixing angle, respectively. The phase  $\delta$  is the Dirac CP violating phase while  $\alpha$  and  $\beta$  are the two Majorana CP violating phases.

The parameters of neutrino oscillations, mixing angles and the mass squared differences,  $\Delta m_{ij}^2 = m_i^2 - m_j^2$ , can be determined by global analysis of the existing neutrino oscillation data. In Table 1.1 we give the result of a recent global fit analysis [24].

| parameter                                    | best fit   | $3\sigma$ range |
|--|------------|-----------------|
| $\Delta m_{21}^2$ [ $10^{-5}\text{eV}^2$ ]   | 7.62       | 7.12–8.20       |
| $ \Delta m_{31}^2 $ [ $10^{-3}\text{eV}^2$ ] | 2.55       | 2.31 – 2.74     |
|  | 2.43       | 2.21 – 2.64     |
| $\sin^2 \theta_{12}$                         | 0.320      | 0.27–0.37       |
| $\sin^2 \theta_{23}$                         | 0.613      | 0.36–0.68       |
|  | 0.600      | 0.37–0.67       |
| $\sin^2 \theta_{13}$                         | 0.0246     | 0.017–0.033     |
|  | 0.0250     |                 |
| $\delta$                                     | $0.80\pi$  | $0 - 2\pi$      |
|  | $-0.03\pi$ |                 |

Table 1.1: A global fit of the neutrino oscillation parameters [24]. For  $\Delta m_{31}^2$ ,  $\sin^2 \theta_{23}$ ,  $\sin^2 \theta_{13}$  and  $\delta$  the upper (lower) row corresponds to normal (inverted) neutrino mass hierarchy.

## § 1.2 Seesaw mechanisms

The existence of neutrino masses represents the first tangible deviation from the standard model. In order to account for the smallness of these masses one has to modify the particle content of the SM by adding new degrees of freedom. The neutrino masses can be realized through an effective dimension-five operator

$$\mathcal{L} = \frac{\bar{l}_L \tilde{H} \tilde{H}^T l_L^c}{\Lambda}, \quad (1.3)$$

introduced by Weinberg [25]. It is the only dimension-five effective operator in the SM and it leads to neutrino masses suppressed by a high mass scale  $\Lambda$ . The Weinberg's operator can be generated both at the tree and at the loop level. At the tree level there are only three realizations of the dimension-five operator [26]: type I [27, 28, 29, 30, 31], type II [32, 33, 34, 35, 36, 37] and type III [38] seesaw mechanisms, mediated by heavy fermion singlet  $N_R$ , scalar triplet  $\Delta$  and a fermion triplet  $\Sigma_R$ , respectively. In the usual seesaw setup the masses of the new degrees of freedom are associated with the scale of Grand Unified Theories. As a consequence, the possibility of direct tests of the seesaw mechanism seems very remote.

### § 1.3 Low scale seesaw mechanisms

Several proposals have been made to bring the high mass scale of the seesaw mechanism down to the TeV range, so that they might be experimentally testable, for instance at the LHC at CERN.

The most straightforward possibility is to have cancellations within the type I seesaw mechanism such that scale of new physics may be relatively low without the need to excessively suppress the Yukawa couplings [39, 40]. The general conditions for this to happen were given in [41]. Cancellations between the type I and type II seesaw contributions to the neutrino masses have also been considered [42, 43]. In the inverse seesaw mechanism [44, 45] there is both a high scale in the TeV range and a low scale in the keV range.

Low scale seesaw mechanism can be achieved by radiatively generated neutrino masses. The loop factors provide a sufficient suppression as it was first introduced at one-loop level in [46]. This idea was later exploited by one [47], two [49, 48, 50] and three-loop level [51, 52] mechanisms.

In a multiple seesaw approach first put forward in [53] and later extended in [54], the involved additional fields and additional discrete symmetries are instrumental in bringing the seesaw mechanism to the TeV scale [55] accessible at the LHC.

## § 1.4 Higher dimensional representations

The gauge group of the standard model is  $SU(3)_C \times SU(2)_L \times U(1)_Y$ . All fermions and scalars of the standard model are either in the singlets or in the fundamental representations of the SM gauge group factors. The multiplets in the higher dimensional representations of the  $SU(2)_L$  weak-isospin gauge group of the SM were used in addressing different beyond the standard model topics such as neutrino masses and dark matter. We will list just a few here.

Among many higher dimensional multiplets considered as minimal dark matter (MDM) candidates in [56], the fermion transforming as  $\Sigma \sim (1, 5, 0)$  under the SM gauge group has been singled out as the best MDM candidate. The phenomenology of this fermionic quintuplet has been considered in a series of publications [57, 58, 59]. Another MDM candidate, a scalar septuplet  $\Phi \sim (1, 7, 0)$  was considered in [60].

Higher dimensional multiplets were also used in models aiming to explain non-zero neutrino masses. Probably the most famous is the already mentioned type III seesaw mechanism [38] using hypercharge zero lepton triplets. In [61] hypercharge non-zero lepton triplets  $\Sigma_{L,R} \sim (1, 3, 2)$  together with scalar quadruplet  $\Phi \sim (1, 4, -3)$  were used to generate neutrino masses at the tree level from a dimension-seven operator.

An attempt to build a model relating radiative seesaw and MDM mass scales without beyond SM gauge symmetry (R $\nu$ MDM) was considered in [62], and later applied for baryon asymmetry in [63]. The stability of MDM candidates in this setup, in which they participate in radiative neutrino mass generation, was examined in [64] where the existence of additional renormalizable operators which spoil the stability of the MDM candidate has been pointed out.



# Chapter 2

## Model with Majorana lepton quintuplet

A seesaw model built upon the zero hypercharge fermionic weak quintuplet has been proposed in [65]. Such a multiplet, in isolation, provides a viable dark matter particle within the so-called minimal dark matter model [56]. It is of interest to explore the conditions under which the quintuplets  $\Sigma_R \sim (1, 5, 0)$  could simultaneously generate the masses of the known neutrinos and provide a stable DM candidate.

The proposed model goes beyond conventional type I, II and III seesaw mechanisms, mediated by a heavy fermion singlet, a scalar triplet, and a fermion triplet, respectively. Fermionic seesaw mediator of isospin larger than one has to be accompanied by a scalar multiplet larger than that of the SM Higgs doublet. We analyze in detail both the tree-level and the radiative neutrino masses generated by hypercharge zero quintuplets  $\Sigma_R \sim (1, 5, 0)$ . Thereby we address also a phenomenology of these states at the LHC and recall that by imposing a  $Z_2$  symmetry, one can reconcile the seesaw mission with the viability as a DM.



## § 2.1 The model

The model proposed here is based on the symmetry of the SM gauge group  $SU(3)_C \times SU(2)_L \times U(1)_Y$ . In addition to the usual SM fermions, we introduce three generations of hypercharge zero lepton quintuplets  $\Sigma_R = (\Sigma_R^{++}, \Sigma_R^+, \Sigma_R^0, \Sigma_R^-, \Sigma_R^{--})$ , transforming as  $(1, 5, 0)$  under the SM gauge group. Also, in addition to the SM Higgs doublet  $H = (H^+, H^0)$  there is a scalar quadruplet  $\Phi = (\Phi^+, \Phi^0, \Phi^-, \Phi^{--})$  transforming as  $(1, 4, -1)$ .

In a tensor notation suitable to cope with higher  $SU(2)_L$  multiplets [62] our additional fields are totally symmetric tensors  $\Sigma_{Rijkl}$  and  $\Phi_{ijk}$  with the following components:

$$\begin{aligned} \Sigma_{R1111} &= \Sigma_R^{++} , \quad \Sigma_{R1112} = \frac{1}{\sqrt{4}}\Sigma_R^+ , \quad \Sigma_{R1122} = \frac{1}{\sqrt{6}}\Sigma_R^0 , \\ \Sigma_{R1222} &= \frac{1}{\sqrt{4}}\Sigma_R^- , \quad \Sigma_{R2222} = \Sigma_R^{--} ; \end{aligned} \quad (2.1)$$

$$\Phi_{111} = \Phi^+ , \quad \Phi_{112} = \frac{1}{\sqrt{3}}\Phi^0 , \quad \Phi_{122} = \frac{1}{\sqrt{3}}\Phi^- , \quad \Phi_{222} = \Phi^{--} . \quad (2.2)$$

The gauge invariant and renormalizable Lagrangian involving these new fields reads

$$\mathcal{L} = \overline{\Sigma_R} i \gamma^\mu D_\mu \Sigma_R + (D^\mu \Phi)^\dagger (D_\mu \Phi) - (\overline{L}_L Y \Phi \Sigma_R + \frac{1}{2} \overline{(\Sigma_R)^C} M \Sigma_R + \text{H.c.}) - V(H, \Phi). \quad (2.3)$$

Here,  $D_\mu$  is the gauge covariant derivative,  $Y$  is the Yukawa-coupling matrix and  $M$  is the mass matrix of the heavy leptons, which we choose to be real and diagonal. For simplicity we drop the flavour indices altogether.

In the adopted tensor notation the terms in Eq. (2.3) read

$$\begin{aligned} \overline{L}_L \Phi \Sigma_R &= \overline{L}_L^i \Phi_{jkl} \Sigma_{Rij'k'l'} \epsilon^{jj'} \epsilon^{kk'} \epsilon^{ll'} , \\ \overline{(\Sigma_R)^C} \Sigma_R &= \overline{(\Sigma_R)^C}_{ijkl} \Sigma_{Ri'j'k'l'} \epsilon^{ii'} \epsilon^{jj'} \epsilon^{kk'} \epsilon^{ll'} . \end{aligned} \quad (2.4)$$

Accordingly, the Majorana mass term for the quintuplet  $\Sigma_R$  is expanded in component fields to give

$$\begin{aligned} \overline{(\Sigma_R)^C} M \Sigma_R &= \overline{(\Sigma_R^{++})^C} M \Sigma_R^{--} - \overline{(\Sigma_R^+)^C} M \Sigma_R^- + \overline{(\Sigma_R^0)^C} M \Sigma_R^0 \\ &\quad - \overline{(\Sigma_R^-)^C} M \Sigma_R^+ + \overline{(\Sigma_R^{--})^C} M \Sigma_R^{++} , \end{aligned} \quad (2.5)$$

the terms containing two charged Dirac fermions and one neutral Majorana fermion

$$\Sigma^{++} = \Sigma_R^{++} + \Sigma_R^{-C} , \quad \Sigma^+ = \Sigma_R^+ - \Sigma_R^{-C} , \quad \Sigma^0 = \Sigma_R^0 + \Sigma_R^{0C} . \quad (2.6)$$

## § 2.2 Scalar potential

The scalar potential has the gauge invariant form

$$\begin{aligned} V(H, \Phi) &= -\mu_H^2 H^{*i} H_i + \mu_\Phi^2 \Phi^{*ijk} \Phi_{ijk} + \lambda_1 (H^{*i} H_i)^2 \\ &+ \lambda_2 (H^* H \Phi^* \Phi)_1 + \lambda_3 (H^* H \Phi^* \Phi)_2 \\ &+ (\lambda_4 e^{i\alpha} H^* H H \Phi + \text{H.c.}) + (\lambda_5 e^{i\beta} H H \Phi \Phi + \text{H.c.}) \\ &+ (\lambda_6 e^{i\gamma} H \Phi^* \Phi \Phi + \text{H.c.}) + \lambda_7 (\Phi^{*ijk} \Phi_{ijk})^2 + \lambda_8 \Phi^* \Phi \Phi^* \Phi , \end{aligned} \quad (2.7)$$

where parameters are real. Detailed analysis of the scalar potential in Eq. (2.7) is given in Appendix A.

Here, for simplicity, it is assumed that all quartic couplings are real and only the main points of the analysis are presented. The electroweak symmetry breaking (EWSB) proceeds in usual way from the vacuum expectation value (vev)  $v_H$  of the Higgs doublet, corresponding to the negative sign in front of the  $\mu_H^2$  term in Eq. (2.7). On the other hand, the electroweak  $\rho$  parameter dictates a small value for vev  $v_\Phi$  of the scalar quadruplet, implying the positive sign in front of the  $\mu_\Phi^2$  term. However, the presence of the  $\lambda_4$  term in Eq. (2.7), given explicitly by

$$\begin{aligned} H^* H H \Phi &= \frac{1}{\sqrt{3}} H^{+*} H^+ H^+ \Phi^- - \frac{2}{\sqrt{3}} H^{0*} H^+ H^0 \Phi^- + H^{0*} H^+ H^+ \Phi^{--} \\ &+ H^{+*} H^0 H^0 \Phi^+ - \frac{2}{\sqrt{3}} H^{+*} H^+ H^0 \Phi^0 + \frac{1}{\sqrt{3}} H^{0*} H^0 H^0 \Phi^0 , \end{aligned} \quad (2.8)$$

leads to the induced vev  $v_\Phi$  for the  $\Phi^0$  field. Since it changes the electroweak  $\rho$  parameter from the unit value to  $\rho \simeq 1 + 6v_\Phi^2/v_H^2$ , a comparison to the experimental value  $\rho = 1.0004_{-0.0004}^{+0.0003}$  [66] gives an upper limit  $v_\Phi \lesssim 3.2$  GeV and constraints the ratio  $v_\Phi/v_H$  to be smaller than 0.01.

After the EWSB the neutral components of the scalar fields acquire the vacuum expectation values and read

$$H^0 = \frac{1}{\sqrt{2}}(v_H + h^0 + i\chi) , \quad \Phi^0 = \frac{1}{\sqrt{2}}(v_\Phi + \varphi^0 + i\eta) . \quad (2.9)$$

Since all quartic couplings in the scalar potential are assumed to be real, the conditions for the minimum of the potential

$$\frac{\partial V_0(v_H, v_\Phi)}{\partial v_H} = 0 , \quad \frac{\partial V_0(v_H, v_\Phi)}{\partial v_\Phi} = 0 \quad (2.10)$$

give

$$\mu_H^2 = \lambda_1 v_H^2 + \left(\frac{1}{2}\lambda_2 + \frac{1}{6}\lambda_3 - \frac{2}{3}\lambda_5\right)v_\Phi^2 + \frac{\sqrt{3}}{2}\lambda_4 v_H v_\Phi - \frac{\sqrt{3}}{9}\lambda_6 \frac{v_\Phi^3}{v_H} , \quad (2.11)$$

$$\mu_\Phi^2 = -\left(\frac{1}{2}\lambda_2 + \frac{1}{6}\lambda_3 - \frac{2}{3}\lambda_5\right)v_H^2 - \frac{\sqrt{3}}{6}\lambda_4 \frac{v_H^3}{v_\Phi} + \frac{\sqrt{3}}{3}\lambda_6 v_H v_\Phi - \left(\lambda_7 + \frac{5}{9}\lambda_8\right)v_\Phi^2 . \quad (2.12)$$

In the leading order in the ratios  $v_\Phi/v_H$  and  $v_\Phi^2/\mu_\Phi^2$ , the vevs of scalar fields are

$$v_H \simeq \sqrt{\frac{\mu_H^2}{\lambda_1}} , \quad v_\Phi \simeq -\frac{1}{2\sqrt{3}}\lambda_4 \frac{v_H^3}{\mu_\Phi^2} , \quad (2.13)$$

as given in Eq. (A.16).

## § 2.3 Neutrino masses

The Yukawa interaction terms from Eq. (2.3), when expressed like in Eq. (2.4), read

$$\begin{aligned} \overline{L}_L \Phi \Sigma_R = & -\frac{\sqrt{3}}{2} \bar{\nu}_L \Phi^- \Sigma_R^+ - \frac{1}{\sqrt{2}} \bar{l}_L \Phi^- \Sigma_R^0 + \frac{\sqrt{3}}{2} \bar{l}_L \Phi^0 \Sigma_R^- + \frac{1}{\sqrt{2}} \bar{\nu}_L \Phi^0 \Sigma_R^0 \\ & - \frac{1}{2} \bar{\nu}_L \Phi^+ \Sigma_R^- - \bar{l}_L \Phi^+ \Sigma_R^{--} + \frac{1}{2} \bar{l}_L \Phi^{--} \Sigma_R^+ + \bar{\nu}_L \Phi^{--} \Sigma_R^{++} . \end{aligned} \quad (2.14)$$

The vev  $v_\Phi$  generates a Dirac mass term connecting  $\nu_L$  and  $\Sigma_R^0$ , a nondiagonal entry in the mass matrix for neutral leptons given by

$$\mathcal{L}_{\nu\Sigma^0} = -\frac{1}{2} \left( \overline{\nu}_L \overline{(\Sigma_R^0)^c} \right) \begin{pmatrix} 0 & \frac{1}{2} Y v_\Phi \\ \frac{1}{2} Y^T v_\Phi & M \end{pmatrix} \begin{pmatrix} (\nu_L)^c \\ \Sigma_R^0 \end{pmatrix} + \text{H.c.} . \quad (2.15)$$

Similar term connecting light and heavy singly charged leptons gives the mass matrix for charged leptons

$$\mathcal{L}_{l\Sigma^-} = - \left( \overline{l_L} \overline{(\Sigma_R^+)^C} \right) \begin{pmatrix} Y_{l\nu} & -\frac{\sqrt{3}}{2\sqrt{2}} Y v_\Phi \\ 0 & M \end{pmatrix} \begin{pmatrix} l_R \\ (\Sigma_L^+)^C \end{pmatrix} + \text{H.c.} . \quad (2.16)$$

After diagonalizing the mass matrix for neutral leptons, light neutrinos acquire the Majorana mass matrix given by

$$m_\nu^{tree} = -\frac{1}{4} v_\Phi^2 Y M^{-1} Y^T . \quad (2.17)$$

In the basis where the matrix of heavy leptons is real and diagonal,  $M = \text{diag}(M_1, M_2, M_3)$ , we can write  $m_\nu^{tree}$  as

$$(m_\nu)_{ij}^{tree} = -\frac{1}{4} v_\Phi^2 \sum_k \frac{Y_{ik} Y_{jk}}{M_k} . \quad (2.18)$$

Together with the induced vev in Eq. (2.13), this gives

$$(m_\nu)_{ij}^{tree} = -\frac{1}{48} \lambda_4^2 \frac{v_H^6}{\mu_\Phi^4} \sum_k \frac{Y_{ik} Y_{jk}}{M_k} , \quad (2.19)$$

which reflects the fact that the light neutrino mass is generated from the dimension-nine operator corresponding to the tree-level seesaw mechanism displayed on Fig. 2.1.

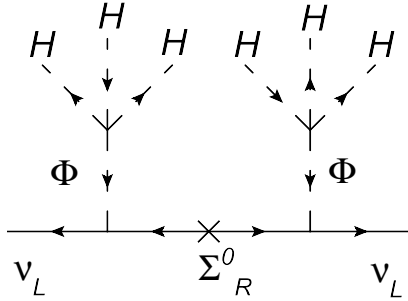


Figure 2.1: Tree-level diagram corresponding to dimension-nine operator in Eq. (2.19). The fermion line flow indicates a Majorana nature of the seesaw mediator.

Besides at the tree level, the light neutrino masses arise also through one-loop diagrams displayed on Fig. 2.2. The crucial quartic  $\lambda_5$  term in Eq. (2.7), when expanded in component fields, gives

$$HH\Phi\Phi = \frac{2}{\sqrt{3}}\Phi^-\Phi^+H^0H^0 - \frac{2}{3}\Phi^-\Phi^-H^+H^+ + \frac{2}{\sqrt{3}}\Phi^{--}\Phi^0H^+H^+ - \frac{2}{3}\Phi^0\Phi^0H^0H^0 + \frac{2}{3}\Phi^-\Phi^0H^+H^0 - 2\Phi^+\Phi^{--}H^+H^0. \quad (2.20)$$

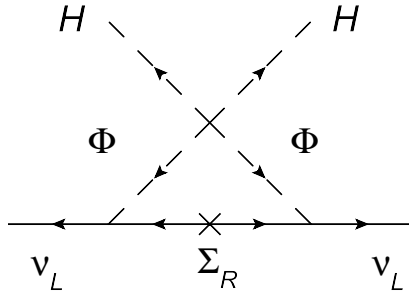


Figure 2.2: One-loop diagrams generating the light neutrino masses.

There are two different contributions on Fig. 2.2, one with heavy neutral fields ( $\Sigma^0, \Phi^0$ ) and the other with heavy charged fields ( $\Sigma^+, \Phi^+, \Phi^-$ ) running in the loop. If we neglect the mass splitting within the  $\Sigma$  and  $\Phi$  multiplets, the contribution to the light neutrino mass matrix is given by

$$(m_\nu)_{ij}^{loop} = \frac{-5\lambda_5 v_H^2}{48\pi^2} \sum_k \frac{Y_{ik}Y_{jk}M_k}{m_\Phi^2 - M_k^2} \left[ 1 - \frac{M_k^2}{m_\Phi^2 - M_k^2} \ln \frac{m_\Phi^2}{M_k^2} \right]. \quad (2.21)$$

This expression can be further specified [47], depending on relative values of the masses for additional fermion and scalar multiplets. For heavy fermions significantly heavier than the new scalars,  $M_k^2 \gg m_\Phi^2$ ,

$$(m_\nu)_{ij}^{loop} = \frac{-5\lambda_5 v_H^2}{48\pi^2} \sum_k \frac{Y_{ik}Y_{jk}}{M_k} \left[ \ln \frac{M_k^2}{m_\Phi^2} - 1 \right]. \quad (2.22)$$

In the opposite case, for  $m_\Phi^2 \gg M_k^2$  [67],

$$(m_\nu)_{ij}^{loop} = \frac{-5\lambda_5 v_H^2}{48\pi^2 m_\Phi^2} \sum_k Y_{ik}Y_{jk}M_k. \quad (2.23)$$

Finally, if  $m_\Phi^2 \simeq M_k^2$ , then

$$(m_\nu)_{ij}^{loop} = \frac{-5\lambda_5 v_H^2}{96\pi^2} \sum_k \frac{Y_{ik} Y_{jk}}{M_k}. \quad (2.24)$$

The tree-level and the loop contributions added together give the light neutrino mass matrix

$$\begin{aligned} (m_\nu)_{ij} &= (m_\nu)_{ij}^{tree} + (m_\nu)_{ij}^{loop} \\ &= \frac{-1}{48} \lambda_4^2 \frac{v_H^6}{\mu_\Phi^4} \sum_k \frac{Y_{ik} Y_{jk}}{M_k} + \frac{-5\lambda_5 v_H^2}{48\pi^2} \sum_k \frac{Y_{ik} Y_{jk} M_k}{m_\Phi^2 - M_k^2} \left[ 1 - \frac{M_k^2}{m_\Phi^2 - M_k^2} \ln \frac{m_\Phi^2}{M_k^2} \right]. \end{aligned} \quad (2.25)$$

In the case of comparable masses of the lepton quintuplet and the scalar quadruplet the light neutrino mass matrix reads

$$(m_\nu)_{ij} = \left[ \frac{-1}{48} \lambda_4^2 \frac{v_H^6}{\mu_\Phi^4} + \frac{-5\lambda_5 v_H^2}{96\pi^2} \right] \sum_k \frac{Y_{ik} Y_{jk}}{M_k}. \quad (2.26)$$

From this expression we can estimate the high energy scale of our model and the corresponding value for  $v_\Phi$  in Eq. (2.13). For illustrative purposes we take the same values for the mass parameters ( $\mu_\Phi = M = \Lambda_{NP}$ ) and the empirical input values  $v_H = 246$  GeV and  $m_\nu \sim 0.1$  eV. For the moderate values  $Y \sim 10^{-3}$ ,  $\lambda_4 \sim 10^{-2}$  and  $\lambda_5 \sim 10^{-4}$  we get  $\Lambda_{NP} \simeq 440$  GeV and  $v_\Phi \simeq 220$  MeV. The corresponding masses of the new states could be tested at the LHC. On Fig. 2.3 we display the part of the parameter space for which the tree-level (loop-level) contribution dominates.

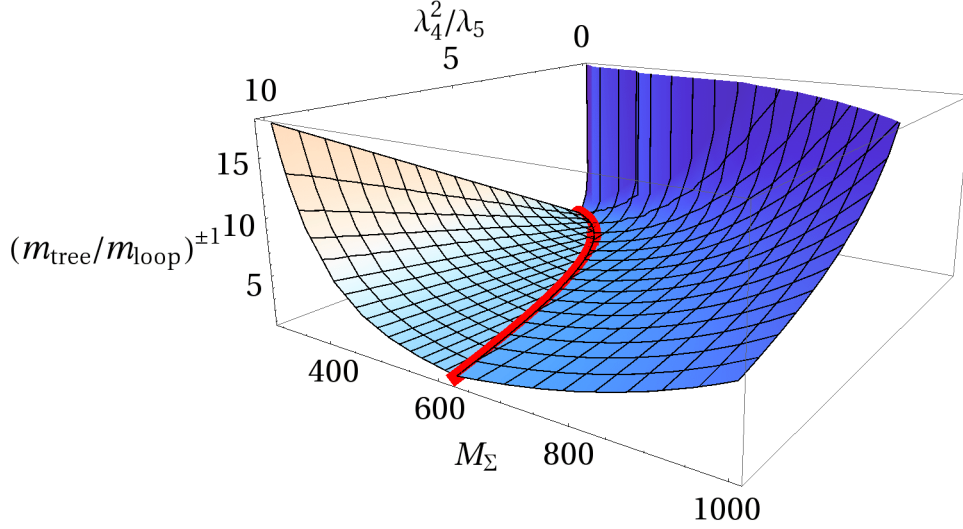


Figure 2.3: For the portion of the parameter space left from the equality-division line, where the tree-level contribution to neutrino masses dominates, we plot  $m_{tree}/m_{loop}$ . Right from the equality-division line the one-loop contribution to neutrino masses dominates, and we plot  $m_{loop}/m_{tree}$ .

## § 2.4 Production of Majorana quintuplet leptons at the LHC

The production channels of the heavy quintuplet leptons in proton-proton collisions are dominated by the quark-antiquark annihilation via neutral and charged gauge bosons

$$q + \bar{q} \rightarrow A \rightarrow \Sigma + \bar{\Sigma}, \quad A = \gamma, Z, W^\pm,$$

where the gauge Lagrangian relevant for the production is given by

$$\begin{aligned} \mathcal{L}_{gauge}^{\Sigma\bar{\Sigma}} = & + e(2\bar{\Sigma}^{++}\gamma^\mu\Sigma^{++} + \bar{\Sigma}^+\gamma^\mu\Sigma^+)A_\mu \\ & + g \cos \theta_W(2\bar{\Sigma}^{++}\gamma^\mu\Sigma^{++} + \bar{\Sigma}^+\gamma^\mu\Sigma^+)Z_\mu \\ & + g(\sqrt{2}\bar{\Sigma}^+\gamma^\mu\Sigma^{++} + \sqrt{3}\bar{\Sigma}^0\gamma^\mu\Sigma^+)W_\mu^- + \text{H.c.} . \end{aligned} \quad (2.27)$$

The cross section for the partonic process is

$$\hat{\sigma}(q\bar{q} \rightarrow \Sigma\bar{\Sigma}) = \frac{\beta(3 - \beta^2)}{48\pi} \hat{s}(V_L^2 + V_R^2), \quad (2.28)$$

where  $\hat{s} \equiv (p_q + p_{\bar{q}})^2$  is the Mandelstam variable  $s$  for the quark-antiquark system, the parameter  $\beta \equiv \sqrt{1 - 4M_\Sigma^2/\hat{s}}$  denotes the heavy lepton velocity, and the left- and right-handed couplings are given by

$$V_{L,R}^{(\gamma+Z)} = \frac{Q_\Sigma Q_q e^2}{\hat{s}} + \frac{g^{Z\Sigma} g_{L,R}^q g^2}{c_W^2(\hat{s} - M_Z^2)}, \quad (2.29)$$

$$V_L^{(W^-)} = \frac{g^{W\Sigma} g^2 V_{ud}}{\sqrt{2}(\hat{s} - M_W^2)} = V_L^{(W^+)*}, \quad (2.30)$$

$$V_R^{(W^\pm)} = 0. \quad (2.31)$$

Here,  $g_L^q = T_3 - s_W^2 Q_q$  and  $g_R^q = -s_W^2 Q_q$  are the SM chiral quark couplings to the  $Z$  boson. The vector couplings of heavy leptons to gauge bosons are

$$g^{Z\Sigma} = T_3 - s_W^2 Q_\Sigma \text{ and } g^{W\Sigma} = \sqrt{2} \text{ or } \sqrt{3}, \quad (2.32)$$

where  $g^{W\Sigma}$  can be read of the last row in Eq. (2.27), relevant for the production of  $\Sigma^{++}\bar{\Sigma}^+$  and  $\Sigma^+\bar{\Sigma}^0$  pairs, respectively.

To obtain the cross sections for a hadron collider, the partonic cross-section from Eq. (2.28) has to be convoluted with the appropriate parton distribution functions (PDFs)  $q(x, \mu^2)$ . For the case of the proton-proton collisions we have

$$\begin{aligned} \frac{d^2\sigma(pp \rightarrow \Sigma\bar{\Sigma})}{dx_1 dx_2} &= \frac{1}{N_c} \sum_{f_1=u,d,\dots} \sum_{f_2=\bar{u},\bar{d},\dots} \hat{\sigma}(q_{f_1} q_{f_2} \rightarrow \Sigma\bar{\Sigma}) \\ &\times (q_{f_1}(x_1, \mu^2) q_{f_2}(x_2, \mu^2) + q_{f_2}(x_1, \mu^2) q_{f_1}(x_2, \mu^2)), \end{aligned} \quad (2.33)$$

leading to the total cross section

$$\begin{aligned} \sigma(pp \rightarrow \Sigma\bar{\Sigma}) &= \frac{1}{N_c} \sum_{f_1=u,d,\dots} \sum_{f_2=\bar{u},\bar{d},\dots} \int_{4M^2/s}^1 d\tau \int_\tau^1 \frac{dx_1}{x_1} \hat{\sigma}(q_{f_1} q_{f_2} \rightarrow \Sigma\bar{\Sigma}) \\ &\times \left( q_{f_1}(x_1, \mu^2) q_{f_2}\left(\frac{\tau}{x_1}, \mu^2\right) + q_{f_2}(x_1, \mu^2) q_{f_1}\left(\frac{\tau}{x_1}, \mu^2\right) \right). \end{aligned} \quad (2.34)$$

Here, the inverse of the  $N_c = 3$  factor is due to the color averaging in the initial state, corresponding to the summation over colors implicit in the standard published PDFs. To evaluate the cross sections we have used CTEQ6.6 PDFs [68] via LHAPDF software library [69] and have chosen  $\mu = M_\Sigma$  as a factorization scale.



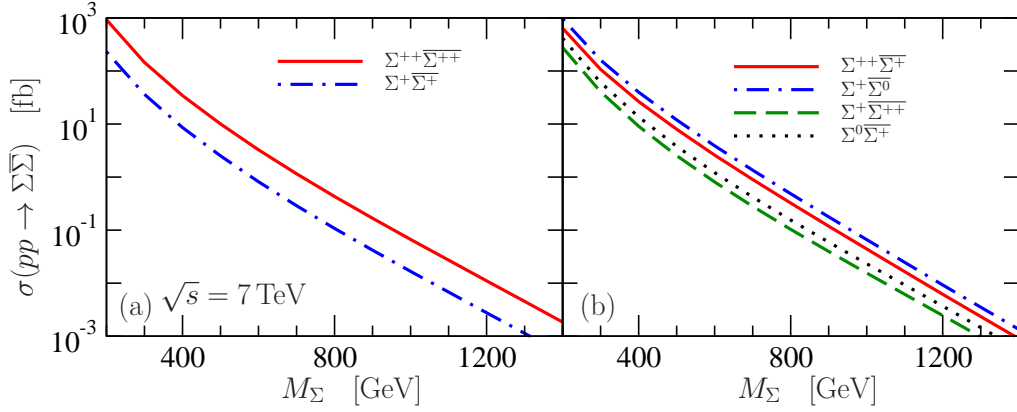


Figure 2.4: The cross sections for production of quintuplet lepton pairs on LHC proton-proton collisions at  $\sqrt{s} = 7$  TeV via neutral  $\gamma, Z$  (a) and charged  $W^{\pm}$  currents (b), in dependence on the heavy quintuplet mass  $M_{\Sigma}$ .

The cross sections for proton-proton collisions are presented on Fig. 2.4 for  $\sqrt{s} = 7$  TeV appropriate for the 2011-12 LHC run, and for designed  $\sqrt{s} = 14$  TeV on Fig. 2.5. Thereby we distinguish separately the production via neutral currents shown on the left panel, and via charged currents shown on the right panel of Figs. 2.4 and 2.5.

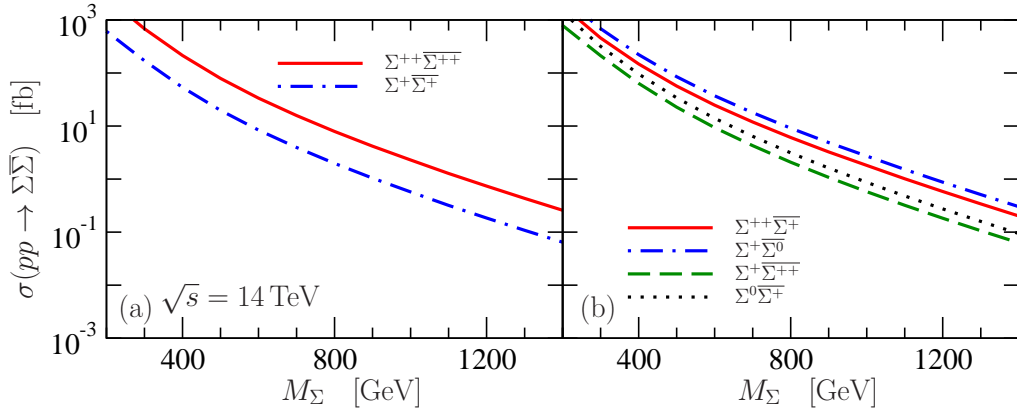


Figure 2.5: Same as Fig. 2.4, but for designed  $\sqrt{s} = 14$  TeV at the LHC.

We extract in Table 2.1 the pair production cross sections from Fig. 2.4 for three selected values of  $M_{\Sigma}$ . From this table we find that the doubly-charged  $\Sigma^{++}$  has the largest production cross section  $\sigma(\Sigma^{++})|_{M_{\Sigma}=400\text{GeV}} = 60.9$  fb and

doubly-charged  $\overline{\Sigma}^{++}$  has the smallest, still comparable  $\sigma(\overline{\Sigma}^{++})|_{M_\Sigma=400\text{GeV}} = 43.5\text{ fb}$ . The production rates of other heavy leptons are in between.

| Produced pair                       | Cross section (fb)          |                             |                             |
|-------------------------------------|-----------------------------|-----------------------------|-----------------------------|
|                                     | $M_\Sigma = 200\text{ GeV}$ | $M_\Sigma = 400\text{ GeV}$ | $M_\Sigma = 800\text{ GeV}$ |
| $\Sigma^{++}\overline{\Sigma}^{++}$ | 924                         | 34.4                        | 0.43                        |
| $\Sigma^+\overline{\Sigma}^+$       | 231                         | 8.6                         | 0.11                        |
| $\Sigma^{++}\overline{\Sigma}^+$    | 641                         | 26.5                        | 0.32                        |
| $\Sigma^+\overline{\Sigma}^0$       | 961                         | 39.8                        | 0.49                        |
| $\Sigma^+\overline{\Sigma}^{++}$    | 276                         | 9.1                         | 0.10                        |
| $\Sigma^0\overline{\Sigma}^+$       | 414                         | 13.6                        | 0.15                        |
| Total                               | 3447                        | 132                         | 1.6                         |

Table 2.1: Production cross sections for  $\Sigma$ - $\overline{\Sigma}$  pairs for the LHC run at  $\sqrt{s} = 7\text{ TeV}$ , for three selected values of  $M_\Sigma$ .

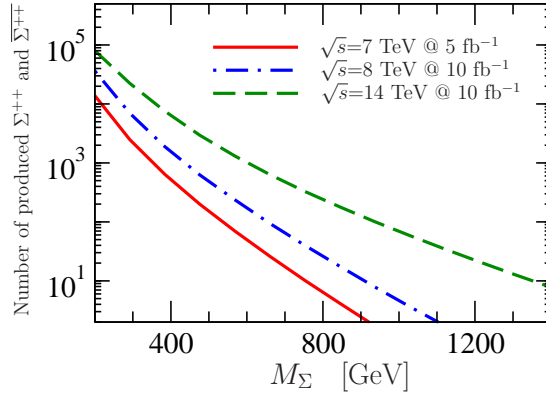


Figure 2.6: Number of  $\Sigma^{++}$  and  $\overline{\Sigma}^{++}$  particles produced for three characteristic LHC collider setups, in dependence on the heavy lepton mass  $M_\Sigma$ .

On Fig. 2.6 we plot the expected number of produced  $\Sigma^{++}$  and  $\overline{\Sigma}^{++}$  particles for three characteristic collider setups. In particular, for  $M_\Sigma = 400\text{ GeV}$  and  $5\text{ fb}^{-1}$  of integrated luminosity of 2011 LHC run at  $\sqrt{s} = 7\text{ TeV}$  and  $21\text{ fb}^{-1}$  of integrated luminosity of 2012 LHC run at  $\sqrt{s} = 8\text{ TeV}$ , there should be about 3200 doubly-charged  $\Sigma^{++}$  or  $\overline{\Sigma}^{++}$  fermions produced. In total, there should be 4000  $\Sigma - \overline{\Sigma}$  pairs produced.

By testing the heavy lepton production cross sections one can hope to identify the quantum numbers of the quintuplet particles, but in order to confirm their relation to neutrinos one has to study their decays.

## § 2.5 Decays of Majorana quintuplet leptons

The focus here is entirely on the decay modes of the heavy lepton states listed in Eq. (2.6). Namely, provided that in our scenario the exotic scalar states are slightly heavier than the exotic leptons, the exotic scalar fields will not appear in the final states of heavy lepton decays. Note that exotic scalar states  $\Phi \sim (1, 4, 1)$  were considered recently in [70], in the context of modified type III seesaw model.

The couplings relevant for the decays at hand stem from off-diagonal entries in the mass matrices in Eqs. (2.15) and (2.16). The diagonalization of these matrices is considered in detail in the Appendix B and here only the main points are presented. The diagonalization of the mass matrices can be achieved by making the following unitary transformations on the lepton fields:

$$\begin{aligned} \begin{pmatrix} (\nu_L)^c \\ \Sigma_R^0 \end{pmatrix} &= U^0 \begin{pmatrix} (\nu_{mL})^c \\ \Sigma_{mR}^0 \end{pmatrix}, \\ \begin{pmatrix} l_L \\ (\Sigma_R^+)^c \end{pmatrix} &= U^L \begin{pmatrix} l_{mL} \\ (\Sigma_{mR}^+)^c \end{pmatrix}, \quad \begin{pmatrix} l_R \\ (\Sigma_L^+)^c \end{pmatrix} = U^R \begin{pmatrix} l_{mR} \\ (\Sigma_{mL}^+)^c \end{pmatrix}. \end{aligned} \quad (2.35)$$

Following the procedure from [71, 72, 73], the matrices  $U^0$  and  $U^{L,R}$  can be expressed in terms of  $Yv_\Phi$  and  $M$ . Thereby, by expanding  $U^0$  and  $U^{L,R}$  in powers of  $M^{-1}$  and keeping only the leading order terms, we get

$$U^0 \equiv \begin{pmatrix} U_{PMNS}^* & \frac{1}{2}v_\Phi Y^* M^{-1} \\ -\frac{1}{2}v_\Phi M^{-1} Y^T U_{PMNS}^* & 1 \end{pmatrix}, \quad (2.36)$$

$$U^L \equiv \begin{pmatrix} 1 & -\frac{\sqrt{3}}{2\sqrt{2}}v_\Phi Y M^{-1} \\ \frac{\sqrt{3}}{2\sqrt{2}}v_\Phi M^{-1} Y^\dagger & 1 \end{pmatrix}, \quad U^R \equiv \begin{pmatrix} 1 & 0 \\ 0 & 1 \end{pmatrix}. \quad (2.37)$$

Here,  $U_{PMNS}$  is a  $3 \times 3$  unitary matrix from Eq. (1.2) which diagonalizes the effective light neutrino mass matrix, and the nondiagonal entries are related to the sought couplings of heavy and light leptons, and are expressed in terms of the matrix-valued quantity

$$(V)_{l\Sigma} = \left( \frac{v_\Phi}{\sqrt{2}} Y M^{-1} \right)_{l\Sigma}. \quad (2.38)$$

Next, for simplicity, we suppress the indices indicating the mass-eigenstate fields. The Lagrangian in the mass-eigenstate basis, relevant for the decays of the heavy leptons, has the neutral current part

$$\begin{aligned} \mathcal{L}_{NCZ} &= \frac{g}{c_W} \left[ \bar{\nu} \left( \frac{1}{2\sqrt{2}} U_{PMNS}^\dagger V \gamma^\mu P_L - \frac{1}{2\sqrt{2}} U_{PMNS}^T V^* \gamma^\mu P_R \right) \Sigma^0 \right. \\ &\quad \left. + \bar{l}^c \left( \frac{\sqrt{3}}{4} V^* \gamma^\mu P_R \right) \Sigma^+ + \text{H.c.} \right] Z_\mu^0, \end{aligned} \quad (2.39)$$

and the charged current part

$$\begin{aligned} \mathcal{L}_{CC} &= g \left[ \bar{\nu} \left( -\sqrt{\frac{3}{2}} U_{PMNS}^\dagger V \gamma^\mu P_L + \frac{-\sqrt{3}}{2\sqrt{2}} U_{PMNS}^T V^* \gamma^\mu P_R \right) \Sigma^+ \right. \\ &\quad \left. + \bar{l} (-V \gamma^\mu P_L) \Sigma^0 \right. \\ &\quad \left. + \bar{l}^c \left( \sqrt{\frac{3}{2}} V^* \gamma^\mu P_R \right) \Sigma^{++} \right] W_\mu^- + \text{H.c.}, \end{aligned} \quad (2.40)$$

as given in Eqs. (B.22) and (B.23).

Let us start our list of the partial decay widths by the decays of neutral  $\Sigma^0$  state:

$$\begin{aligned} \Gamma(\Sigma^0 \rightarrow \ell^\mp W^\pm) &= \frac{g^2}{32\pi} |V_{\ell\Sigma}|^2 \frac{M_\Sigma^3}{M_W^2} \left( 1 - \frac{M_W^2}{M_\Sigma^2} \right)^2 \left( 1 + 2 \frac{M_W^2}{M_\Sigma^2} \right), \\ \sum_{m=1}^3 \Gamma(\Sigma^0 \rightarrow \nu_m Z^0) &= \frac{g^2}{32\pi c_W^2} \sum_{\ell=\{e,\mu,\tau\}} \frac{1}{4} |V_{\ell\Sigma}|^2 \frac{M_\Sigma^3}{M_Z^2} \left( 1 - \frac{M_Z^2}{M_\Sigma^2} \right)^2 \left( 1 + 2 \frac{M_Z^2}{M_\Sigma^2} \right). \end{aligned} \quad (2.41)$$

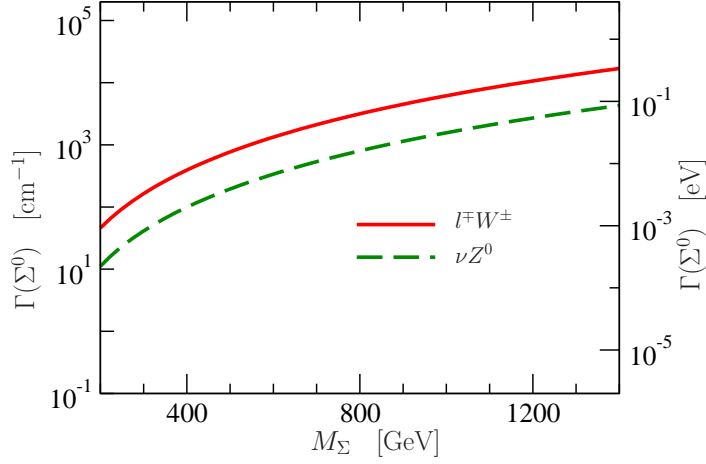


Figure 2.7: Partial decay widths of  $\Sigma^0$  quintuplet lepton for  $|V_{\ell\Sigma}| = 3.5 \cdot 10^{-7}$ , in dependence on heavy quintuplet mass  $M_\Sigma$ .

The positive singly-charged heavy lepton  $\Sigma^+$  has the following partial decay widths:

$$\begin{aligned} \Gamma(\Sigma^+ \rightarrow \ell^+ Z^0) &= \frac{g^2}{32\pi c_W^2} \frac{3}{16} |V_{\ell\Sigma}|^2 \frac{M_\Sigma^3}{M_Z^2} \left(1 - \frac{M_Z^2}{M_\Sigma^2}\right)^2 \left(1 + 2\frac{M_Z^2}{M_\Sigma^2}\right), \\ \sum_{m=1}^3 \Gamma(\Sigma^+ \rightarrow \nu_m W^+) &= \frac{g^2}{32\pi} \sum_{\ell=\{e,\mu,\tau\}} \frac{15}{8} |V_{\ell\Sigma}|^2 \frac{M_\Sigma^3}{M_W^2} \left(1 - \frac{M_W^2}{M_\Sigma^2}\right)^2 \left(1 + 2\frac{M_W^2}{M_\Sigma^2}\right). \end{aligned} \quad (2.42)$$

Finally, the doubly-charged  $\Sigma^{++}$  state decays exclusively via a charged current, with the partial decay width

$$\Gamma(\Sigma^{++} \rightarrow \ell^+ W^+) = \frac{g^2}{32\pi} \frac{3}{2} |V_{\ell\Sigma}|^2 \frac{M_\Sigma^3}{M_W^2} \left(1 - \frac{M_W^2}{M_\Sigma^2}\right)^2 \left(1 + 2\frac{M_W^2}{M_\Sigma^2}\right). \quad (2.43)$$

The mass difference induced by loops of SM gauge bosons between two components of  $\Sigma$  quintuplet with electric charges  $Q$  and  $Q'$  is explicitly cal-

culated in [56]

$$M_Q - M_{Q'} = \frac{\alpha_2 M_\Sigma}{4\pi} \left\{ (Q^2 - Q'^2) s_W^2 f\left(\frac{M_Z}{M_\Sigma}\right) + (Q - Q')(Q + Q' - Y) \left[ f\left(\frac{M_W}{M_\Sigma}\right) - f\left(\frac{M_Z}{M_\Sigma}\right) \right] \right\}, \quad (2.44)$$

$$f(r) = \frac{r}{2} \left[ 2r^3 \ln r - 2r + (r^2 - 4)^{1/2} (r^2 + 2) \ln \left( \frac{r^2 - 2 - r\sqrt{r^2 - 4}}{2} \right) \right].$$

The values for the mass splittings  $\Delta M_{ij} = M_i - M_j$  for  $M_\Sigma = 400$  GeV are

$$\Delta M_{21} \equiv M_{\Sigma^{++}} - M_{\Sigma^+} \simeq 490 \text{ MeV}, \quad \Delta M_{10} \equiv M_{\Sigma^+} - M_{\Sigma^0} \simeq 163 \text{ MeV}, \quad (2.45)$$

which opens additional decay channels, like  $\Sigma^{++} \rightarrow \pi^+ \Sigma^+$  and  $\Sigma^+ \rightarrow \pi^+ \Sigma^0$ .

The decay rate for a single pion finale state is given by

$$\Gamma(\Sigma^i \rightarrow \Sigma^j \pi^+) = (g^{W\Sigma})_{ij}^2 \frac{2}{\pi} G_F^2 |V_{ud}|^2 f_\pi^2 (\Delta M_{ij})^3 \sqrt{1 - \frac{m_\pi^2}{(\Delta M_{ij})^2}} \quad (2.46)$$

where  $(g^{W\Sigma})_{ij}^2$  is given in Eq. (2.32). These decays are suppressed by small mass differences.

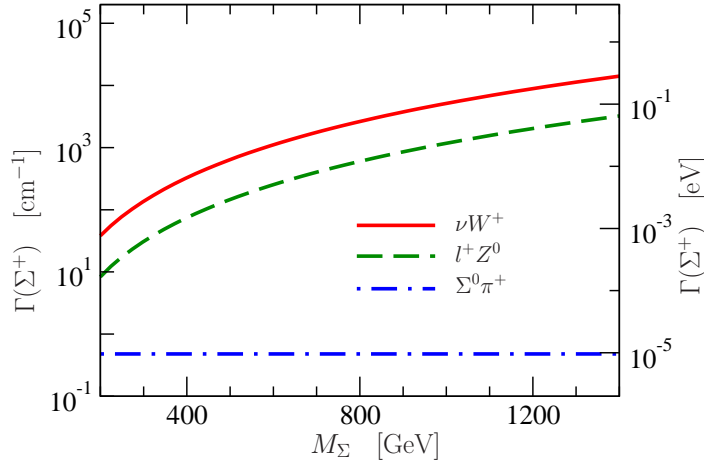


Figure 2.8: Partial decay widths of  $\Sigma^+$  quintuplet lepton for  $|V_{l\Sigma}| = 3.5 \cdot 10^{-7}$ , in dependence on heavy quintuplet mass  $M_\Sigma$ .

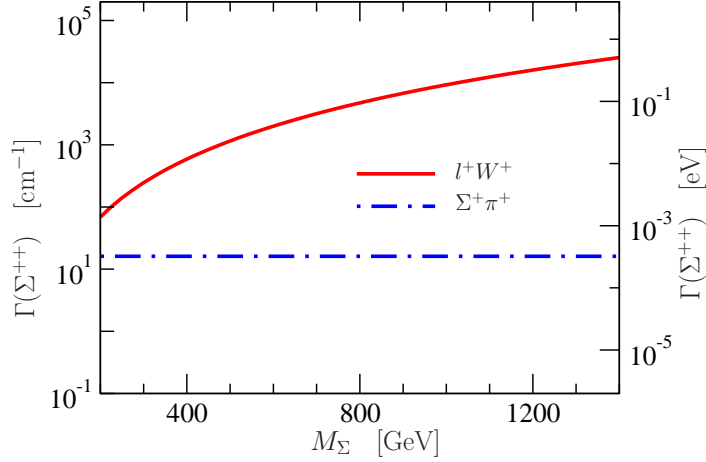


Figure 2.9: Partial decay widths of  $\Sigma^{++}$  quintuplet lepton for  $|V_{l\Sigma}| = 3.5 \cdot 10^{-7}$ , in dependence on heavy quintuplet mass  $M_\Sigma$ .

In Figs. 2.7, 2.8 and 2.9 we plot the partial widths of the decays of  $\Sigma^0$ ,  $\Sigma^+$  and  $\Sigma^{++}$  given in Eqs. (2.41), (2.42) and (2.43), respectively. Figures. 2.8 and 2.9 also show the pion final state decays from Eq. (2.46). We list the representative final states of these decays in Table 2.2, which includes same-sign dilepton events as distinguished signatures at the LHC.

|  | $\Sigma^{++} \rightarrow \ell^- W^-$<br>(0.66) | $\Sigma^+ \rightarrow \ell^- Z^0$<br>(0.06) | $\Sigma^0 \rightarrow \ell^+ W^-$<br>(0.30) | $\Sigma^0 \rightarrow \ell^- W^+$<br>(0.30) |
|--|--|---|---|---|
| $\Sigma^{++} \rightarrow \ell^+ W^+$<br>(0.66) | $\ell^+ \ell^- W^+ W^-$<br>(0.44)              | $\ell^+ \ell^- W^+ Z^0$<br>(0.04)           | -   | -   |
| $\Sigma^+ \rightarrow \ell^+ Z^0$<br>(0.06)    | $\ell^+ \ell^- Z^0 W^-$<br>(0.04)              | $\ell^+ \ell^- Z^0 Z^0$<br>(0.004)          | $\ell^+ \ell^+ Z^0 W^-$<br>(0.02)           | $\ell^+ \ell^- Z^0 W^+$<br>(0.02)           |
| $\Sigma^0 \rightarrow \ell^- W^+$<br>(0.30)    | -  | $\ell^- \ell^- W^+ Z^0$<br>(0.02)           | -   | -   |
| $\Sigma^0 \rightarrow \ell^+ W^-$<br>(0.30)    | -  | $\ell^+ \ell^- W^- Z^0$<br>(0.02)           | -   | -   |

Table 2.2: Decays of exotic leptons to SM charged leptons, including multi-lepton and same-sign dilepton events, together with their branching ratios (restricted to  $l = e, \mu$ ) and for  $M_\Sigma = 400$  GeV.

## § 2.6 Possible role as dark matter

The fermionic quintuplet of the present model was selected previously as a viable MDM candidate in [56]. To employ it as a seesaw mediator requires additional scalar multiplets, what makes the neutral component of the quintuplet unstable. If we employ a  $Z_2$  symmetry under which  $\Sigma \rightarrow -\Sigma$ ,  $\Phi \rightarrow -\Phi$  and all SM fields are unchanged, the lightest component of the  $\Sigma$  and  $\Phi$  multiplets is again a DM candidate. The quartic  $\lambda_5$  term in the scalar potential is still allowed so that neutrinos acquire radiatively generated masses given by Eq. (2.21).

If  $\Sigma^0$  is the DM particle, its mass is fixed by the relic abundance to the value  $M_\Sigma \approx 10$  TeV in [56]. The choice  $\lambda_5 = 10^{-7}$  gives enough suppression to have small neutrino masses with large Yukawa,  $Y \sim 0.1$ . In this part of the parameter space the model could have interesting LFV effects like in [62].

The neutral component of the scalar multiplet  $\Phi$  could also be a DM particle, despite its tree level coupling to the  $Z$  boson. Similar to the inert doublet model, the  $\lambda_5$  term in the scalar potential in Eq. (2.7) splits the real and imaginary parts of the  $\Phi^0$  field. If the mass splitting is large enough, the inelastic scattering through the  $Z$  boson exchange is kinematically forbidden in direct detection experiments. In this case the new states could be within reach of the LHC. To ensure a large enough mass splitting, the coupling  $\lambda_5$  cannot be too small. Accordingly, from Eq. (2.21), it follows that the Yukawa couplings have to be smaller, suppressing the LFV effects.

## § 2.7 Loop induced Higgs decays

The recently discovered resonance with mass  $m_h \simeq 125 - 126$  GeV [74, 75] strongly resembles the SM Higgs boson. There is a hint that the loop-induced  $h \rightarrow \gamma\gamma$  event rate [76, 77] deviates, modulo QCD uncertainties [78], by a factor 1.5 - 2 [79, 80] from its SM value,

$$\frac{[\sigma(gg \rightarrow h) \times \text{BR}(h \rightarrow \gamma\gamma)]_{\text{LHC}}}{[\sigma(gg \rightarrow h) \times \text{BR}(h \rightarrow \gamma\gamma)]_{\text{SM}}} = 1.71 \pm 0.33 . \quad (2.47)$$



This indicates the existence of additional charged particle(s) on which the tree-level Higgs decay modes are much less sensitive. The history of the “pre-discovery” of charmed and top quarks through the loop amplitudes may be repeated in the scalar sector.

On the other hand, if this enhancement in  $h \rightarrow \gamma\gamma$  disappears with a larger integrated luminosity, it will still constrain the parameter space of various extensions of the SM containing new charged states which should affect this loop amplitude. In this spirit there is a number of theoretical attempts to match the indicated discrepancy by the effects of an extended Higgs sector [81, 82, 83, 84].

Notable, the  $h \rightarrow \gamma\gamma$  decay rate is sensitive on the doubly charged scalar fields such as those existing in scalar triplet from the type II seesaw mechanism. These states have been in focus of both the direct searches at the LHC [85, 86, 87] and of theoretical investigations [88, 89, 90, 91, 92]. The effects of singly and doubly charged components of a scalar quadruplet  $\Phi \sim (1, 4, -1)$  [93] accompanying the Majorana quintuplet of the seesaw model at hand are presented in this section.

### 2.7.1 Exotic scalar couplings to Higgs boson

The mixing between singly charged and between neutral components of  $H$  and  $\Phi$  multiplets will occur after the EWSB and it is considered in Appendix A. Let us illustrate this on the  $h^0 - \varphi^0$  mass terms arising from the scalar potential from Eq. (2.7)

$$\begin{aligned} \mathcal{L}_{h^0\varphi^0} = & -\frac{1}{2} \left( -\mu_H^2 + 3\lambda_1 v_H^2 + \left( \frac{1}{2}\lambda_2 + \frac{1}{6}\lambda_3 - \frac{2}{3}\lambda_5 \right) v_\Phi^2 + \sqrt{3}\lambda_4 v_H v_\Phi \right) h^0 h^0 \\ & - \left( \left( \lambda_2 + \frac{1}{3}\lambda_3 - \frac{4}{3}\lambda_5 \right) v_H v_\Phi + \frac{\sqrt{3}}{2}\lambda_4 v_H^2 - \frac{1}{\sqrt{3}}\lambda_6 v_\Phi^2 \right) h^0 \varphi^0 \\ & - \frac{1}{2} \left( \mu_\Phi^2 + \left( \frac{1}{2}\lambda_2 + \frac{1}{6}\lambda_3 - \frac{2}{3}\lambda_5 \right) v_H^2 + \frac{2}{\sqrt{3}}\lambda_6 v_H v_\Phi + \left( 3\lambda_7 + \frac{5}{3}\lambda_8 \right) v_\Phi^2 \right) \varphi^0 \varphi^0 . \end{aligned} \quad (2.48)$$

The mass term that mixes  $h^0$  and  $\varphi^0$  is small because it is proportional either to  $v_\Phi$  from  $\lambda_{2,3,6}$  terms in Eq. (2.7), or to small lepton number violating

couplings  $\lambda_{4,5}$  dictated to be small from considerations of neutrino masses. Therefore we neglect the mixing between the components of  $H$  and  $\Phi$  multiplets and we neglect the terms of higher order in  $v_\Phi/v_H$  whenever possible.

In the approximations given above, the masses of charged components of the quadruplet  $\Phi$  are

$$\begin{aligned} m^2(\Phi^+) &= \mu_\Phi^2 + \frac{1}{2}\lambda_2 v_H^2, \\ m^2(\Phi^-) &= \mu_\Phi^2 + \frac{1}{2}\lambda_2 v_H^2 + \frac{1}{3}\lambda_3 v_H^2, \\ m^2(\Phi^{--}) &= \mu_\Phi^2 + \frac{1}{2}\lambda_2 v_H^2 + \frac{1}{2}\lambda_3 v_H^2. \end{aligned} \quad (2.49)$$

Their couplings to the Higgs boson relevant for the  $h \rightarrow \gamma\gamma$  decay are

$$-\mathcal{L} = c_{\Phi^+} v_H h^0 \Phi^{+*} \Phi^+ + c_{\Phi^-} v_H h^0 \Phi^{-*} \Phi^- + c_{\Phi^{--}} v_H h^0 \Phi^{--*} \Phi^{--}, \quad (2.50)$$

where the newly introduced couplings

$$c_{\Phi^+} = \lambda_2, \quad c_{\Phi^-} = \lambda_2 + \frac{2}{3}\lambda_3, \quad c_{\Phi^{--}} = \lambda_2 + \lambda_3, \quad (2.51)$$

are expressed in terms of the quartic couplings  $\lambda_2$  and  $\lambda_3$  which, for simplicity, we assume to be equal in the following.

### 2.7.2 Higgs diphoton-decay width

In the model presented here, in addition to the dominant SM contributions from the  $W$  boson and top quark loops to the  $h \rightarrow \gamma\gamma$  decay rate only the charged scalars contribute substantially. They are colourless so that the Higgs boson production through gluon fusion at the LHC is unaffected. Also, since the Higgs boson total decay width is only marginally affected, a dominant change in  $h \rightarrow \gamma\gamma$  event rate comes from the change in Higgs boson diphoton partial decay width.

The analytic expression for the diphoton  $h \rightarrow \gamma\gamma$  partial width reads [81, 94, 95, 96]

$$\Gamma(h \rightarrow \gamma\gamma) = \frac{\alpha^2 m_h^3}{256\pi^3 v_H^2} \left| A_1(\tau_W) + N_c Q_t^2 A_{1/2}(\tau_t) + N_{c,S} Q_S^2 \frac{c_S}{2} \frac{v_H^2}{m_S^2} A_0(\tau_S) \right|^2, \quad (2.52)$$

where the three contributions corresponding to  $\tau_i \equiv 4m_i^2/m_h^2$  ( $i = W, t, S$ ) refer to spin-1 ( $W$  boson), spin-1/2 (top quark) and charged spin-0 particles in the loop. The electric charges for fermions and scalars,  $Q_t = +2/3$  and  $Q_S$ , are given in units of  $|e|$ , and their respective number of colors are  $N_c = 3$  and  $N_{c,S} = 1$  for color singlet scalars under consideration here. The loop functions for spin-1, spin-1/2, and spin-0 particles are given as

$$A_1(x) = -x^2 [2x^{-2} + 3x^{-1} + 3(2x^{-1} - 1)f(x^{-1})], \quad (2.53)$$

$$A_{1/2}(x) = 2x^2 [x^{-1} + (x^{-1} - 1)f(x^{-1})], \quad (2.54)$$

$$A_0(x) = -x^2 [x^{-1} - f(x^{-1})], \quad (2.55)$$

where, for a Higgs mass below the kinematic threshold of the loop particle  $m_h < 2 m_{\text{loop}}$ , we have

$$f(x) = \arcsin^2 \sqrt{x}. \quad (2.56)$$

We now look at the possible enhancement of the  $h \rightarrow \gamma\gamma$  decay rate through extra contributions with charged components of scalar quadruplet  $\Phi$  running in the loops. Following [81] we define the enhancement factor with respect to the SM decay width

$$R_{\gamma\gamma} = \left| 1 + \sum_{S=\Phi^+, \Phi^-, \Phi^{--}} Q_S^2 \frac{c_S}{2} \frac{v_H^2}{m_S^2} \frac{A_0(\tau_S)}{A_1(\tau_W) + N_c Q_t^2 A_{1/2}(\tau_t)} \right|^2. \quad (2.57)$$

In order to get an enhancement of the  $h \rightarrow \gamma\gamma$  decay rate, the contribution of the new charged scalars has to interfere constructively with the dominant SM contribution of the  $W$  boson. Since this requires negative couplings  $c_S$  in Eq. (2.52), we assume  $\lambda_{2,3} < 0$ . The biggest effect on the  $h \rightarrow \gamma\gamma$  decay rate comes from  $\Phi^{--}$  for two reasons. First, it has a charge  $|Q_{\Phi^{--}}| = 2$  and second, for  $\lambda_3 < 0$  it is the lightest of the charged  $\Phi$  components. We will not consider  $\lambda_{2,3} > 0$  case for which to get a significant enhancement in  $R_{\gamma\gamma}$

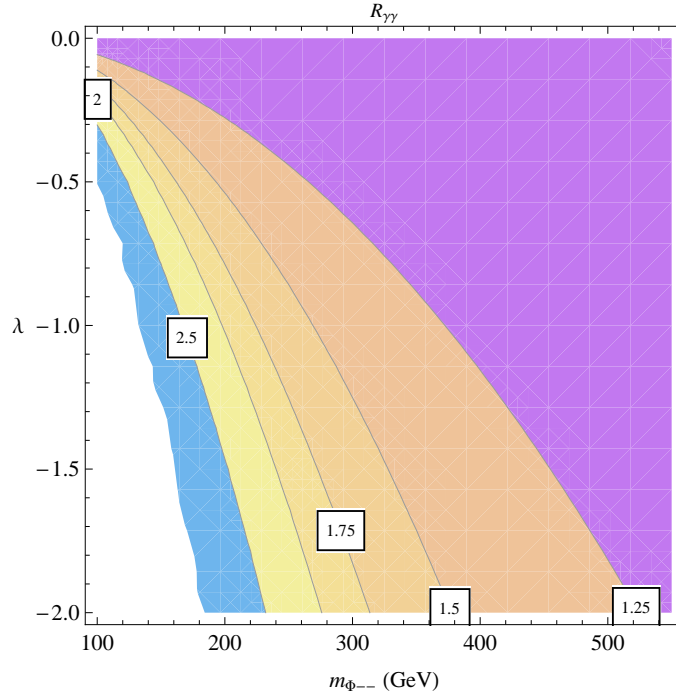


Figure 2.10: Enhancement factor  $R_{\gamma\gamma} = (2.5, 2, 1.75, 1.5, 1.25)$  for the  $h \rightarrow \gamma\gamma$  branching ratio in dependence on scalar coupling  $\lambda = \lambda_2 = \lambda_3$  and the mass of the lightest charged component of the  $\Phi$  multiplet,  $m(\Phi^{--})$ .

the charged scalars should be too light or the couplings should be big.

On Fig. 2.10 we plot the enhancement factor  $R_{\gamma\gamma}$  as a function of the scalar couplings  $\lambda_{2,3}$  and the mass of the lightest charged scalar  $m(\Phi^{--})$ . For simplicity we assume  $\lambda_2 = \lambda_3 = \lambda$ , and in order to keep the stability of the scalar potential, we restrict ourselves to the interval  $\lambda \in [-2, 0]$ . In this interval the value  $R_{\gamma\gamma} = 2$  can be achieved up to  $m(\Phi^{--}) = 280$  GeV and the value  $R_{\gamma\gamma} = 1.25$  up to  $m(\Phi^{--}) = 520$  GeV.

### 2.7.3 Higgs to Z-photon decay width

Another loop mediated Higgs decay sensitive to new charged particles is  $h \rightarrow Z\gamma$ . It is sensitive both on the charge and weak isospin of the particles in the loop. After adding a contribution of a new scalar to the SM contributions

from the  $W$  boson and top quark the decay rate is given by [81]

$$\Gamma(h \rightarrow Z\gamma) = \frac{\alpha^2 m_h^3}{128\pi^3 v_H^2 \sin^2 \theta_w} \left(1 - \frac{m_Z^2}{m_h^2}\right)^3 |\mathcal{A}_{SM} + \mathcal{A}_S|^2, \quad (2.58)$$

where

$$\mathcal{A}_{SM} = \cos \theta_w A_1(\tau_W, \sigma_W) + N_c \frac{Q_t(2T_3^{(t)} - 4Q_t \sin^2 \theta_w)}{\cos \theta_w} A_{1/2}(\tau_t, \sigma_t), \quad (2.59)$$

$$\mathcal{A}_S = \frac{v_H \sin \theta_w}{2} \frac{c_S v_H}{m_S^2} Q_S \frac{T_3^{(S)} - Q_S \sin^2 \theta_w}{\cos \theta_w \sin \theta_w} A_0(\tau_S, \sigma_S). \quad (2.60)$$

Here  $\sigma_i = 4m_i^2/m_Z^2$  and  $T_3^{(t)} = 1/2$  and  $T_3^{(S)}$  correspond to the weak isospin of the top quark and the new scalar. The loop functions are given by

$$\begin{aligned} A_1(x, y) &= 4(3 - \tan^2 \theta_w) I_2(x, y) + [(1 + 2x^{-1}) \tan^2 \theta_w - (5 + 2x^{-1})] I_1(x, y), \\ A_{1/2}(x, y) &= I_1(x, y) - I_2(x, y), \\ A_0(x, y) &= I_1(x, y), \end{aligned} \quad (2.61)$$

where

$$\begin{aligned} I_1(x, y) &= \frac{xy}{2(x-y)} + \frac{x^2 y^2}{2(x-y)^2} [f(x^{-1}) - f(y^{-1})] + \frac{x^2 y}{(x-y)^2} [g(x^{-1}) - g(y^{-1})], \\ I_2(x, y) &= -\frac{xy}{2(x-y)} [f(x^{-1}) - f(y^{-1})]. \end{aligned} \quad (2.62)$$

For the Higgs mass below the kinematic threshold of the loop particle,  $m_h < 2 m_{\text{loop}}$ , we have

$$g(x) = \sqrt{x^{-1} - 1} \arcsin \sqrt{x}. \quad (2.63)$$

The additional contributions in a model with scalar quadruplet lead to the modification factor  $R_{Z\gamma}$  for the  $h \rightarrow Z\gamma$  decay rate with respect to the SM decay width

$$R_{Z\gamma} = \left| 1 + \sum_{S=\Phi^+, \Phi^-, \Phi^{--}} \frac{\mathcal{A}_S}{\mathcal{A}_{SM}} \right|^2. \quad (2.64)$$

On Fig. 2.11 we plot the modification factor  $R_{Z\gamma}$  as a function of the scalar couplings  $\lambda_{2,3}$  (assuming  $\lambda_2 = \lambda_3 = \lambda$ ) and the mass of the lightest

charged scalar  $m(\Phi^{--})$ . We obtain a moderate suppression of the  $h \rightarrow Z\gamma$  decay rate in the region of the parameter space where the  $h \rightarrow \gamma\gamma$  decay rate is enhanced. In the chosen interval  $\lambda \in [-2, 0]$  the factor  $R_{Z\gamma} = 0.6$  is achieved up to  $m(\Phi^{--}) = 220$  GeV and  $R_{Z\gamma} = 0.9$  up to  $m(\Phi^{--}) = 480$  GeV.

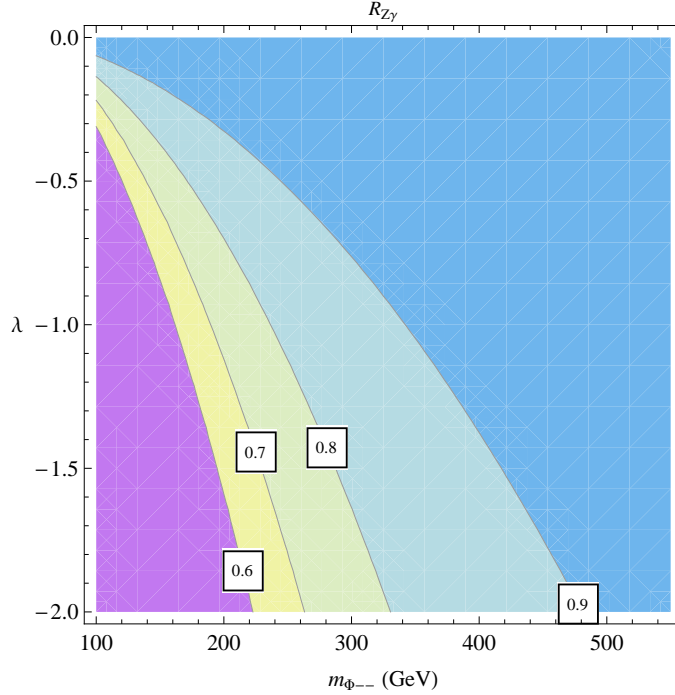


Figure 2.11: Modification factor  $R_{Z\gamma}=(0.6, 0.7, 0.8, 0.9)$  for the  $h \rightarrow Z\gamma$  branching ratio in dependence on the scalar coupling  $\lambda = \lambda_2 = \lambda_3$  and the mass of the lightest charged component of the  $\Phi$  multiplet,  $m(\Phi^{--})$ .

## § 2.8 Direct and indirect bounds on new scalars

The measurement of the  $h \rightarrow \gamma\gamma$  rare decay mode may mark a spectacular onset of a virtual physics at the LHC. The interaction with virtual particles is essential both for the production and the decay factor in Eq. (2.47). It is in order to discuss the features of additional charged scalars, which determine their possible appearance both in the Higgs boson loop decays under

consideration and in their direct searches.

Now, an essential point is a lack of Yukawa couplings of the scalar quadruplet to a pair of SM fermions. The lack of these Yukawa couplings means that a doubly charged  $\Phi^{--}$  does not decay to a pair of charged SM leptons, which has decisive repercussions. The direct searches for doubly charged scalars through resonance in the invariant mass of a pair of charged leptons at the LHC [85, 86] leave the quadruplet scalar states unconstrained. The strongest bound in the range (383 GeV, 408 GeV) set in the inclusive search for the CMS benchmark points depends on  $\Phi^{--}$  production analysis, and counts all possible final state lepton pairs in  $\text{BR}(\Phi^{--} \rightarrow l_i^- l_j^-)$ ,  $i, j = e, \mu, \tau$ . Of course,  $\Phi^{--}$  can decay also to  $W^- W^-$  final state, but this channel has not been measured yet and doesn't constrain the quadruplet scalar mass.

In comparison, the studies of  $h \rightarrow \gamma\gamma$  enhancement by the doubly charged scalar from the scalar triplet from the type II seesaw mechanism [88, 89, 90, 91] also lead to their rather small masses, which already seem to be excluded by the above mentioned direct searches at the LHC [85, 86]. In case that the decay of the doubly-charged component of the triplet scalar to  $W^- W^-$  were the dominant one, it would invalidate the discussed CMS search and no limit on the triplet mass would be placed either.

## § 2.9 Testability at the LHC

Newly introduced heavy degrees of freedom are expected to be abundantly produced at the LHC, and the distinctive signatures could come from doubly-charged components of the fermionic quintuplets. For already accumulated integrated luminosity at the LHC,  $5 \text{ fb}^{-1}$  in 2011 run and  $21 \text{ fb}^{-1}$  in 2012 run, there could be  $\sim 3000$  produced doubly-charged  $\Sigma^{++}$  or  $\bar{\Sigma}^{++}$  fermions, with mass  $M_\Sigma = 400 \text{ GeV}$ .

The decays of these states to SM charged leptons have an interesting multilepton signature. There are, in addition, same-sign dilepton events displayed in Table 2.2. These events have a negligible SM background, as demonstrated [97, 98, 99, 100] in generic new physics scenario with lepton number violation. In particular, the detailed studies of fermionic triplets from type III seesaw scenario [73, 97, 98] apply to our case of fermionic quintuplets.

The signals which are good for the discovery correspond to a relatively high signal rate and small SM background, which is calculated by MadGraph [101]. In order to compare the signal and SM background cross sections, we assume a particular choice of parameters leading to the branching ratios given in Table 2.2, restricted to  $l = e, \mu$  leptons in the final states. In this respect we distinguish four classes of events containing  $\Sigma^+$  decaying to  $e^+$  or  $\mu^+$  lepton and  $Z^0 \rightarrow (\ell^+\ell^-, q\bar{q})$  resonance to help in  $\Sigma^+$  identification:

$$(i) \quad pp \rightarrow \Sigma^+ \overline{\Sigma^+} \rightarrow (\ell^+ Z^0) (\ell^- Z^0),$$

which has too small cross section of 0.03 fb with respect to the SM background of 0.6 fb at 7 TeV LHC;

$$(ii) \quad pp \rightarrow \Sigma^+ \overline{\Sigma^0} \rightarrow (\ell^+ Z^0) (\ell^- W^+),$$

which has a cross section of 0.7 fb, comparable to the SM background of 0.8 fb;

$$(iii) \quad pp \rightarrow \Sigma^+ \overline{\Sigma^0} \rightarrow (\ell^+ Z^0) (\ell^+ W^-),$$

the LNV event having 0.7 fb with the same-sign dilepton state, which is nonexistent in the SM and thus devoid of the SM background;

$$(iv) \quad pp \rightarrow \Sigma^{++} \overline{\Sigma^+} \rightarrow (\ell^+ W^+) (\ell^- Z^0),$$

having relatively high signal rate of 1.1 fb with respect to the SM background of 0.8 fb. The classes (iii) and (iv) lead to signals elaborately detailed in [73, 97, 98].





# Chapter 3

## Model with Dirac lepton quintuplet

The heaviness of the top quark and the lightness of the Higgs boson have been the landmarks for several extensions of the SM which rely on vectorlike rather than on sequential fourth generation fermions. Such a line of research has been followed in the examination [102] of the vectorlike top quark partner, which by a sort of Dirac seesaw mechanism increases the mass of the top quark [103].

By generalizing this idea from the quark sector to the leptons, it is worth to explore a possible role of TeV-scale vectorlike Dirac fermions as seesaw mediators. By relying only on the **gauge symmetry** and the **renormalizability** of the SM, novel seesaw mechanism supported by non-zero hypercharge fermions in higher isomultiplets is found. Under these conditions there are only two options for seesaw mediators, the triplet fermions introduced in [61] and the quintuplet fermions proposed in [104], on which we focus in this chapter.

In order to generate a tree-level seesaw diagram the hypercharge non-zero Dirac leptons have to be in conjunction with appropriate new scalar fields. Let us first systemize all possible realizations of such tree-level mechanism and then focus to dimension-nine model with Dirac lepton quintuplet  $\Sigma_{L,R} \sim (1, 5, 2)$ . This model generates neutrino masses both at the tree-level and at the loop level. Finally we investigate the phenomenology of new Dirac-type heavy lepton quintuplet at the LHC.

### § 3.1 Dirac vectorlike multiplets in seesaw mechanism

In order to add something new to already existing tree-level seesaw mechanisms, we employ vectorlike fermionic multiplets with non-zero hypercharge. In contrast to chiral SM fermions, the masses of such vectorlike fermions are not restricted to the electroweak scale, so that they can be naturally adjusted to the new physics scale. In order to produce a tree-level seesaw, the newly introduced fermion multiplets have to have a neutral component which will mix with light neutrinos. Accompanying new scalar multiplets also have to have a neutral component which could acquire a vev. Their weak isospin can not be higher than three half, in order that they couple linearly with the Higgs doublet and develop an induced vev after the spontaneous symmetry breaking of the SM gauge group. This will lead to tree-level neutrino masses from higher dimensional operators.

The effective operators of the form  $(LLHH)(H^\dagger H)^n$ , leading to neutrino masses, have already been studied in [105, 106] and more recently in [107], where it has been pointed out that the mass operator at each higher dimension is unique, independent of the mechanism leading to it. Since the sought-after dimension-nine operator can be relevant only in the absence of possible dimension-five operator, we forbid the appearance of the states which generate conventional seesaw mechanisms. In first place, we should avoid a scalar triplet  $\Delta \sim (1, 3, 2)$  generating type II seesaw, and a fermion singlet  $N_R \sim (1, 1, 0)$  or triplet  $N_R \sim (1, 3, 0)$  generating type I and III seesaw, respectively. Note that type I, II, and III mechanisms correspond to single appearance of exotic (EX) scalar/fermion particles in the Yukawa term

$$L_Y^{single} \sim (\text{SM} - \text{fermion})(\text{SM} - \text{scalar/fermion})(\text{EX} - \text{fermion/scalar}). \quad (3.1)$$

The study of exotic triplets in [108, 109] also restricts to such minimal Yukawa terms. We go beyond them to new Yukawa terms with double appearance of exotic particles,

$$L_Y^{conjunction} \sim (\text{SM} - \text{fermion})(\text{EX} - \text{scalar})(\text{EX} - \text{fermion}), \quad (3.2)$$

where a conjunct exotic scalar-fermion pair can lead to the neutrino mass operators of dimension larger than five, as shown in Table 3.1.

| Seesaw Type       | Exotic Fermion        | Exotic Scalar                   | Scalar Coupling              | $m_\nu$ at   |
|-------------------|-----------------------|---------------------------------|------------------------------|--------------|
| Type I            | $N_R \sim (1, 0)$     | -                               | -                            | dim 5        |
| Type II           | -                     | $\Delta \sim (3, 2)$            | $\mu\Delta HH$               | dim 5        |
| Type III          | $N_R \sim (3, 0)$     | -                               | -                            | dim 5        |
| Conjunct Mediator | Exotic Fermion Pair   | Exotic Scalars $\Phi_1, \Phi_2$ | Scalar - Higgs Couplings     | $m_\nu$ at   |
| doublet           | $\Sigma_{L,R} (2, 1)$ | $(3, -2), (3, 0)$               | $\mu_{1,2}\Phi_{1,2}HH$      | dim 5        |
| <b>triplet</b>    | $\Sigma_{L,R} (3, 2)$ | $(4, -3), (2, -1)$              | $\lambda_1\Phi_1HHH$         | <b>dim 7</b> |
| quadruplet        | $\Sigma_{L,R} (4, 1)$ | $(3, -2), (3, 0)$               | $\mu_{1,2}\Phi_{1,2}HH$      | dim 5        |
| <b>quintuplet</b> | $\Sigma_{L,R} (5, 2)$ | $(4, -3), (4, -1)$              | $\lambda_{1,2}\Phi_{1,2}HHH$ | <b>dim 9</b> |

Table 3.1: The assignments of electroweak charges for exotic particles leading to the tree-level seesaw operator up to dimension nine.

To obtain the gauge invariant interaction in Eq. (3.2), the conjunct EX scalar-fermion pair should form an object with the weak isospin half and the hypercharge one. One possible way to achieve this is shown in the doublet and quadruplet ‘‘Seesaw Type’’ rows in Table 3.1, where new fermion fields of isospin one half (doublet) or three half (quadruplet) hold together with a scalar of isospin one (triplet). However the latter appears already in type II seesaw and would lead to dimension-five operator for neutrino masses. Then we are left with new fermion fields which should be of either isospin one (**triplet**) or isospin two (**quintuplet**). Whereas the first option corresponds to dimension-seven operator introduced in [61], we adopt the latter case corresponding to dimension-nine operator which might be more accessible for tests at the LHC.

## § 3.2 The model

The model pursued here starts from three generations of SM model leptons  $L_L$  and  $l_R$  and adds to them  $n_\Sigma$  isospin  $T = 2$  vectorlike quintuplets of leptons with hypercharge two, where both left and right components transform as

$(1, 5, 2)$  under the SM gauge group,

$$\Sigma_{L,R} = \begin{pmatrix} \Sigma^{+++} \\ \Sigma^{++} \\ \Sigma^+ \\ \Sigma^0 \\ \Sigma^- \end{pmatrix}_{L,R} \sim (1, 5, 2) . \quad (3.3)$$

Besides the SM Higgs doublet  $H$ , there are two additional scalar quadruplets  $\Phi_1$  and  $\Phi_2$  transforming as  $(1, 4, -3)$  and  $(1, 4, -1)$ , respectively:

$$\Phi_1 = \begin{pmatrix} \phi_1^0 \\ \phi_1^- \\ \phi_1^{--} \\ \phi_1^{---} \end{pmatrix} \sim (4, -3), \quad \Phi_2 = \begin{pmatrix} \phi_2^+ \\ \phi_2^0 \\ \phi_2^- \\ \phi_2^{--} \end{pmatrix} \sim (4, -1). \quad (3.4)$$

For this choice of EX fields the conjunct Yukawa interaction in Eq. (3.2) is explicated by the second row in the following gauge invariant Lagrangian:

$$\begin{aligned} \mathcal{L} &= \overline{\Sigma}_L i \not{D} \Sigma_L + \overline{\Sigma}_R i \not{D} \Sigma_R - \overline{\Sigma}_R M_\Sigma \Sigma_L - \overline{\Sigma}_L M_\Sigma^\dagger \Sigma_R \\ &+ \left( \overline{\Sigma}_R Y_1 L_L \Phi_1^* + \overline{(\Sigma_L)^c} Y_2 L_L \Phi_2 + \text{H.c.} \right) . \end{aligned} \quad (3.5)$$

This contains the bare Dirac mass terms for the introduced vectorlike lepton quintuplet fields

$$\begin{aligned} -\mathcal{L}_D &= \overline{\Sigma}_R^{+++} M_\Sigma \Sigma_L^{+++} + \overline{\Sigma}_R^{++} M_\Sigma \Sigma_L^{++} \\ &+ \overline{\Sigma}_R^+ M_\Sigma \Sigma_L^+ + \overline{\Sigma}_R^0 M_\Sigma \Sigma_L^0 + \overline{\Sigma}_R^- M_\Sigma \Sigma_L^- + \text{H.c.} . \end{aligned} \quad (3.6)$$

Turning to the scalar potential, we restrict ourselves only to renormalizable terms relevant for our mechanism:

$$\begin{aligned} V(H, \Phi_1, \Phi_2) &\sim -\mu_H^2 H^\dagger H + \mu_{\Phi_1}^2 \Phi_1^\dagger \Phi_1 + \mu_{\Phi_2}^2 \Phi_2^\dagger \Phi_2 + \lambda_H (H^\dagger H)^2 \\ &+ \{ \lambda_1 \Phi_1^* H^* H^* H^* + \text{H.c.} \} + \{ \lambda_2 \Phi_2^* H H^* H^* + \text{H.c.} \} \\ &+ \{ \lambda_3 \Phi_1^* \Phi_2 H^* H^* + \text{H.c.} \} . \end{aligned} \quad (3.7)$$

The electroweak symmetry breaking proceeds in the usual way from the vev  $v_H = 246$  GeV of the Higgs doublet. On the other hand, the electroweak  $\rho$  parameter dictates the vevs  $v_{\Phi_1}$  and  $v_{\Phi_2}$  to be small, implying  $\mu_{\Phi_1}^2, \mu_{\Phi_2}^2 > 0$ .

However, the  $\lambda_1$  and  $\lambda_2$  terms in Eq. (3.7) result in the induced vevs for the scalar quadruplets,

$$v_{\Phi_1} \simeq -\lambda_1 \frac{v_H^3}{\mu_{\Phi_1}^2}, \quad v_{\Phi_2} \simeq -\lambda_2 \frac{v_H^3}{\mu_{\Phi_2}^2}. \quad (3.8)$$

The non-vanishing vevs in Eq. (3.8) change the electroweak  $\rho$  parameter to  $\rho(\Phi_1) \simeq 1 - 12v_{\Phi_1}^2/v_H^2$  and  $\rho(\Phi_2) \simeq 1 + 12v_{\Phi_2}^2/v_H^2$ , respectively. If these vevs are taken separately, the experimental value  $\rho = 1.0004_{-0.0004}^{+0.0003}$  [66] leads to the upper bounds  $v_{\Phi_1} \leq 1.4$  GeV and  $v_{\Phi_2} \leq 2.2$  GeV, respectively. Thus, the value of a few GeV can be considered as an upper bound on both  $v_{\Phi_1}$  and  $v_{\Phi_2}$  if there is no fine-tuning between them.

### § 3.3 Neutrino masses

Due to the induced vevs,  $v_{\Phi_1}$  and  $v_{\Phi_2}$  the Yukawa terms in Eq. (3.5) lead to the mass terms connecting the SM lepton doublet with new Dirac quintuplet lepton. Thereby, the triply and doubly charged states do not mix with SM leptons whereas the singly-charged and neutral states have peculiar mixing with SM leptons which we present in detail in Appendix C.

When extracting the mass matrices produced by the mass and Yukawa terms we suppress the generation indices of the fields. Three neutral left-handed fields  $\nu_L$ ,  $\Sigma_L^0$  and  $(\Sigma_R^0)^c$  span the symmetric neutral mass matrix as follows:

$$\mathcal{L}_{\nu\Sigma^0} = -\frac{1}{2} \left( \overline{(\nu_L)^c} \overline{(\Sigma_L^0)^c} \overline{\Sigma_R^0} \right) \begin{pmatrix} 0 & m_2^T & m_1^T \\ m_2 & 0 & M_\Sigma^T \\ m_1 & M_\Sigma & 0 \end{pmatrix} \begin{pmatrix} \nu_L \\ \Sigma_L^0 \\ (\Sigma_R^0)^c \end{pmatrix} + \text{H.c.} \quad (3.9)$$

For singly-charged fermions we arrive at the nonsymmetric mass matrix which explicates the mixing between the SM leptons and new singly-charged states

$$\mathcal{L}_{l\Sigma} = - \left( \overline{l_R} \overline{\Sigma_R^-} \overline{(\Sigma_L^+)^c} \right) \begin{pmatrix} m_l & 0 & 0 \\ m_3 & M_\Sigma & 0 \\ m_4 & 0 & M_\Sigma^T \end{pmatrix} \begin{pmatrix} l_L \\ \Sigma_L^- \\ (\Sigma_R^+)^c \end{pmatrix} + \text{H.c.} \quad (3.10)$$

Here  $M_\Sigma$  is given in Eq. (3.6), while  $m_1$  and  $m_2$  entries in the neutral sector in Eq. (3.9) and  $m_3$  and  $m_4$  in the charged sector in Eq. (3.10) come from the respective terms in Eq. (3.5):

$$\begin{aligned} m_1 &= \sqrt{\frac{1}{10}} Y_1 v_{\Phi_1}^* , & m_2 &= -\sqrt{\frac{3}{20}} Y_2 v_{\Phi_2} , \\ m_3 &= \sqrt{\frac{2}{5}} Y_1 v_{\Phi_1}^* , & m_4 &= \sqrt{\frac{1}{10}} Y_2 v_{\Phi_2} . \end{aligned} \quad (3.11)$$

Accordingly, the masses  $m_i$  ( $i = 1, 2, 3, 4$ ) are determined by the vev  $v_{\Phi_1}$  and vev  $v_{\Phi_2}$  of the neutral components of the scalar quadruplets, whereas  $M_\Sigma$  is on the new physics scale which is larger than the electroweak scale.

The diagonalization of the mass matrices proceeds by unitary transformations presented in Appendix C, following a procedure developed in [72]. Thereby, we write the leading order expressions up to  $M_\Sigma^{-2}$  in the basis in which the matrices  $m_l$  and  $M_\Sigma$  are already diagonalized. Block diagonalization of the neutral mass matrix in Eq. (3.9) gives to this order

$$\tilde{m}_\nu \simeq -m_2^T M_\Sigma^{-1} m_1 - m_1^T M_\Sigma^{-1} m_2 , \quad (3.12)$$

where a familiar unitary  $U_{PMNS}$  matrix diagonalizes the obtained effective light neutrino mass matrix:

$$U_{PMNS}^T \tilde{m}_\nu U_{PMNS} = m_\nu . \quad (3.13)$$

The same formalism has been applied in [73, 110] and the results in our Appendix C agree with theirs, when taking the appropriate limits.

By merging Eqs. (3.11), (3.12) and (3.8) we obtain for the light neutrino mass

$$m_\nu^{tree} \sim \frac{Y_1 Y_2 \lambda_1 \lambda_2 v_H^6}{M_\Sigma \mu_{\Phi_1}^2 \mu_{\Phi_2}^2} , \quad (3.14)$$

which reflects the fact that it is generated by an effective dimension-nine operator corresponding to the tree-level seesaw mechanism displayed on Fig.(3.1)

Neutrino masses in this model can also arise from dimension-five operator generated at the one loop level by the quartic coupling  $\lambda_3$  in Eq. (3.7). It gives a contribution to the neutrino masses

$$m_\nu^{loop} \sim \frac{Y_1 Y_2 \lambda_3 v_H^2}{16\pi^2 M_\Sigma} . \quad (3.15)$$

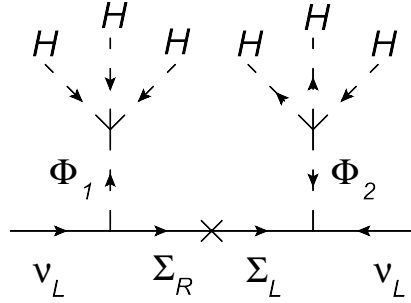


Figure 3.1: Tree-level diagram corresponding to dimension-nine operator in Eq. (3.14). The fermion line flow indicates a Dirac nature of the seesaw mediator.

As explained in [104], there is a restricted range of the parameter space where the dimension-five loop-level contribution shown on Fig. 3.2 is smaller than the dimension-nine tree-level contribution shown on Fig. 3.1. With an extra assumption on the scalar field coupling strengths,  $\lambda_3 \simeq \lambda_1 \cdot \lambda_2$ , the dimension-nine mechanism turns out to be the leading one for the mass scale of the new states  $\Lambda_{NP} \sim \text{few } 100 \text{ GeV}$ .

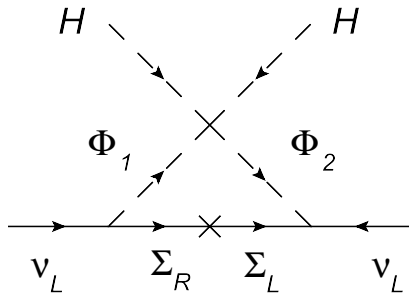


Figure 3.2: Dimension-five operator arising from the one-loop seesaw diagram given by the  $\lambda_3$  coupling from Eq. (3.7).



## § 3.4 Production of Dirac quintuplet leptons at the LHC

The production channels of the heavy quintuplet leptons in proton-proton collisions are dominated by the quark-antiquark annihilation via neutral and charged gauge bosons

$$q + \bar{q} \rightarrow A \rightarrow \Sigma + \bar{\Sigma}, \quad A = \gamma, Z, W^\pm,$$

where the gauge Lagrangian relevant for the production

$$\begin{aligned} \mathcal{L}_{gauge}^{\Sigma\bar{\Sigma}} = & + e(3\bar{\Sigma}^{++++}\gamma^\mu\Sigma^{++++} + 2\bar{\Sigma}^{++}\gamma^\mu\Sigma^{++} + \bar{\Sigma}^+\gamma^\mu\Sigma^+ - \bar{\Sigma}^-\gamma^\mu\Sigma^-)A_\mu \\ & + \frac{g}{c_W}((2 - 3s_W^2)\bar{\Sigma}^{++++}\gamma^\mu\Sigma^{++++} + (1 - 2s_W^2)\bar{\Sigma}^{++}\gamma^\mu\Sigma^{++})Z_\mu \\ & + \frac{g}{c_W}((-s_W^2)\bar{\Sigma}^+\gamma^\mu\Sigma^+ + (-1)\bar{\Sigma}^0\gamma^\mu\Sigma^0 + (-2 + s_W^2)\bar{\Sigma}^-\gamma^\mu\Sigma^-)Z_\mu \\ & + g(\sqrt{2}\bar{\Sigma}^{++}\gamma^\mu\Sigma^{++} + \sqrt{3}\bar{\Sigma}^+\gamma^\mu\Sigma^+ \\ & + \sqrt{3}\bar{\Sigma}^0\gamma^\mu\Sigma^0 + \sqrt{2}\bar{\Sigma}^-\gamma^\mu\Sigma^-)W_\mu^- + \text{H.c.} \end{aligned} \quad (3.16)$$

is contained in Eq. (C.17) in Appendix C.

The cross section for the partonic process is determined entirely by gauge couplings and is given by

$$\hat{\sigma}(q\bar{q} \rightarrow \Sigma\bar{\Sigma}) = \frac{\beta(3 - \beta^2)}{48\pi} \hat{s}(V_L^2 + V_R^2), \quad (3.17)$$

where  $\hat{s} \equiv (p_q + p_{\bar{q}})^2$  is the Mandelstam variable  $s$  for the quark-antiquark system, the parameter  $\beta \equiv \sqrt{1 - 4M_\Sigma^2/\hat{s}}$  denotes the heavy lepton velocity, and the left- and right-handed couplings are given by

$$V_{L,R}^{(\gamma+Z)} = \frac{Q_\Sigma Q_q e^2}{\hat{s}} + \frac{g^{Z\Sigma} g_{L,R}^q g^2}{c_W^2(\hat{s} - M_Z^2)}, \quad (3.18)$$

$$V_L^{(W^-)} = \frac{g^{W\Sigma} g^2 V_{ud}}{\sqrt{2}(\hat{s} - M_W^2)} = V_L^{(W^+)*}, \quad (3.19)$$

$$V_R^{(W^\pm)} = 0. \quad (3.20)$$

Here,  $g_L^q = T_3 - s_W^2 Q_q$  and  $g_R^q = -s_W^2 Q_q$  are the SM chiral quark couplings to the  $Z$  boson. The vector couplings of heavy leptons to gauge bosons are

$$g^{Z\Sigma} = T_3 - s_W^2 Q_\Sigma, \quad g^{W\Sigma} = \sqrt{2}, \sqrt{3}, \sqrt{3} \text{ and } \sqrt{2}, \quad (3.21)$$

where  $g^{W\Sigma}$  can be read of the last two rows in Eq. (3.16) relevant for the production of  $\Sigma^{+++}\overline{\Sigma^{++}}$ ,  $\Sigma^{++}\overline{\Sigma^+}$ ,  $\Sigma^+\overline{\Sigma^0}$  and  $\Sigma^0\overline{\Sigma^-}$  pairs, respectively.

In evaluating the cross sections for a hadron collider, the partonic cross section from Eq. (2.28) has been convoluted with the parton distribution functions, using CTEQ6.6 PDFs [68] via LHAPDF software library [69].

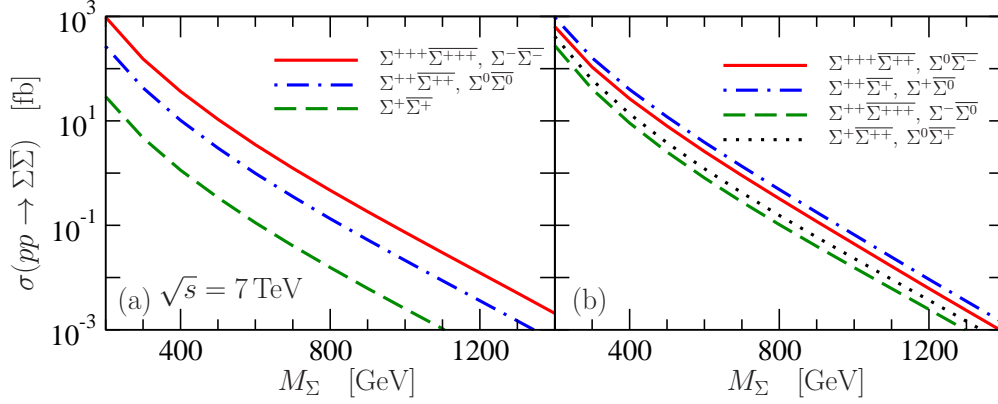


Figure 3.3: The cross sections for production of Dirac quintuplet lepton pairs on LHC proton-proton collisions at  $\sqrt{s} = 7$  TeV via neutral  $\gamma, Z$  (a) and charged  $W^\pm$  currents (b), in dependence on the heavy quintuplet mass  $M_\Sigma$ .

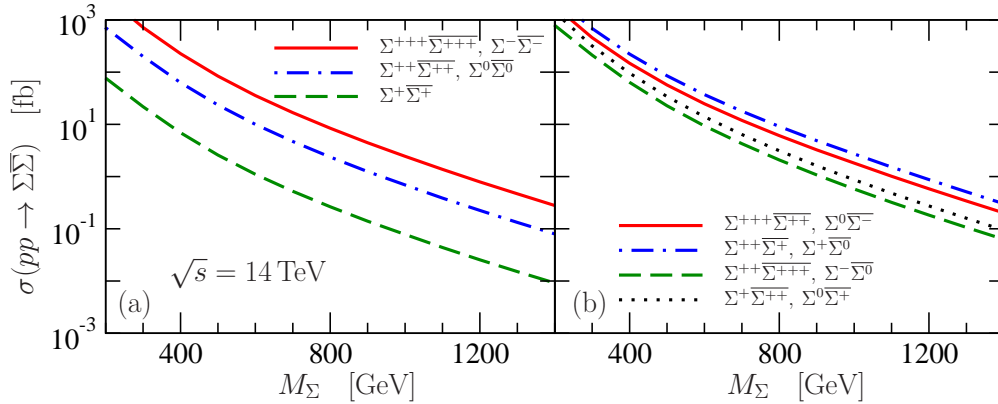


Figure 3.4: Same as Fig. 3.3, but for designed  $\sqrt{s} = 14$  TeV at the LHC.

The cross sections for proton-proton collisions are presented at  $\sqrt{s} = 7$  TeV, appropriate for the 2011-12 LHC run, on Fig. 3.3, and for designed  $\sqrt{s} = 14$  TeV on Fig. 3.4. Thereby we distinguish separately the production via neutral currents shown on LHS, and via charged currents shown on RHS of Figs. 3.3 and 3.4.

| Produced pair                         | Cross section (fb)   |                      |                      |
|---------------------------------------|----------------------|----------------------|----------------------|
|                                       | $M_\Sigma = 200$ GeV | $M_\Sigma = 400$ GeV | $M_\Sigma = 800$ GeV |
| $\Sigma^{+++}\overline{\Sigma}^{+++}$ | 967                  | 36.6                 | 0.47                 |
| $\Sigma^{++}\overline{\Sigma}^{++}$   | 267                  | 10.3                 | 0.13                 |
| $\Sigma^+\overline{\Sigma}^+$         | 29                   | 1.1                  | 0.02                 |
| $\Sigma^0\overline{\Sigma}^0$         | 253                  | 9.3                  | 0.11                 |
| $\Sigma^-\overline{\Sigma}^-$         | 939                  | 34.6                 | 0.43                 |
| $\Sigma^{+++}\overline{\Sigma}^{++}$  | 641                  | 26.5                 | 0.32                 |
| $\Sigma^{++}\overline{\Sigma}^+$      | 961                  | 39.8                 | 0.49                 |
| $\Sigma^+\overline{\Sigma}^0$         | 961                  | 39.8                 | 0.49                 |
| $\Sigma^0\overline{\Sigma}^-$         | 641                  | 26.5                 | 0.32                 |
| $\Sigma^{++}\overline{\Sigma}^{+++}$  | 276                  | 9.1                  | 0.10                 |
| $\Sigma^+\overline{\Sigma}^{++}$      | 414                  | 13.6                 | 0.16                 |
| $\Sigma^0\overline{\Sigma}^+$         | 414                  | 13.6                 | 0.16                 |
| $\Sigma^-\overline{\Sigma}^0$         | 276                  | 9.1                  | 0.10                 |
| Total                                 | 7040                 | 269.9                | 3.30                 |

Table 3.2: Production cross sections for  $\Sigma$ - $\overline{\Sigma}$  pairs for the LHC run at  $\sqrt{s} = 7$  TeV, for three selected values of  $M_\Sigma$ .

We extract the pair production cross sections shown in Fig. 3.3 for three selected values of  $M_\Sigma$  which we show in Table 3.2. From this table we find that the triply-charged  $\Sigma^{+++}$  has the biggest production cross section  $\sigma(\Sigma^{+++})|_{M_\Sigma=400\text{GeV}} = 63.1$  fb and singly-charged  $\Sigma^-$  has the smallest, but comparable, production cross section  $\sigma(\Sigma^-)|_{M_\Sigma=400\text{GeV}} = 43.7$  fb. Production cross sections for all other particles and antiparticles from the Dirac quintuplet are in between. In particular, for  $5\text{ fb}^{-1}$  of integrated luminosity of 2011 LHC run at  $\sqrt{s} = 7$  TeV and  $21\text{ fb}^{-1}$  of integrated luminosity of 2012 LHC run at  $\sqrt{s} = 8$  TeV, there could be 8000  $\Sigma$ - $\overline{\Sigma}$  pairs in total produced for  $M_\Sigma = 400$  GeV, among which 3300 triply-charged  $\Sigma^{+++}$  or  $\overline{\Sigma}^{+++}$  fermions. By testing the heavy lepton production cross sections one can hope to identify the quantum numbers of Dirac quintuplet particles, but in order to confirm their relation to neutrinos one has to study their decays.

## § 3.5 Decays of Dirac quintuplet leptons

Provided that in our scenario the exotic scalar states in Eq. (3.4) are slightly heavier than the exotic leptons in Eq. (3.3), the exotic scalars will not appear in the final states in heavy lepton decays. Here the focus is entirely on the decay modes of the Dirac quintuplet lepton states in Eq. (3.3), where the triply charged state will be phenomenologically most interesting.

The electroweak mass difference induced by loops of SM gauge bosons between two components of Dirac quintuplet lepton with electric charges  $Q$  and  $Q'$  is explicitly calculated in [56] and given in Eq. (2.44). For  $M_\Sigma = 400$  GeV we get

$$\begin{aligned} M_{\Sigma^{+++}} - M_{\Sigma^{++}} &\simeq 1130 \text{ MeV}, \quad M_{\Sigma^{++}} - M_{\Sigma^+} \simeq 804 \text{ MeV}, \\ M_{\Sigma^+} - M_{\Sigma^0} &\simeq 477 \text{ MeV}, \quad M_{\Sigma^0} - M_{\Sigma^-} \simeq 150 \text{ MeV}. \end{aligned} \quad (3.22)$$

The neutral  $\Sigma^0$  and singly-charged  $\Sigma^+$  states, receive additional corrections given in Eqs. (C.12) and (C.16), respectively. However, being of the order of magnitude of the light neutrino masses, these corrections are completely negligible. The splitting  $\sim 1$  GeV between triply and doubly charged quintuplet states opens additional decay channels, in particular, the  $\rho$  resonance enhanced decay channel to the two pions in the final state.

### 3.5.1 Pointlike decays

The Lagrangian in the mass-eigenstate basis relevant for the decays of the heavy leptons, has the neutral part

$$\begin{aligned} \mathcal{L}_{NCZ} &= \frac{g}{c_W} \left[ \bar{\nu} \left( \frac{3}{2} U_{PMNS}^\dagger V_1 \gamma^\mu P_L - \frac{\sqrt{3}}{2\sqrt{2}} U_{PMNS}^T V_2^* \gamma^\mu P_R \right) \Sigma^0 \right. \\ &\quad \left. + \bar{l} (3V_1 \gamma^\mu P_L) \Sigma^- + \bar{l}^c \left( \frac{1}{2} V_2^* \gamma^\mu P_R \right) \Sigma^+ \right] Z_\mu^0 + \text{H.c.}, \end{aligned} \quad (3.23)$$

and the charged current part

$$\begin{aligned}
\mathcal{L}_{CC} &= g \left[ \bar{\nu} (-\sqrt{3} U_{PMNS}^\dagger V_1 \gamma^\mu P_L + \sqrt{2} U_{PMNS}^T V_2^* \gamma^\mu P_R) \Sigma^+ \right. \\
&+ \bar{\Sigma}^- (\sqrt{3} V_2^T U_{PMNS}^* \gamma^\mu P_R) \nu + \bar{l} \left( -\frac{3}{\sqrt{2}} V_1 \gamma^\mu P_L \right) \Sigma^0 \\
&\left. + \bar{\Sigma}^0 \left( -\frac{\sqrt{3}}{2} V_2^T \gamma^\mu P_R \right) l^c + \bar{l}^c \left( -\sqrt{3} V_2^* \gamma^\mu P_R \right) \Sigma^{++} \right] W_\mu^- + \text{H.c.} ,
\end{aligned} \tag{3.24}$$

as given in Eqs. (C.25) and (C.26) in Appendix C.

Here, all the couplings can be expressed in terms of the matrix-valued quantities  $V_1$  and  $V_2$  explicated in the Appendix C, corresponding to the mass matrices in Eq. (3.11)

$$V_1 = \sqrt{\frac{1}{10}} Y_1^\dagger v_{\Phi_1} M_\Sigma^{-1}, V_2 = \sqrt{\frac{1}{10}} Y_2^\dagger v_{\Phi_2}^* M_\Sigma^{-1}. \tag{3.25}$$

Out of the five  $\Sigma$ -states in Eq. (3.3), the four lying lowest have the point-like decays to the gauge bosons and SM leptons. Here, in contrast to type III triplet states, the decays of quintuplet states into the SM Higgs boson are suppressed.

Let us start our list of the partial decay widths by the decays of neutral  $\Sigma^0$  state:

$$\begin{aligned}
\Gamma(\Sigma^0 \rightarrow \ell^- W^+) &= \frac{g^2}{32\pi} \left| \frac{3}{\sqrt{2}} V_1^{\ell\Sigma} \right|^2 \frac{M_\Sigma^3}{M_W^2} \left( 1 - \frac{M_W^2}{M_\Sigma^2} \right)^2 \left( 1 + 2 \frac{M_W^2}{M_\Sigma^2} \right), \\
\Gamma(\Sigma^0 \rightarrow \ell^+ W^-) &= \frac{g^2}{32\pi} \left| \frac{\sqrt{3}}{2} V_2^{\ell\Sigma} \right|^2 \frac{M_\Sigma^3}{M_W^2} \left( 1 - \frac{M_W^2}{M_\Sigma^2} \right)^2 \left( 1 + 2 \frac{M_W^2}{M_\Sigma^2} \right), \\
\sum_{m=1}^3 \Gamma(\Sigma^0 \rightarrow \nu_m Z^0) &= \frac{g^2}{32\pi c_W^2} \sum_{\ell=\{e,\mu,\tau\}} \left( \left| \frac{3}{2} V_1^{\ell\Sigma} \right|^2 + \left| \frac{\sqrt{3}}{2\sqrt{2}} V_2^{\ell\Sigma} \right|^2 \right) \\
&\quad \frac{M_\Sigma^3}{M_Z^2} \left( 1 - \frac{M_Z^2}{M_\Sigma^2} \right)^2 \left( 1 + 2 \frac{M_Z^2}{M_\Sigma^2} \right).
\end{aligned} \tag{3.26}$$

These three decays, for two chosen set of couplings  $V_1$  and  $V_2$ , are displayed on Figs. 3.6 and 3.5. Only the product of  $V_1$  and  $V_2$  is constrained by neutrino masses from Eq. (2.1). Decays of  $\Sigma^0$  to leptons (antileptons) are governed by  $V_1$  ( $V_2$ ), so that the branching ratios to leptons or antileptons are strongly

dependent on the hierarchy between  $V_1$  and  $V_2$ , as illustrated in Figs. 3.6 and 3.5.

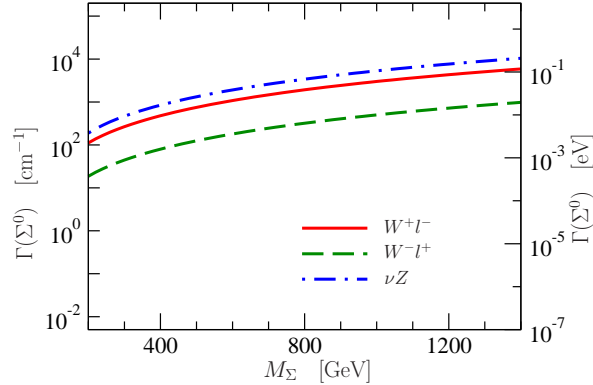


Figure 3.5: Partial decay widths of  $\Sigma^0$  Dirac quintuplet lepton for  $|V_1^{l\Sigma}| = |V_2^{l\Sigma}| = 10^{-6} \sqrt{\frac{20}{M_\Sigma(\text{GeV})}}$ , in dependence on heavy quintuplet mass  $M_\Sigma$ .

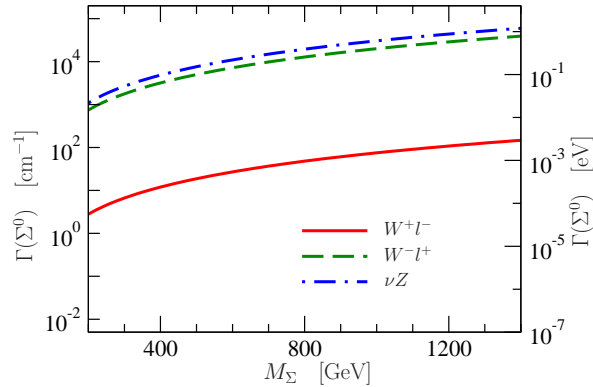


Figure 3.6: Partial decay widths of  $\Sigma^0$  Dirac quintuplet lepton for  $|V_1^{l\Sigma}| = 10^{-6} \sqrt{\frac{0.5}{M_\Sigma(\text{GeV})}}$  different from  $|V_2^{l\Sigma}| = 10^{-6} \sqrt{\frac{800}{M_\Sigma(\text{GeV})}}$ , in dependence on heavy quintuplet mass  $M_\Sigma$ .

Besides the representative  $\Sigma^0$  decays above, let us present also the rest of the pointlike decays. For a negative singly-charged heavy lepton  $\Sigma^-$  the

partial decay widths are given by:

$$\begin{aligned}\Gamma(\Sigma^- \rightarrow \ell^- Z^0) &= \frac{g^2}{32\pi c_W^2} \left| 3V_1^{\ell\Sigma} \right|^2 \frac{M_\Sigma^3}{M_Z^2} \left( 1 - \frac{M_Z^2}{M_\Sigma^2} \right)^2 \left( 1 + 2\frac{M_Z^2}{M_\Sigma^2} \right), \\ \sum_{m=1}^3 \Gamma(\Sigma^- \rightarrow \nu_m W^-) &= \frac{g^2}{32\pi} \sum_{\ell=\{e,\mu,\tau\}} \left| \sqrt{3}V_2^{\ell\Sigma} \right|^2 \\ &\quad \frac{M_\Sigma^3}{M_W^2} \left( 1 - \frac{M_W^2}{M_\Sigma^2} \right)^2 \left( 1 + 2\frac{M_W^2}{M_\Sigma^2} \right).\end{aligned}\quad (3.27)$$

The positive singly-charged  $\Sigma^+$  state has the following partial decay widths:

$$\begin{aligned}\Gamma(\Sigma^+ \rightarrow \ell^+ Z^0) &= \frac{g^2}{32\pi c_W^2} \left| \frac{1}{2}V_2^{\ell\Sigma} \right|^2 \frac{M_\Sigma^3}{M_Z^2} \left( 1 - \frac{M_Z^2}{M_\Sigma^2} \right)^2 \left( 1 + 2\frac{M_Z^2}{M_\Sigma^2} \right), \\ \sum_{m=1}^3 \Gamma(\Sigma^+ \rightarrow \nu_m W^+) &= \frac{g^2}{32\pi} \sum_{\ell=\{e,\mu,\tau\}} \left( \left| \sqrt{3}V_1^{\ell\Sigma} \right|^2 + \left| \sqrt{2}V_2^{\ell\Sigma} \right|^2 \right) \\ &\quad \frac{M_\Sigma^3}{M_W^2} \left( 1 - \frac{M_W^2}{M_\Sigma^2} \right)^2 \left( 1 + 2\frac{M_W^2}{M_\Sigma^2} \right).\end{aligned}\quad (3.28)$$

Finally, the doubly-charged  $\Sigma^{++}$  state decays exclusively via a charged current, with the partial decay width

$$\Gamma(\Sigma^{++} \rightarrow \ell^+ W^+) = \frac{g^2}{32\pi} \left| \sqrt{3}V_2^{\ell\Sigma} \right|^2 \frac{M_\Sigma^3}{M_W^2} \left( 1 - \frac{M_W^2}{M_\Sigma^2} \right)^2 \left( 1 + 2\frac{M_W^2}{M_\Sigma^2} \right).\quad (3.29)$$

Let us stress that there is no such pointlike decay for the triply-charged  $\Sigma^{+++}$ . This state, instead, has other interesting decays presented in the next subsections.

In Table 3.3 we list all possible events coming from the decays of the neutral and singly-charged Dirac quintuplet states to the SM charged leptons. This includes the same-sign dilepton events as a distinguished signature at the LHC.

|                                   | $\overline{\Sigma^+} \rightarrow \ell^- Z^0$ | $\overline{\Sigma^0} \rightarrow \ell^+ W^-$ | $\overline{\Sigma^0} \rightarrow \ell^- W^+$ | $\overline{\Sigma^-} \rightarrow \ell^+ Z^0$ |
|-----------------------------------|--|--|--|--|
| $\Sigma^+ \rightarrow \ell^+ Z^0$ | $\ell^+ \ell^- Z^0 Z^0$                      | $\ell^+ \ell^+ Z^0 W^-$                      | $\ell^+ \ell^- Z^0 W^+$                      | -  |
| $\Sigma^0 \rightarrow \ell^- W^+$ | $\ell^- \ell^- W^+ Z^0$                      | $\ell^- \ell^+ W^+ W^-$                      | $\ell^- \ell^- W^+ W^+$                      | $\ell^- \ell^+ W^+ Z^0$                      |
| $\Sigma^0 \rightarrow \ell^+ W^-$ | $\ell^+ \ell^- W^- Z^0$                      | $\ell^+ \ell^+ W^- W^-$                      | $\ell^+ \ell^- W^- W^+$                      | $\ell^+ \ell^+ W^- Z^0$                      |
| $\Sigma^- \rightarrow \ell^- Z^0$ | -  | $\ell^- \ell^+ Z^0 W^-$                      | $\ell^- \ell^- Z^0 W^+$                      | $\ell^- \ell^+ Z^0 Z^0$                      |

Table 3.3: Decays of exotic leptons to SM particles including same sign dilepton events

### 3.5.2 Cascade decays

Besides previous decays, there are also decays of  $\Sigma^i$  to a lighter  $\Sigma^j$  state. The decay rate for a single pion finale state is given by

$$\Gamma(\Sigma^i \rightarrow \Sigma^j \pi^+) = (g^{W\Sigma})_{ij}^2 \frac{2}{\pi} G_F^2 |V_{ud}|^2 f_\pi^2 (\Delta M_{ij})^3 \sqrt{1 - \frac{m_\pi^2}{(\Delta M_{ij})^2}}. \quad (3.30)$$

The corresponding leptonic decay is

$$\Gamma(\Sigma^i \rightarrow \Sigma^j l^+ \nu) = (g^{W\Sigma})_{ij}^2 \frac{2}{15\pi^3} G_F^2 (\Delta M_{ij})^5 \sqrt{1 - \frac{m_l^2}{(\Delta M_{ij})^2}} \quad (3.31)$$

where  $(g^{W\Sigma})_{ij}^2$  is given in Eq. (3.21) and  $\Delta M_{ij} = M_i - M_j$  is given in Eq. (3.22).

Such decays are suppressed by small mass differences, except for  $\Sigma^{+++}$  where the mass difference  $\Delta M_{32}$  between the  $\Sigma^{+++}$  and  $\Sigma^{++}$  state is large enough to enable also the two pions in the final state. This three-body decay is dominated by a  $\rho(770)$  resonance, and we obtain for it an analytical formula expressed in terms of the meson decay constants,  $f_\pi \simeq 130$  MeV and  $f_\rho \simeq 150$  MeV,

$$\Gamma(\Sigma^{+++} \rightarrow \Sigma^{++} \pi^+ \pi^0) \simeq \Gamma(\Sigma^{+++} \rightarrow \Sigma^{++} \rho^+) = \frac{24}{\pi} G_F^2 V_{ud}^2 f_\rho^2 (\Delta M_{32})^3 \left(1 - \frac{4m_\pi^2}{m_\rho^2}\right)^{-1} \sqrt{1 - \frac{m_\rho^2}{(\Delta M_{32})^2}}. \quad (3.32)$$

This decay shows an enhancement with respect to the single pion decay

$$\frac{\Gamma(\Sigma^{+++} \rightarrow \Sigma^{++} \pi^+ \pi^0)}{\Gamma(\Sigma^{+++} \rightarrow \Sigma^{++} \pi^+)} = 6 \frac{f_\rho^2}{f_\pi^2} \frac{\sqrt{1 - \frac{m_\rho^2}{(\Delta M_{32})^2}}}{\sqrt{1 - \frac{m_\pi^2}{(\Delta M_{32})^2}}} \left(1 - \frac{4m_\pi^2}{m_\rho^2}\right)^{-1}. \quad (3.33)$$



These decays will serve as the referent decays for the golden decay mode of the triply-charged state studied in the following subsection.

### 3.5.3 Golden $\Sigma^{+++} \rightarrow W^+W^+l^+$ decay

We now turn to evaluation of the decay rate for  $\Sigma^{+++} \rightarrow W^+W^+l^+$  with on-shell  $W$  bosons. The Feynman diagram on Fig. 3.7 and its crossed, contribute with an off-shell  $\Sigma^{++}$  in the intermediate state.

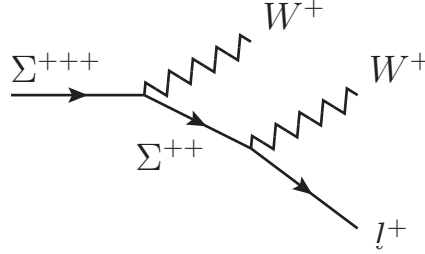


Figure 3.7: Feynman diagram contributing to the triply-charged golden decay

The expression for the amplitude squared is lengthy so we give the analytical expression for decay width only in the limit  $M_\Sigma \gg M_W$ :

$$\Gamma(\Sigma^{+++} \rightarrow W^+W^+l^+) \Big|_{M_\Sigma \gg M_W} = \frac{g^2}{384\pi^2 s_W^2} \left| \sqrt{3} V_2^{\ell\Sigma} \right|^2 \frac{M_\Sigma^5}{M_W^4}. \quad (3.34)$$

Obviously, this decay is governed by the same mixing factor as in  $\Sigma^{++}$  decay in Eq. (3.29). Full numerical calculation, using FormCalc package [111], results in a partial width plotted on Figs. 3.8 and 3.9 for same choices of the mixing factor  $V_2$  as on previous figures. On the same figures we plot the partial widths of the decays of  $\Sigma^{+++}$  given in Eqs. (3.30)-(3.32).

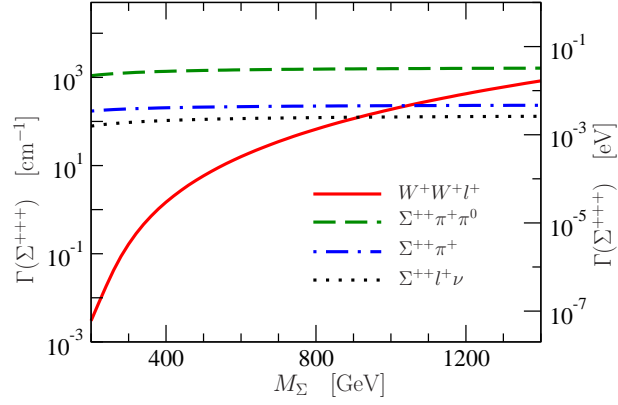


Figure 3.8: Selected partial decay widths of  $\Sigma^{+++}$  Dirac quintuplet lepton for  $|V_2^{l\Sigma}| = 10^{-6} \sqrt{\frac{20}{M_\Sigma(\text{GeV})}}$  in dependence of heavy quintuplet mass  $M_\Sigma$ .

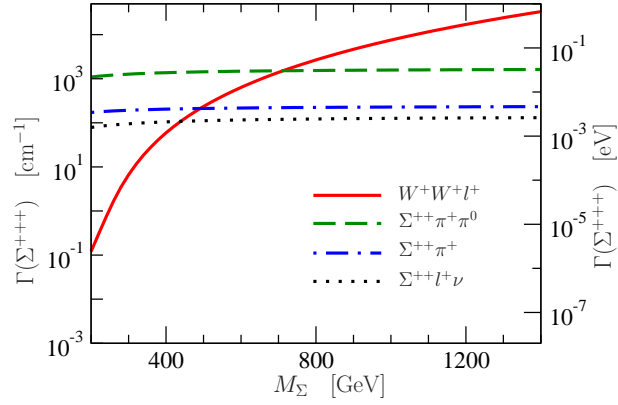


Figure 3.9: Selected partial decay widths of  $\Sigma^{+++}$  Dirac quintuplet lepton for  $|V_2^{l\Sigma}| = 10^{-6} \sqrt{\frac{800}{M_\Sigma(\text{GeV})}}$  in dependence of heavy quintuplet mass  $M_\Sigma$ .

For the sake of being definite, let us explicate the branching ratios for the choice of heavy-light mixing  $V_2$  taken on Fig. 3.9, for two values of heavy-lepton mass  $M_\Sigma$

$$\begin{aligned} \sum_l BR(\Sigma^{+++} \rightarrow W^+W^+l^+) \Big|_{M_\Sigma=400\text{GeV}} &= 0.09 \\ \sum_l BR(\Sigma^{+++} \rightarrow W^+W^+l^+) \Big|_{M_\Sigma=800\text{GeV}} &= 0.80 . \end{aligned} \quad (3.35)$$

As stated before, for  $5 \text{ fb}^{-1}$  of integrated luminosity of 2011 LHC run at  $\sqrt{s} = 7 \text{ TeV}$  and  $21 \text{ fb}^{-1}$  of integrated luminosity of 2012 LHC run at  $\sqrt{s} = 8 \text{ TeV}$ , there could be  $\sim 3300$  triply-charged  $\Sigma^{+++}$  or  $\overline{\Sigma}^{+++}$  fermions produced. This would result in  $\sim 300$  decays  $\Sigma^{+++}(\overline{\Sigma}^{+++}) \rightarrow W^\pm W^\pm l^\pm$  for  $M_\Sigma = 400 \text{ GeV}$  and  $|V_2^{l\Sigma}| = 10^{-6} \sqrt{\frac{800}{M_\Sigma(\text{GeV})}}$ .

# Chapter 4

## Concluding remarks

The advent of LHC offers a possibility for discovering new particles. Neutrino masses are the first tangible deviation from the SM so that best motivated such particles appear in attempts to explain neutrino masses at the TeV scale. Conventional seesaw models rely on isomultiplets up to triplets and lead to high seesaw scale. If such states are not realized in nature, there is a possibility that TeV scale higher multiplets may explain neutrino masses. This thesis presents two such models based on fermionic quintuplets. In the first model a Majorana quintuplet has a neutral component which may provide a DM candidate. In the other one, a Dirac quintuplet has a triply charged component falsifiable at LHC.

Both proposed models are based only on the gauge symmetry and the renormalizability of the SM. Neutrino masses in these models arise at the tree level from dimension-nine operators and from loop-suppressed dimension-five operator. The components of lepton quintuplets can be abundantly produced and tested at the LHC due to their nontrivial gauge charges. They decay to multilepton final states, including same-sign dilepton events. One can question the possibility of distinction between Majorana and Dirac type quintuplets. A triply-charged component of Dirac quintuplet leads to spectacular falsifiable signatures. Consequently, a nonobservance of triply-charged fermion would put a study of Majorana quintuplet in a forefront. In case when quintuplets are kinematically out of the direct LHC reach, they can still provide radiative neutrino masses, and the neutral component of Majorana quintuplet could be a viable DM candidate.



# Appendices



# Appendix A

## Scalar potential

In a tensor notation suitable to cope with higher  $SU(2)_L$  multiplets scalar fields are totally symmetric tensors  $H_i$  for Higgs doublet and  $\Phi_{ijk}$  for scalar quadruplet with the following components:

$$H_1 = H^+ \quad , \quad H_2 = H^0 \quad , \quad (A.1)$$

$$\Phi_{111} = \Phi^+ \quad , \quad \Phi_{112} = \frac{1}{\sqrt{3}}\Phi^0 \quad , \quad \Phi_{122} = \frac{1}{\sqrt{3}}\Phi^- \quad , \quad \Phi_{222} = \Phi^{--} \quad . \quad (A.2)$$

The scalar potential has the gauge invariant form

$$\begin{aligned} V(H, \Phi) = & -\mu_H^2 H^{*i} H_i + \mu_\Phi^2 \Phi^{*ijk} \Phi_{ijk} + \lambda_1 (H^{*i} H_i)^2 \\ & + \lambda_2 (H^* H \Phi^* \Phi)_1 + \lambda_3 (H^* H \Phi^* \Phi)_2 \\ & + (\lambda_4 e^{i\alpha} H^* H H \Phi + \text{H.c.}) + (\lambda_5 e^{i\beta} H H \Phi \Phi + \text{H.c.}) \\ & + (\lambda_6 e^{i\gamma} H \Phi^* \Phi \Phi + \text{H.c.}) + \lambda_7 (\Phi^{*ijk} \Phi_{ijk})^2 + \lambda_8 \Phi^* \Phi \Phi^* \Phi . \end{aligned} \quad (A.3)$$

All parameters of the scalar potential in Eq. (A.3) are real.



The terms in Eq. (A.3) in tensor notation read

$$\begin{aligned}
(H^* H \Phi^* \Phi)_1 &= H^{*i} H_i \Phi^{*jkl} \Phi_{jkl} , \\
(H^* H \Phi^* \Phi)_2 &= H^{*i} H_j \Phi^{*jkl} \Phi_{ikl} , \\
H^* H H \Phi &= H^{*i} H_j H_k \Phi_{ij'k'} \epsilon^{jj'} \epsilon^{kk'} , \\
H H \Phi \Phi &= H_i \Phi_{jkl} H_{i'} \Phi_{j'k'l'} \epsilon^{ij} \epsilon^{i'j'} \epsilon^{kk'} \epsilon^{ll'} , \\
H \Phi^* \Phi \Phi &= H_i \Phi^{*ijk} \Phi_{jlm} \Phi_{kl'm'} \epsilon^{ll'} \epsilon^{mm'} , \\
\Phi^* \Phi \Phi^* \Phi &= \Phi^{*ijk} \Phi_{i'jk} \Phi^{*i'j'k'} \Phi_{ij'k'} .
\end{aligned} \tag{A.4}$$

The EWSB proceeds in usual way from the vev of the Higgs doublet, corresponding to the negative sign in front of the  $\mu_H^2$  term in Eq. (A.3). On the other hand, the electroweak  $\rho$  parameter dictates a small value for vev of the scalar quadruplet, implying the positive sign in front of the  $\mu_\Phi^2$  term. After the EWSB the neutral components of the scalar fields acquire a vacuum expectation value and read

$$H^0 = \frac{1}{\sqrt{2}}(v_H + h^0 + i\chi^0) , \quad \Phi^0 = \frac{1}{\sqrt{2}} e^{i\theta} (v_\Phi + \varphi^0 + i\eta^0) , \tag{A.5}$$

where  $v_H$  and  $v_\Phi$  are real. The value of the minimum of the potential  $\langle 0|V(H, \Phi)|0\rangle$ , reads

$$\begin{aligned}
V_0(v_H, v_\Phi) &= -\frac{1}{2}\mu_H^2 v_H^2 + \frac{1}{2}\mu_\Phi^2 v_\Phi^2 + \frac{1}{4}\lambda_1 v_H^4 + \frac{1}{4}\lambda_2 v_H^2 v_\Phi^2 + \frac{1}{12}\lambda_3 v_H^2 v_\Phi^2 \\
&+ \frac{1}{2\sqrt{3}}\lambda_4 \cos(\alpha + \theta) v_H^3 v_\Phi - \frac{1}{3}\lambda_5 \cos(\beta + 2\theta) v_H^2 v_\Phi^2 \\
&- \frac{1}{3\sqrt{3}}\lambda_6 \cos(\gamma + \theta) v_H v_\Phi^3 + \frac{1}{4}\lambda_7 v_\Phi^4 + \frac{5}{38}\lambda_8 v_\Phi^4 .
\end{aligned} \tag{A.6}$$

The conditions for the minimum of the potential

$$\frac{\partial V_0(v_H, v_\Phi)}{\partial v_H} = 0 , \quad \frac{\partial V_0(v_H, v_\Phi)}{\partial v_\Phi} = 0 , \quad \frac{\partial V_0(v_H, v_\Phi)}{\partial \theta} = 0 \tag{A.7}$$

give

$$\begin{aligned}
3v_H \left[ 6\lambda_1 v_H^2 + \left( 3\lambda_2 + \lambda_3 - 4\lambda_5 \cos(\beta + 2\theta) \right) v_\Phi^2 - 6\mu_H^2 \right. \\
\left. + 3\sqrt{3}\lambda_4 v_H v_\Phi \cos(\alpha + \theta) \right] = 2\sqrt{3}\lambda_6 \cos(\gamma + \theta) v_\Phi^3 ,
\end{aligned} \tag{A.8}$$

$$v_\Phi \left[ 3(3\lambda_2 + \lambda_3)v_H^2 + 18\mu_\Phi^2 + 2(9\lambda_7 + 5\lambda_8)v_\Phi^2 \right] + 3\sqrt{3}\lambda_4 v_H^3 \cos(\alpha + \theta) = \\ = 6v_H v_\Phi \left[ 2\lambda_5 \cos(\beta + 2\theta)v_H + \sqrt{3}\lambda_6 \cos(\gamma + \theta)v_\Phi \right], \quad (\text{A.9})$$

$$3\sqrt{3}\lambda_4 v_H^2 \sin(\alpha + \theta) - 2v_\Phi \left[ 6\lambda_5 \sin(\beta + 2\theta)v_H + \sqrt{3}\lambda_6 \sin(\gamma + \theta)v_\Phi \right] = 0. \quad (\text{A.10})$$

In the leading order in the ratio  $v_\Phi/v_H$ , the parameters of the vevs of scalar fields are

$$v_H \simeq \sqrt{\frac{\mu_H^2}{\lambda_1}}, \quad \theta \simeq -\alpha + \pi, \\ v_\Phi \simeq \frac{\sqrt{3}\lambda_4 v_H^3}{6\mu_\Phi^2 + (3\lambda_2 + \lambda_3 - 4\lambda_5 \cos(\beta - 2\alpha))v_H^2}. \quad (\text{A.11})$$

From now on we will consider a simplified case where all quartic couplings in the scalar potential are real, which means

$$\alpha = 0, \quad \beta = 0, \quad \gamma = 0 \quad \text{and we take} \quad \theta = 0. \quad (\text{A.12})$$

In this case the conditions for the minimum of the potential

$$\frac{\partial V_0(v_H, v_\Phi)}{\partial v_H} = 0, \quad \frac{\partial V_0(v_H, v_\Phi)}{\partial v_\Phi} = 0 \quad (\text{A.13})$$

give

$$\mu_H^2 = \lambda_1 v_H^2 + \left(\frac{1}{2}\lambda_2 + \frac{1}{6}\lambda_3 - \frac{2}{3}\lambda_5\right)v_\Phi^2 + \frac{\sqrt{3}}{2}\lambda_4 v_H v_\Phi - \frac{\sqrt{3}}{9}\lambda_6 \frac{v_\Phi^3}{v_H}, \quad (\text{A.14}) \\ \mu_\Phi^2 = -\left(\frac{1}{2}\lambda_2 + \frac{1}{6}\lambda_3 - \frac{2}{3}\lambda_5\right)v_H^2 - \frac{\sqrt{3}}{6}\lambda_4 \frac{v_H^3}{v_\Phi} + \frac{\sqrt{3}}{3}\lambda_6 v_H v_\Phi - (\lambda_7 + \frac{5}{9}\lambda_8)v_\Phi^2. \quad (\text{A.15})$$

In the leading order in the ratios  $v_\Phi/v_H$  and  $v_\Phi^2/\mu_\Phi^2$ , the vevs of scalar fields are

$$v_H \simeq \sqrt{\frac{\mu_H^2}{\lambda_1}}, \quad v_\Phi \simeq -\frac{1}{2\sqrt{3}}\lambda_4 \frac{v_H^3}{\mu_\Phi^2}. \quad (\text{A.16})$$

The mixing between neutral components and between singly charged components of  $H$  and  $\Phi$  multiplets will occur after the EWSB. The mass terms for neutral fields ( $h^0, \varphi^0$ ) arising from the scalar potential in Eq. (A.3) are

$$\begin{aligned}
\mathcal{L}_{h^0\varphi^0} = & -\frac{1}{2} \left( -\mu_H^2 + 3\lambda_1 v_H^2 + \left( \frac{1}{2}\lambda_2 + \frac{1}{6}\lambda_3 - \frac{2}{3}\lambda_5 \right) v_\Phi^2 + \sqrt{3}\lambda_4 v_H v_\Phi \right) h^0 h^0 \\
& - \left( \left( \lambda_2 + \frac{1}{3}\lambda_3 - \frac{4}{3}\lambda_5 \right) v_H v_\Phi + \frac{\sqrt{3}}{2}\lambda_4 v_H^2 - \frac{1}{\sqrt{3}}\lambda_6 v_\Phi^2 \right) h^0 \varphi^0 \\
& - \frac{1}{2} \left( \mu_\Phi^2 + \left( \frac{1}{2}\lambda_2 + \frac{1}{6}\lambda_3 - \frac{2}{3}\lambda_5 \right) v_H^2 + \frac{2}{\sqrt{3}}\lambda_6 v_H v_\Phi + \left( 3\lambda_7 + \frac{5}{3}\lambda_8 \right) v_\Phi^2 \right) \varphi^0 \varphi^0 .
\end{aligned} \tag{A.17}$$

The mass terms for neutral fields ( $\chi^0, \eta^0$ ) arising from the scalar potential in Eq. (A.3) are

$$\begin{aligned}
\mathcal{L}_{\chi^0\eta^0} = & -\frac{1}{2} \left( -\mu_H^2 + \lambda_1 v_H^2 + \left( \frac{1}{2}\lambda_2 + \frac{1}{6}\lambda_3 + \frac{2}{3}\lambda_5 \right) v_\Phi^2 + \frac{1}{\sqrt{3}}\lambda_4 v_H v_\Phi \right) \chi^0 \chi^0 \\
& - \left( -\frac{1}{2\sqrt{3}}\lambda_4 v_H^2 + \frac{4}{3}\lambda_5 v_H v_\Phi + \frac{1}{3\sqrt{3}}\lambda_6 v_\Phi^2 \right) \chi^0 \eta^0 \\
& - \frac{1}{2} \left( \mu_\Phi^2 + \left( \frac{1}{2}\lambda_2 + \frac{1}{6}\lambda_3 + \frac{2}{3}\lambda_5 \right) v_H^2 - \frac{2}{3\sqrt{3}}\lambda_6 v_H v_\Phi + \left( \lambda_7 + \frac{10}{18}\lambda_8 \right) v_\Phi^2 \right) \eta^0 \eta^0 .
\end{aligned} \tag{A.18}$$

The mass terms for singly charged fields ( $H^+$ ,  $\Phi^+$ ,  $\Phi^-$ ) arising from the scalar potential in Eq. (A.3) are

$$\begin{aligned}
\mathcal{L}_{H^+\Phi^+\Phi^-} = & - \left( -\mu_H^2 + \lambda_1 v_H^2 + \left( \frac{1}{2}\lambda_2 + \frac{1}{3}\lambda_3 \right) v_\Phi^2 - \frac{2}{\sqrt{3}} \lambda_4 v_H v_\Phi \right) H^+ H^{+*} \\
& - \left( \frac{1}{2\sqrt{3}} \lambda_3 v_H v_\Phi + \frac{1}{2} \lambda_4 v_H^2 - \frac{1}{3} \lambda_6 v_\Phi^2 \right) H^+ \Phi^{+*} + \text{H.c.} \\
& - \left( \frac{1}{3} \lambda_3 v_H v_\Phi - \frac{1}{\sqrt{3}} \lambda_4 v_H^2 + \frac{1}{3} \lambda_5 v_H v_\Phi - \frac{1}{3\sqrt{3}} \lambda_6 v_\Phi^2 \right) H^+ \Phi^- + \text{H.c.} \\
& - \left( \mu_\Phi^2 + \frac{1}{2} \lambda_2 v_H^2 + (\lambda_7 + \lambda_8) v_\Phi^2 \right) \Phi^+ \Phi^{+*} \\
& - \left( \frac{1}{\sqrt{3}} \lambda_5 v_H^2 + \frac{1}{3} \lambda_6 v_H v_\Phi + \frac{2}{3\sqrt{3}} \lambda_8 v_\Phi^2 \right) \Phi^+ \Phi^- + \text{H.c.} \\
& - \left( \mu_\Phi^2 + \left( \frac{1}{2}\lambda_2 + \frac{1}{3}\lambda_3 \right) v_H^2 - \frac{2}{3\sqrt{3}} \lambda_6 v_H v_\Phi + (\lambda_7 + \frac{8}{9}\lambda_8) v_\Phi^2 \right) \Phi^{*-} \Phi^- .
\end{aligned} \tag{A.19}$$

The mass of the doubly charged field  $\Phi^{--}$  arising from the scalar potential in Eq. (A.3) is

$$m^2(\Phi^{--}) = \mu_\Phi^2 + \frac{1}{2}\lambda_2 v_H^2 + \frac{1}{2}\lambda_3 v_H^2 + \frac{2}{\sqrt{3}}\lambda_6 v_H v_\Phi + \lambda_7 v_\Phi^2 + \frac{1}{3}\lambda_8 v_\Phi^2 . \tag{A.20}$$

The mass terms that mix components of  $H$  and  $\Phi$  multiplets are small because they are proportional either to  $v_\Phi$  or to small lepton number violating couplings  $\lambda_{4,5}$ . Both are dictated to be small from considerations of neutrino masses. Therefore we neglect the mixing between the components of  $H$  and  $\Phi$  multiplets and we neglect the terms of higher order in  $v_\Phi/v_H$  whenever possible. In this approximation,  $H^+$  and  $\chi^0$  are Goldstone bosons and the

masses of the scalar fields are

$$\begin{aligned}
m^2(h^0) &= 2\lambda_1 v_H^2, \\
m^2(\Phi^+) &= \mu_\Phi^2 + \frac{1}{2}\lambda_2 v_H^2, \\
m^2(\varphi^0) &= \mu_\Phi^2 + \frac{1}{2}\lambda_2 v_H^2 + \frac{1}{6}\lambda_3 v_H^2, \\
m^2(\eta^0) &= \mu_\Phi^2 + \frac{1}{2}\lambda_2 v_H^2 + \frac{1}{6}\lambda_3 v_H^2, \\
m^2(\Phi^-) &= \mu_\Phi^2 + \frac{1}{2}\lambda_2 v_H^2 + \frac{1}{3}\lambda_3 v_H^2, \\
m^2(\Phi^{--}) &= \mu_\Phi^2 + \frac{1}{2}\lambda_2 v_H^2 + \frac{1}{2}\lambda_3 v_H^2.
\end{aligned} \tag{A.21}$$

# Appendix B

## Majorana quintuplet interactions in the mass basis

In this model, in addition to SM particles, there are three zero hypercharge Majorana lepton quintuplets  $\Sigma_R \sim (1, 5, 0)$ . We write the additional fields as totally symmetric tensors  $\Sigma_{Rijkl}$  with the following components:

$$\begin{aligned}\Sigma_{R1111} &= \Sigma_R^{++} , \quad \Sigma_{R1112} = \frac{1}{\sqrt{4}}\Sigma_R^+ , \quad \Sigma_{R1122} = \frac{1}{\sqrt{6}}\Sigma_R^0 , \\ \Sigma_{R1222} &= \frac{1}{\sqrt{4}}\Sigma_R^- , \quad \Sigma_{R2222} = \Sigma_R^{--} .\end{aligned}\tag{B.1}$$

The gauge invariant and renormalizable Lagrangian involving these Majorana lepton quintuplets reads

$$\mathcal{L} = \overline{\Sigma_R} i \gamma^\mu D_\mu \Sigma_R - (\overline{L}_L Y \Phi \Sigma_R + \frac{1}{2} \overline{(\Sigma_R)^C} M \Sigma_R + \text{H.c.}) .\tag{B.2}$$

Here,  $D_\mu$  is the gauge covariant derivative,  $Y$  is the Yukawa-coupling matrix and  $M$  is the mass matrix of the heavy leptons, which we choose to be real and diagonal.

In the adopted tensor notation the terms in Eq. (B.2) read

$$\begin{aligned}\overline{L}_L \Phi \Sigma_R &= \overline{L}_L^i \Phi_{jkl} \Sigma_{Rij'k'l'} \epsilon^{jj'} \epsilon^{kk'} \epsilon^{ll'} , \\ \overline{(\Sigma_R)^C} \Sigma_R &= \overline{(\Sigma_R)^C}_{ijkl} \Sigma_{Ri'j'k'l'} \epsilon^{ii'} \epsilon^{jj'} \epsilon^{kk'} \epsilon^{ll'} .\end{aligned}\tag{B.3}$$

Accordingly, the Majorana mass term for the quintuplet  $\Sigma_R$  is expanded in component fields to give

$$\begin{aligned} \overline{(\Sigma_R)^C} M \Sigma_R &= \overline{(\Sigma_R^{++})^C} M \Sigma_R^{--} - \overline{(\Sigma_R^+)^C} M \Sigma_R^- + \overline{(\Sigma_R^0)^C} M \Sigma_R^0 \\ &- \overline{(\Sigma_R^-)^C} M \Sigma_R^+ + \overline{(\Sigma_R^{--})^C} M \Sigma_R^{++} , \end{aligned} \quad (\text{B.4})$$

the terms containing two charged Dirac fermions and one neutral Majorana fermion

$$\Sigma^{++} = \Sigma_R^{++} + \Sigma_R^{--C} , \quad \Sigma^+ = \Sigma_R^+ - \Sigma_R^{-C} , \quad \Sigma^0 = \Sigma_R^0 + \Sigma_R^{0C} . \quad (\text{B.5})$$

With a non-zero vacuum expectation value for the scalar fields, the doublet leptons receive mass and mix with the quintuplet leptons. The neutral lepton mass matrix including the neutrino mass loop contribution from Eq. (2.21) is

$$\mathcal{L}_{\nu\Sigma^0} = -\frac{1}{2} \left( \overline{\nu_L} \overline{(\Sigma_R^0)^C} \right) \begin{pmatrix} m_\nu^{loop} & \frac{1}{2} Y v_\Phi \\ \frac{1}{2} Y^T v_\Phi & M \end{pmatrix} \begin{pmatrix} (\nu_L)^c \\ \Sigma_R^0 \end{pmatrix} + \text{H.c.} . \quad (\text{B.6})$$

Singly charged lepton mass matrix is

$$\mathcal{L}_{l\Sigma^-} = - \left( \overline{l_L} \overline{(\Sigma_R^+)^C} \right) \begin{pmatrix} \frac{1}{\sqrt{2}} Y_l v_H & -\frac{\sqrt{3}}{2\sqrt{2}} Y v_\Phi \\ 0 & M \end{pmatrix} \begin{pmatrix} l_R \\ (\Sigma_L^+)^c \end{pmatrix} + \text{H.c.} . \quad (\text{B.7})$$

For detailed studies one needs to understand these mass matrices and their diagonalization which can be achieved by making the following unitary transformations on the leptons

$$\begin{aligned} \begin{pmatrix} (\nu_L)^c \\ \Sigma_R^0 \end{pmatrix} &= U^0 \begin{pmatrix} (\nu_{mL})^c \\ \Sigma_{mR}^0 \end{pmatrix} , \\ \begin{pmatrix} l_L \\ (\Sigma_R^+)^c \end{pmatrix} &= U^L \begin{pmatrix} l_{mL} \\ (\Sigma_{mR}^+)^c \end{pmatrix} , \quad \begin{pmatrix} l_R \\ (\Sigma_L^+)^c \end{pmatrix} = U^R \begin{pmatrix} l_{mR} \\ (\Sigma_{mL}^+)^c \end{pmatrix} , \end{aligned} \quad (\text{B.8})$$

different for a symmetric neutral mass matrix and a nonsymmetric charged mass matrix

$$\begin{aligned} U^{0T} \begin{pmatrix} m_\nu^{loop} & \frac{1}{2} Y v_\Phi \\ \frac{1}{2} Y^T v_\Phi & M \end{pmatrix} U^0 &= \begin{pmatrix} m_{neutrino} & 0 \\ 0 & M_0 \end{pmatrix} , \\ U^{L\dagger} \begin{pmatrix} \frac{1}{\sqrt{2}} Y_l v_H & -\frac{\sqrt{3}}{2\sqrt{2}} Y v_\Phi \\ 0 & M \end{pmatrix} U^R &= \begin{pmatrix} m_{lepton} & 0 \\ 0 & M_+ \end{pmatrix} . \end{aligned} \quad (\text{B.9})$$

For three light doublet fields and three Majorana lepton quintuplets the matrices  $U_{L,R}$  and  $U_0$  are  $6 \times 6$  unitary matrices, which can be decomposed into the  $3 \times 3$  block matrices as follows:

$$U^0 \equiv \begin{pmatrix} U_{\nu\nu}^0 & U_{\nu(\Sigma_R^0)^c}^0 \\ U_{(\Sigma_R^0)^c\nu}^0 & U_{(\Sigma_R^0)^c(\Sigma_R^0)^c}^0 \end{pmatrix}, \quad (\text{B.10})$$

$$U^L \equiv \begin{pmatrix} U_{ll}^L & U_{l(\Sigma_R^+)^c}^L \\ U_{(\Sigma_R^+)^cl}^L & U_{(\Sigma_R^+)^c(\Sigma_R^+)^c}^L \end{pmatrix}, \quad (\text{B.11})$$

$$U^R \equiv \begin{pmatrix} U_{ll}^R & U_{l(\Sigma_L^+)^c}^R \\ U_{(\Sigma_L^+)^cl}^R & U_{(\Sigma_L^+)^c(\Sigma_L^+)^c}^R \end{pmatrix}. \quad (\text{B.12})$$

In principle, the matrices  $U^0$  and  $U^{L,R}$  can be expressed in terms of  $Y$ ,  $Y_l$  and  $M$  sub-blocks. Since, in order for the seesaw mechanism to work the factors  $Y M^{-1}$  should be small, one can expand  $U^0$  and  $U^{L,R}$  in powers of  $M^{-1}$  and keep a track of the leading order contributions. For this purpose, without loss of generality, it is convenient to write the leading order expressions up to  $M^{-2}$  in the basis where  $Y_l$  and  $M$  are already diagonalized. Following the procedure of [71, 72, 73] we first obtain results for the entries  $U^0$ :

$$\begin{aligned} U_{\nu\nu}^0 &= \left(1 - \frac{1}{8} v_\Phi^2 Y^* M^{-2} Y^T\right) U_{PMNS}^*, \\ U_{\nu(\Sigma_R^0)^c}^0 &= \frac{1}{2} v_\Phi Y^* M^{-1}, \\ U_{(\Sigma_R^0)^c\nu}^0 &= -\frac{1}{2} v_\Phi M^{-1} Y^T U_{PMNS}^*, \\ U_{(\Sigma_R^0)^c(\Sigma_R^0)^c}^0 &= 1 - \frac{1}{8} v_\Phi^2 M^{-1} Y^T Y^* M^{-1}. \end{aligned} \quad (\text{B.13})$$

Here,  $U_{PMNS}$  is a  $3 \times 3$  unitary matrix given in Eq. (1.2) which diagonalizes the effective light neutrino mass matrix:

$$m_\nu \simeq m_\nu^{loop} - \frac{1}{4} v_\Phi^2 Y M^{-1} Y^T, \quad U_{PMNS}^\dagger m_\nu U_{PMNS}^* = m_{neutrino}. \quad (\text{B.14})$$

The mass matrix for heavy neutral leptons acquires corrections of the order  $M^{-1}$ ,

$$\tilde{M}_0 \simeq M + \frac{1}{8} v_\Phi^2 (Y^T Y^* M^{-1} + M^{-1} Y^\dagger Y), \quad (\text{B.15})$$



which, being of the order of light neutrino masses, are completely negligible for our phenomenological considerations.

Next, we obtain the leading order expressions up to  $M^{-2}$  for the entries in  $U^L$ :

$$\begin{aligned}
U_{ll}^L &= 1 - \frac{3}{16}v_\Phi^2 Y M^{-2} Y^\dagger , \\
U_{l(\Sigma_R^+)^c}^L &= \frac{-\sqrt{3}}{2\sqrt{2}}v_\Phi Y M^{-1} , \\
U_{(\Sigma_R^+)^c l}^L &= \frac{\sqrt{3}}{2\sqrt{2}}v_\Phi M^{-1} Y^\dagger , \\
U_{(\Sigma_R^+)^c(\Sigma_R^+)^c}^L &= 1 - \frac{3}{16}v_\Phi v_\Phi^* M^{-1} Y^\dagger Y M^{-1} . \tag{B.16}
\end{aligned}$$

Similarly, for  $U^R$ , the leading order expressions up to  $M^{-2}$  are:

$$\begin{aligned}
U_{ll}^R &= 1 , \quad U_{l(\Sigma_L^+)^c}^R = \frac{-\sqrt{3}}{4}v_H v_\Phi Y_l Y M^{-2} , \\
U_{(\Sigma_L^+)^c l}^R &= \frac{\sqrt{3}}{4}v_H v_\Phi M^{-2} Y^\dagger Y_l , \quad U_{(\Sigma_L^+)^c(\Sigma_L^+)^c}^R = 1 . \tag{B.17}
\end{aligned}$$

As a result, the mass matrix for the light singly-charged leptons gets corrections of the order  $M^{-2}$

$$m_l \simeq \frac{1}{\sqrt{2}}Y_l v_H \left(1 - \frac{3}{16}v_\Phi^2 Y^* M^{-2} Y^T\right) , \tag{B.18}$$

while, the mass matrix for the heavy singly-charged leptons gets corrections of the order  $M^{-1}$

$$\tilde{M} \simeq M + \frac{3}{16}v_\Phi^2 Y^T Y^* M^{-1} . \tag{B.19}$$

Both corrections are completely negligible for our phenomenological considerations.

Our studies of particle production require a knowledge of gauge couplings to leptonic fields. In the weak interaction basis, they can be written as

$$\begin{aligned}
\mathcal{L}_{gauge}^{\Sigma\bar{\Sigma}} &= + e(2\overline{\Sigma^{++}}\gamma^\mu\Sigma^{++} + \overline{\Sigma^+}\gamma^\mu\Sigma^+)A_\mu \\
&+ g \cos\theta_W(2\overline{\Sigma^{++}}\gamma^\mu\Sigma^{++} + \overline{\Sigma^+}\gamma^\mu\Sigma^+)Z_\mu \\
&+ g(\sqrt{2}\overline{\Sigma^+}\gamma^\mu\Sigma^{++} + \sqrt{3}\overline{\Sigma^0}\gamma^\mu\Sigma^+)W_\mu^- + \text{H.c.} . \tag{B.20}
\end{aligned}$$

where  $c_W = \cos \theta_W$  and  $s_W = \sin \theta_W$ .

In the mass-eigenstate basis we obtain the terms involving the heavy fermion, light fermion and gauge boson fields that are relevant for the decays of heavy leptons. In the following, we focus only on the above terms and restrict to couplings of the order  $M^{-1}$ . Whereas the photon couplings to all leptons and  $Z$  couplings to doubly charged leptons are diagonal in the mass-eigenstate basis, the couplings of  $Z$  boson and  $W$  boson to singly-charged and neutral leptons are more complicated.

Couplings of heavy and light leptons are expressed in terms of the matrix-valued quantity

$$(V)_{l\Sigma} = \left( \frac{v_\Phi}{\sqrt{2}} Y M^{-1} \right)_{l\Sigma}. \quad (\text{B.21})$$

Next, for simplicity, we suppress the indices indicating the mass-eigenstate fields. The Lagrangian in the mass-eigenstate basis, relevant for the decays of the heavy leptons, has the neutral current part

$$\begin{aligned} \mathcal{L}_{NCZ} &= \frac{g}{c_W} \left[ \bar{\nu} \left( \frac{1}{2\sqrt{2}} U_{PMNS}^\dagger V \gamma^\mu P_L - \frac{1}{2\sqrt{2}} U_{PMNS}^T V^* \gamma^\mu P_R \right) \Sigma^0 \right. \\ &\quad \left. + \bar{l}^c \left( \frac{\sqrt{3}}{4} V^* \gamma^\mu P_R \right) \Sigma^+ + \text{H.c.} \right] Z_\mu^0, \end{aligned} \quad (\text{B.22})$$

and the charged current part

$$\begin{aligned} \mathcal{L}_{CC} &= g \left[ \bar{\nu} \left( -\sqrt{\frac{3}{2}} U_{PMNS}^\dagger V \gamma^\mu P_L + \frac{-\sqrt{3}}{2\sqrt{2}} U_{PMNS}^T V^* \gamma^\mu P_R \right) \Sigma^+ \right. \\ &\quad \left. + \bar{l} (-V \gamma^\mu P_L) \Sigma^0 \right. \\ &\quad \left. + \bar{l}^c \left( \sqrt{\frac{3}{2}} V^* \gamma^\mu P_R \right) \Sigma^{++} \right] W_\mu^- + \text{H.c.} . \end{aligned} \quad (\text{B.23})$$

Note that the interactions involving light neutrinos in the above have the additional  $U_{PMNS}$  factor compared with those involving light charged leptons.



# Appendix C

## Dirac quintuplet interactions in the mass basis

The novel seesaw model employs, in addition to the SM particles,  $n_\Sigma$  vectorlike quintuplets of leptons with hypercharge two,  $\Sigma_{L,R} \sim (1, 5, 2)$  under  $SU(3)_C \times SU(2)_L \times U(1)_Y$ . We write the component fields as

$$\Sigma_L = \begin{pmatrix} \Sigma_L^{+++} \\ \Sigma_L^{++} \\ \Sigma_L^+ \\ \Sigma_L^0 \\ \Sigma_L^- \end{pmatrix}, \quad \Sigma_R = \begin{pmatrix} \Sigma_R^{+++} \\ \Sigma_R^{++} \\ \Sigma_R^+ \\ \Sigma_R^0 \\ \Sigma_R^- \end{pmatrix}. \quad (\text{C.1})$$

The renormalizable Lagrangian involving  $\Sigma_L$  and  $\Sigma_R$  is given by

$$\begin{aligned} \mathcal{L} = & \overline{\Sigma}_L i \not{D} \Sigma_L + \overline{\Sigma}_R i \not{D} \Sigma_R - \overline{\Sigma}_R M_\Sigma \Sigma_L - \overline{\Sigma}_L M_\Sigma^\dagger \Sigma_R \\ & + \overline{\Sigma}_R Y_1 L_L \Phi_1^* + \overline{(\Sigma_L)^c} Y_2 L_L \Phi_2 + \text{H.c.} . \end{aligned} \quad (\text{C.2})$$

With a non-zero vacuum expectation value for the scalar fields, doublet leptons receive mass and mix with the quintuplet leptons. Lepton mass terms

in the Lagrangian are

$$\begin{aligned}
\mathcal{L}_m &= -\frac{1}{2} \left( \overline{(\nu_L)^c} \overline{(\Sigma_L^0)^c} \overline{\Sigma_R^0} \right) \begin{pmatrix} 0 & m_2^T & m_1^T \\ m_2 & 0 & M_\Sigma^T \\ m_1 & M_\Sigma & 0 \end{pmatrix} \begin{pmatrix} \nu_L \\ \Sigma_L^0 \\ (\Sigma_R^0)^c \end{pmatrix} + \text{H.c.} \\
&- \left( \overline{l_R} \overline{\Sigma_R^-} \overline{(\Sigma_L^+)^c} \right) \begin{pmatrix} m_l & 0 & 0 \\ m_3 & M_\Sigma & 0 \\ m_4 & 0 & M_\Sigma^T \end{pmatrix} \begin{pmatrix} l_L \\ \Sigma_L^- \\ (\Sigma_R^+)^c \end{pmatrix} + \text{H.c.} \\
&- \overline{\Sigma_R^{++}} M_\Sigma \Sigma_L^{++} - \overline{\Sigma_R^{++}} M_\Sigma \Sigma_L^{++} + \text{H.c.} , \tag{C.3}
\end{aligned}$$

with

$$\begin{aligned}
m_1 &= \sqrt{\frac{1}{10}} Y_1 v_{\Phi_1}^* , & m_2 &= -\sqrt{\frac{3}{20}} Y_2 v_{\Phi_2} , \\
m_3 &= \sqrt{\frac{2}{5}} Y_1 v_{\Phi_1}^* , & m_4 &= \sqrt{\frac{1}{10}} Y_2 v_{\Phi_2} . \tag{C.4}
\end{aligned}$$

For detailed studies, one needs to understand these mass matrices and their diagonalization. The diagonalization of the mass matrices can be achieved by making the following unitary transformations on the leptons

$$\begin{aligned}
\begin{pmatrix} \nu_L \\ \Sigma_L^0 \\ (\Sigma_R^0)^c \end{pmatrix} &= U^0 \begin{pmatrix} \nu_{mL} \\ \Sigma_{mL}^0 \\ (\Sigma_{mR}^0)^c \end{pmatrix} , \\
\begin{pmatrix} l_L \\ \Sigma_L^- \\ (\Sigma_R^+)^c \end{pmatrix} &= U^L \begin{pmatrix} l_{mL} \\ \Sigma_{mL}^- \\ (\Sigma_{mR}^+)^c \end{pmatrix} , & \begin{pmatrix} l_R \\ \Sigma_R^- \\ (\Sigma_L^+)^c \end{pmatrix} &= U^R \begin{pmatrix} l_{mR} \\ \Sigma_{mR}^- \\ (\Sigma_{mL}^+)^c \end{pmatrix} , \tag{C.5}
\end{aligned}$$

different for a symmetric neutral and a nonsymmetric charged mass matrix

$$\begin{aligned}
U^{0T} \begin{pmatrix} 0 & m_2^T & m_1^T \\ m_2 & 0 & M_\Sigma^T \\ m_1 & M_\Sigma & 0 \end{pmatrix} U^0 &= \begin{pmatrix} m_\nu & 0 \\ 0 & M_0 \end{pmatrix} , \\
U^{R\dagger} \begin{pmatrix} m_l & 0 & 0 \\ m_3 & M_\Sigma & 0 \\ m_4 & 0 & M_\Sigma^T \end{pmatrix} U^L &= \begin{pmatrix} m_{lepton} & 0 \\ 0 & M \end{pmatrix} . \tag{C.6}
\end{aligned}$$

For three light doublet fields and  $n_\Sigma$  heavy quintuplet vectorlike lepton fields the matrices  $U_{L,R}$  and  $U_0$  are  $(3 + 2n_\Sigma) \times (3 + 2n_\Sigma)$  unitary matrices, which we decompose into the block matrices as follows:

$$U^0 \equiv \begin{pmatrix} U_{\nu\nu}^0 & U_{\nu\Sigma_L^0}^0 & U_{\nu(\Sigma_R^0)^c}^0 \\ U_{\Sigma_L^0\nu}^0 & U_{\Sigma_L^0\Sigma_L^0}^0 & U_{\Sigma_L^0(\Sigma_R^0)^c}^0 \\ U_{(\Sigma_R^0)^c\nu}^0 & U_{(\Sigma_R^0)^c\Sigma_L^0}^0 & U_{(\Sigma_R^0)^c(\Sigma_R^0)^c}^0 \end{pmatrix}, \quad (\text{C.7})$$

$$U^L \equiv \begin{pmatrix} U_{ll}^L & U_{l\Sigma_L^-}^L & U_{l(\Sigma_R^+)^c}^L \\ U_{\Sigma_L^-l}^L & U_{\Sigma_L^-\Sigma_L^-}^L & U_{\Sigma_L^-(\Sigma_R^+)^c}^L \\ U_{(\Sigma_R^+)^cl}^L & U_{(\Sigma_R^+)^c\Sigma_L^-}^L & U_{(\Sigma_R^+)^c(\Sigma_R^+)^c}^L \end{pmatrix}, \quad (\text{C.8})$$

$$U^R \equiv \begin{pmatrix} U_{ll}^R & U_{l\Sigma_R^-}^R & U_{l(\Sigma_L^+)^c}^R \\ U_{\Sigma_R^-l}^R & U_{\Sigma_R^-\Sigma_R^-}^R & U_{\Sigma_R^-(\Sigma_L^+)^c}^R \\ U_{(\Sigma_L^+)^cl}^R & U_{(\Sigma_L^+)^c\Sigma_R^-}^R & U_{(\Sigma_L^+)^c(\Sigma_L^+)^c}^R \end{pmatrix}. \quad (\text{C.9})$$

Here, we distinguish the entries  $U_{\nu\nu}^0$ ,  $U_{ll}^L$  and  $U_{ll}^R$  which are  $3 \times 3$  matrices, the entries  $U_{\nu\Sigma_L^0}^0$ ,  $U_{\nu(\Sigma_R^0)^c}^0$ ,  $U_{l\Sigma_L^-}^L$ ,  $U_{l(\Sigma_R^+)^c}^L$ ,  $U_{l\Sigma_R^-}^R$  and  $U_{l(\Sigma_L^+)^c}^R$  which are  $3 \times n_\Sigma$  matrices, and the entries  $U_{\Sigma_L^0\nu}^0$ ,  $U_{(\Sigma_R^0)^c\nu}^0$ ,  $U_{\Sigma_L^-l}^L$ ,  $U_{(\Sigma_R^+)^cl}^L$ ,  $U_{\Sigma_R^-l}^R$  and  $U_{(\Sigma_L^+)^cl}^R$  which are  $n_\Sigma \times 3$  matrices. The remaining entries are  $n_\Sigma \times n_\Sigma$  matrices.

In principle, the matrices  $U^0$  and  $U^{L,R}$  can be expressed in terms of  $m_{1,2,3,4}$ ,  $m_l$  and  $M_\Sigma$  sub-blocks. Since, in order for the seesaw mechanism to work, the factors  $m_{1,2,3,4}M_\Sigma^{-1}$  should be small, one can expand  $U^0$  and  $U^{L,R}$  in powers of  $M_\Sigma^{-1}$  and keep a track of the leading order contributions. For this purpose, without loss of generality, it is convenient to write the leading order expressions up to  $M_\Sigma^{-2}$  in the basis where  $m_l$  and  $M_\Sigma$  are already diagonalized. Following the procedure of [72, 73] we first obtain results for the entries  $U^0$ :

$$\begin{aligned} U_{\nu\nu}^0 &= (1 - \frac{1}{2}m_1^\dagger M_\Sigma^{-2} m_1 - \frac{1}{2}m_2^\dagger M_\Sigma^{-2} m_2) V_{PMNS}, & U_{\nu\Sigma_L^0}^0 &= m_1^\dagger M_\Sigma^{-1}, \\ U_{\nu(\Sigma_R^0)^c}^0 &= m_2^\dagger M_\Sigma^{-1}, & U_{\Sigma_L^0\nu}^0 &= -M_\Sigma^{-1} m_1 V_{PMNS}, \\ U_{\Sigma_L^0\Sigma_L^0}^0 &= 1 - \frac{1}{2}M_\Sigma^{-1} m_1 m_1^\dagger M_\Sigma^{-1}, & U_{\Sigma_L^0(\Sigma_R^0)^c}^0 &= -\frac{1}{2}M_\Sigma^{-1} m_1 m_2^\dagger M_\Sigma^{-1}, \\ U_{(\Sigma_R^0)^c\nu}^0 &= -M_\Sigma^{-1} m_2 V_{PMNS}, & U_{(\Sigma_R^0)^c\Sigma_L^0}^0 &= -\frac{1}{2}M_\Sigma^{-1} m_2 m_1^\dagger M_\Sigma^{-1}, \\ U_{(\Sigma_R^0)^c(\Sigma_R^0)^c}^0 &= 1 - \frac{1}{2}M_\Sigma^{-1} m_2 m_2^\dagger M_\Sigma^{-1}. \end{aligned} \quad (\text{C.10})$$

Here,  $U_{PMNS}$  is a  $3 \times 3$  unitary matrix which diagonalizes the effective light neutrino mass matrix:

$$\tilde{m}_\nu \simeq -m_2^T M_\Sigma^{-1} m_1 - m_1^T M_\Sigma^{-1} m_2, \quad U_{PMNS}^T \tilde{m}_\nu U_{PMNS} = m_\nu. \quad (\text{C.11})$$

The mass matrix for heavy neutral leptons acquires corrections of the order  $M_\Sigma^{-1}$ ,

$$\begin{aligned} \tilde{M}_0 \simeq & \begin{pmatrix} 0 & M_\Sigma \\ M_\Sigma & 0 \end{pmatrix} + \frac{1}{2} \begin{pmatrix} m_2 m_1^\dagger M_\Sigma^{-1} & m_2 m_2^\dagger M_\Sigma^{-1} \\ m_1 m_1^\dagger M_\Sigma^{-1} & m_1 m_2^\dagger M_\Sigma^{-1} \end{pmatrix} \\ & + \frac{1}{2} \begin{pmatrix} M_\Sigma^{-1} m_1^* m_2^T & M_\Sigma^{-1} m_1^* m_1^T \\ M_\Sigma^{-1} m_2^* m_2^T & M_\Sigma^{-1} m_2^* m_1^T \end{pmatrix}, \quad (\text{C.12}) \end{aligned}$$

which, being of the order of light neutrino masses, are completely negligible for our phenomenological considerations. In principle, for every vector-like Dirac quintuplet we would get two nearly degenerate heavy Majorana fermions, with mass splitting of the order  $m_\nu$ . By neglecting these corrections we treat heavy neutral leptons as Dirac fermions for all practical phenomenological considerations.

Next, we obtain the leading order expressions up to  $M_\Sigma^{-2}$  for the entries in  $U^L$ :

$$\begin{aligned} U_l^L &= 1 - \frac{1}{2} m_3^\dagger M_\Sigma^{-2} m_3 - \frac{1}{2} m_4^\dagger M_\Sigma^{-2} m_4, \quad U_{l\Sigma_L^-}^L = m_3^\dagger M_\Sigma^{-1}, \\ U_{l(\Sigma_R^+)^c}^L &= m_4^\dagger M_\Sigma^{-1}, \quad U_{\Sigma_L^- l}^L = -M_\Sigma^{-1} m_3, \\ U_{\Sigma_L^- \Sigma_L^-}^L &= 1 - \frac{1}{2} M_\Sigma^{-1} m_3 m_3^\dagger M_\Sigma^{-1}, \quad U_{\Sigma_L^- (\Sigma_R^+)^c}^L = -\frac{1}{2} M_\Sigma^{-1} m_3 m_4^\dagger M_\Sigma^{-1}, \\ U_{(\Sigma_R^+)^c l}^L &= -M_\Sigma^{-1} m_4, \quad U_{(\Sigma_R^+)^c \Sigma_L^-}^L = -\frac{1}{2} M_\Sigma^{-1} m_4 m_3^\dagger M_\Sigma^{-1}, \\ U_{(\Sigma_R^+)^c (\Sigma_R^+)^c}^L &= 1 - \frac{1}{2} M_\Sigma^{-1} m_4 m_4^\dagger M_\Sigma^{-1}. \quad (\text{C.13}) \end{aligned}$$

Similarly, for  $U^R$ , the leading order expressions up to  $M_\Sigma^{-2}$  are:

$$\begin{aligned} U_l^R &= 1, \quad U_{l\Sigma_R^-}^R = m_l m_3^\dagger M_\Sigma^{-2}, \quad U_{l(\Sigma_L^+)^c}^R = m_l m_4^\dagger M_\Sigma^{-2}, \\ U_{\Sigma_R^- l}^R &= -M_\Sigma^{-2} m_3 m_l, \quad U_{\Sigma_R^- \Sigma_R^-}^R = 1, \quad U_{\Sigma_R^- (\Sigma_L^+)^c}^R = 0, \\ U_{(\Sigma_L^+)^c l}^R &= -M_\Sigma^{-2} m_4 m_l, \quad U_{(\Sigma_L^+)^c \Sigma_R^-}^R = 0, \quad U_{(\Sigma_L^+)^c (\Sigma_L^+)^c}^R = 1. \quad (\text{C.14}) \end{aligned}$$

As a result, the mass matrix for the light singly-charged leptons gets corrections of the order  $M_\Sigma^{-2}$

$$\tilde{m}_l \simeq m_l \left( 1 - \frac{1}{2} m_3^\dagger M_\Sigma^{-2} m_3 - \frac{1}{2} m_4^\dagger M_\Sigma^{-2} m_4 \right), \quad (\text{C.15})$$

while, the mass matrix for the heavy singly-charged leptons gets corrections of the order  $M_\Sigma^{-1}$

$$\tilde{M} \simeq \begin{pmatrix} M_\Sigma & 0 \\ 0 & M_\Sigma \end{pmatrix} + \frac{1}{2} \begin{pmatrix} m_3 m_3^\dagger M_\Sigma^{-1} & m_3 m_4^\dagger M_\Sigma^{-1} \\ m_4 m_3^\dagger M_\Sigma^{-1} & m_4 m_4^\dagger M_\Sigma^{-1} \end{pmatrix}. \quad (\text{C.16})$$

Both corrections are completely negligible for our phenomenological considerations.

Our studies of particle production require a knowledge of gauge couplings to leptonic fields. In the weak interaction basis, they can be written as

$$\begin{aligned} \mathcal{L}_{gauge} = & e(3\overline{\Sigma^{++++}}\gamma^\mu\Sigma^{++++} + 2\overline{\Sigma^{++}}\gamma^\mu\Sigma^{++} + \overline{\Sigma^+}\gamma^\mu\Sigma^+ - \overline{\Sigma^-}\gamma^\mu\Sigma^- - \bar{l}\gamma^\mu l)A_\mu \\ & + \frac{g}{c_W}((2 - 3s_W^2)\overline{\Sigma^{++++}}\gamma^\mu\Sigma^{++++} + (1 - 2s_W^2)\overline{\Sigma^{++}}\gamma^\mu\Sigma^{++})Z_\mu \\ & - \frac{g}{c_W}s_W^2(\overline{\Sigma^+}\gamma^\mu\Sigma^+ - \overline{\Sigma^-}\gamma^\mu\Sigma^- - \bar{l}\gamma^\mu l)Z_\mu \\ & + \frac{g}{c_W}(\bar{\nu}_L\gamma^\mu\nu_L + \overline{\Sigma_L^0}\gamma^\mu\Sigma_L^0 - \overline{\Sigma_R^0}\gamma^\mu\Sigma_R^0)Z_\mu \\ & + \frac{g}{c_W}(-\frac{1}{2}\bar{\nu}_L\gamma^\mu\nu_L - 2\overline{\Sigma_L^0}\gamma^\mu\Sigma_L^0 - \frac{1}{2}\bar{l}_L\gamma^\mu l_L - 2\overline{\Sigma_L^-}\gamma^\mu\Sigma_L^- - 2\overline{\Sigma_R^-}\gamma^\mu\Sigma_R^-)Z_\mu \\ & + g\left[\sqrt{2}\overline{\Sigma_L^{++}}\gamma^\mu\Sigma_L^{++} + \sqrt{3}\overline{\Sigma_L^+}\gamma^\mu\Sigma_L^+ + \sqrt{3}\overline{\Sigma_L^0}\gamma^\mu\Sigma_L^0 + \sqrt{2}\overline{\Sigma_L^-}\gamma^\mu\Sigma_L^- \right. \\ & + \sqrt{2}\overline{\Sigma_R^{++}}\gamma^\mu\Sigma_R^{++} + \sqrt{3}\overline{\Sigma_R^+}\gamma^\mu\Sigma_R^+ + \sqrt{3}\overline{\Sigma_R^0}\gamma^\mu\Sigma_R^0 + \sqrt{2}\overline{\Sigma_R^-}\gamma^\mu\Sigma_R^- \\ & \left. + \frac{1}{\sqrt{2}}\bar{l}_L\gamma^\mu\nu_L\right]W_\mu^- + \text{H.c.}, \quad (\text{C.17}) \end{aligned}$$

where  $c_W = \cos\theta_W$  and  $s_W = \sin\theta_W$ .

In the mass-eigenstate basis we obtain the terms involving the heavy fermion, light fermion and gauge boson fields that are relevant for the decays of heavy leptons. In the following, we focus only on the above terms and restrict to couplings of the order  $M_\Sigma^{-1}$ . Whereas the photon couplings to all leptons and  $Z$  couplings to triply and doubly charged leptons are diagonal in the mass-eigenstate basis, the couplings of  $Z$ -boson to singly-charged and neutral leptons are more complicated. They are given by

$$\mathcal{L}_{NCZ} \equiv (\mathcal{L}_{NCZ}^A + \mathcal{L}_{NCZ}^B + \mathcal{L}_{NCZ}^C + \text{H.c.}), \quad (\text{C.18})$$



where

$$\begin{aligned}
\mathcal{L}_{NCZ}^A &= \frac{g}{c_W} \overline{l}_m V_{Zl\Sigma^-}^L \gamma^\mu P_L \Sigma_{m'}^- Z_\mu^0, \\
\mathcal{L}_{NCZ}^B &= \frac{g}{c_W} (\overline{l}_m)^c V_{Zl\Sigma^+}^R \gamma^\mu P_R \Sigma_{m'}^+ Z_\mu^0, \\
\mathcal{L}_{NCZ}^C &= \frac{g}{c_W} [\overline{\nu}_m V_{Z\nu\Sigma^0}^L \gamma^\mu P_L \Sigma_{m'}^0 Z_\mu^0 + \overline{\nu}_m V_{Z\nu\Sigma^0}^R \gamma^\mu P_R \Sigma_{m'}^0 Z_\mu^0].
\end{aligned} \tag{C.19}$$

Here, the matrix couplings, up to order  $M_\Sigma^{-1}$ , are given by

$$\begin{aligned}
V_{Zl\Sigma^-}^L &= -2U_{\Sigma^- l}^{L\dagger} - \frac{1}{2}U_{l\Sigma^-}^L, & V_{Zl\Sigma^+}^R &= \frac{1}{2}U_{l(\Sigma_R^+)^c}^{L*}, \\
V_{Z\nu\Sigma^0}^L &= -2U_{\Sigma^0 L\nu}^{0\dagger} - \frac{1}{2}U_{\nu\nu}^{0\dagger}U_{\nu\Sigma^0}^0, & V_{Z\nu\Sigma^0}^R &= \frac{1}{2}U_{\nu\nu}^{0T}U_{\nu(\Sigma_R^0)^c}^{0*}.
\end{aligned} \tag{C.20}$$

Analogously, the charged current interactions are given by

$$\mathcal{L}_{CC} \equiv (\mathcal{L}_{CC}^A + \mathcal{L}_{CC}^B + \mathcal{L}_{CC}^C + \mathcal{L}_{CC}^D + \mathcal{L}_{CC}^E + \text{H.c.}), \tag{C.21}$$

where

$$\begin{aligned}
\mathcal{L}_{CC}^A &= g[\overline{\nu}_m V_{\nu\Sigma^+}^L \gamma^\mu P_L \Sigma_{m'}^+ W_\mu^- + \overline{\nu}_m V_{\nu\Sigma^+}^R \gamma^\mu P_R \Sigma_{m'}^+ W_\mu^-], \\
\mathcal{L}_{CC}^B &= g[\overline{\Sigma}_m^- V_{\Sigma^- \nu}^L \gamma^\mu P_L \nu_{m'} W_\mu^- + \overline{\Sigma}_m^- V_{\Sigma^- \nu}^R \gamma^\mu P_R \nu_{m'} W_\mu^-], \\
\mathcal{L}_{CC}^C &= g\overline{l}_m V_{l\Sigma^0}^L \gamma^\mu P_L \Sigma_{m'}^0 W_\mu^-, \\
\mathcal{L}_{CC}^D &= g\overline{\Sigma}_m^0 V_{\Sigma^0 l}^R \gamma^\mu P_R (l_{m'})^c W_\mu^-, \\
\mathcal{L}_{CC}^E &= g(\overline{l}_m)^c V_{l\Sigma^{++}}^R \gamma^\mu P_R \Sigma_{m'}^{++} W_\mu^-,
\end{aligned} \tag{C.22}$$

and up to order  $M_\Sigma^{-1}$

$$\begin{aligned}
V_{\nu\Sigma^+}^L &= \sqrt{3}U_{\Sigma^0 L\nu}^{0\dagger}, & V_{\nu\Sigma^+}^R &= \sqrt{3}U_{(\Sigma_R^0)^c\nu}^{0T} - \frac{1}{\sqrt{2}}U_{\nu\nu}^{0T}U_{l(\Sigma_R^+)^c}^{L*}, \\
V_{\Sigma^- \nu}^L &= \frac{1}{\sqrt{2}}U_{l\Sigma^-}^{L\dagger}U_{\nu\nu}^0 + \sqrt{2}U_{\Sigma^0 L\nu}^0, & V_{\Sigma^- \nu}^R &= \sqrt{2}U_{(\Sigma_R^0)^c\nu}^{0*}, \\
V_{l\Sigma^0}^L &= \sqrt{2}U_{\Sigma^- l}^{L\dagger} + \frac{1}{\sqrt{2}}U_{\nu\Sigma^0}^0, & V_{\Sigma^0 l}^R &= \sqrt{3}U_{(\Sigma_R^+)^c l}^{L*} - \frac{1}{\sqrt{2}}U_{\nu(\Sigma_R^0)^c}^{0T}, \\
V_{l\Sigma^{++}}^R &= \sqrt{3}U_{(\Sigma_R^+)^c l}^{LT}.
\end{aligned} \tag{C.23}$$

Finally, by suppressing the indices  $m$  and  $m'$  and by defining

$$V_1 = \sqrt{\frac{1}{10}} Y_1^\dagger v_{\Phi_1} M_\Sigma^{-1}, V_2 = \sqrt{\frac{1}{10}} Y_2^\dagger v_{\Phi_2}^* M_\Sigma^{-1}, \quad (\text{C.24})$$

we obtain more compact expressions

$$\begin{aligned} \mathcal{L}_{NCZ} &= \frac{g}{c_W} \left[ \bar{\nu} \left( \frac{3}{2} V_{PMNS}^\dagger V_1 \gamma^\mu P_L + \frac{-\sqrt{3}}{2\sqrt{2}} V_{PMNS}^T V_2^* \gamma^\mu P_R \right) \Sigma^0 \right. \\ &\quad \left. + \bar{l} (3V_1 \gamma^\mu P_L) \Sigma^- + \bar{l}^c \left( \frac{1}{2} V_2^* \gamma^\mu P_R \right) \Sigma^+ \right] Z_\mu^0 + \text{H.c.} \end{aligned} \quad (\text{C.25})$$

and

$$\begin{aligned} \mathcal{L}_{CC} &= g \left[ \bar{\nu} \left( -\sqrt{3} V_{PMNS}^\dagger V_1 \gamma^\mu P_L + \sqrt{2} V_{PMNS}^T V_2^* \gamma^\mu P_R \right) \Sigma^+ \right. \\ &\quad \left. + \bar{\Sigma}^- \left( \sqrt{3} V_2^T V_{PMNS}^* \gamma^\mu P_R \right) \nu + \bar{l} \left( -\frac{3}{\sqrt{2}} V_1 \gamma^\mu P_L \right) \Sigma^0 \right. \\ &\quad \left. + \bar{\Sigma}^0 \left( -\frac{\sqrt{3}}{2} V_2^T \gamma^\mu P_R \right) l^c + \bar{l}^c \left( -\sqrt{3} V_2^* \gamma^\mu P_R \right) \Sigma^{++} \right] W_\mu^- + \text{H.c.} . \end{aligned}$$

Note that the interactions involving light neutrinos in the above have the additional  $U_{PMNS}$  factor compared with those involving light charged leptons.



# Chapter 5

## Prošireni sažetak: Kvintuplet teških leptona i mehanizam njihalice na skali TeV-a

Ova disertacija izlaže dva originalna modela njihalice koja se temelje na uvođenju leptona smještenih u kvintupletnu reprezentaciju slabog izospina. U prvom modelu riječ je o Majoraninom kvintupletu hipernaboja nula praćenog sa skalarnim kvadrupletom. U drugom modelu Diracov kvintuplet neisčezavajućeg hipernaboja praćen je s dva skalarna kvadrupleta. U oba modela neutrinske mase se pojavljuju ili na granastoj razini od operatora dimenzije devet ili na razini petlje od operatora dimenzije pet. To omogućuje da novouvedena stanja budu u doseg velikog hadronskog sudarivača (LHC, od engl. Large Hadron Collider).

### § 5.1 Oscilacije, mase i miješanja neutrina

Potvrđeno je da neutriini nastali u slabom procesu nakon proputovanja konačne udaljenosti mijenjaju svoju vrstu, okus. Promjenu okusa neutrina tijekom propagacije nazivamo neutrinskim oscilacijama [1, 2, 3], jer vjerojatnost promjene okusa neutrina oscilatorno ovisi o energiji neutrina i udaljenosti propagacije. U mnogim neutrinskim eksperimentima opaženo je nestajanje ili pojavljivanje pojedinog neutrinskog okusa zbog neutrinskih

oscilacija:

- Nestajanje solarnih elektronskih neutrina  $\nu_e$  u solarnim neutrinским pokusima [4, 5, 6, 7, 8, 9, 10, 11, 12].
- Nestajanje atmosferskih mionskih neutrina  $\nu_\mu$  i antineutrina  $\bar{\nu}_\mu$  u pokusu Super-Kamiokande [13, 14].
- Nestajanje reaktorskih elektronskih antineutrina  $\bar{\nu}_e$  u reaktorskom pokusu KamLAND [15, 16].
- Nestajanje mionskih neutrina  $\nu_\mu$  u pokusima dugih snopova (engl. long-baseline) akcelerskih neutrina K2K [17] i MINOS [18, 19].
- Pojavljivanje elektronskih neutrina  $\nu_e$  u snopu mionskih neutrina  $\nu_\mu$  u pokusima dugih snopova akcelerskih neutrina T2K [20] i MINOS [21].
- Nestajanje reaktorskih elektronskih antineutrina  $\bar{\nu}_e$  u bliskim (engl. short-baseline) reaktorskim pokusima Daya Bay [22] i RENO [23].

Ti pokusi pokazuju da su poznata okusna stanja ( $\nu_e, \nu_\mu, \nu_\tau$ ) koja se pojavljuju u nabijenim slabim strujama linearna kombinacija vlastitih stanja neutrinских masa ( $\nu_1, \nu_2, \nu_3$ )

$$\nu_l(x) = \sum_{i=1}^3 U_{li} \nu_i(x), \quad l = e, \mu, \tau. \quad (5.1)$$

$U$  je unitarna matrica neutrinškog miješanja [1, 2, 3], nazvana Pontecorvo-Maki-Nakagawa-Sakata-*inom* ( $U_{PMNS}$ ) parametriziranom na način

$$U_{PMNS} = \begin{pmatrix} c_{12}c_{13} & s_{12}c_{13} & s_{13}e^{-i\delta} \\ -s_{12}c_{23} - c_{12}s_{23}s_{13}e^{i\delta} & c_{12}c_{23} - s_{12}s_{23}s_{13}e^{i\delta} & s_{23}c_{13} \\ s_{12}s_{23} - c_{12}c_{23}s_{13}e^{i\delta} & -c_{12}s_{23} - s_{12}c_{23}s_{13}e^{i\delta} & c_{23}c_{13} \end{pmatrix} \times P, \quad (5.2)$$

gdje je  $P = \text{diag}(1, e^{i\alpha}, e^{i\beta})$ ,  $c_{ij} = \cos \theta_{ij}$  and  $s_{ij} = \sin \theta_{ij}$ . Ovdje su  $\theta_{12}$ ,  $\theta_{23}$  i  $\theta_{13}$  solarni, atmosferski i reaktorski kut miješanja. Faza  $\delta$  je Diracova faza CP narušenja, a faze  $\alpha$  and  $\beta$  su dvije Majoranine faze CP narušenja.

Globalna analiza [24] postojećih podataka o neutrinским oscilacijama daje vrijednosti za veličine prikazane u tablici 5.1.

| parametar                                | prilagodba fit | interval $3\sigma$ |
|--|----------------|--------------------|
| $\Delta m_{21}^2 [10^{-5}\text{eV}^2]$   | 7.62           | 7.12–8.20          |
| $ \Delta m_{31}^2  [10^{-3}\text{eV}^2]$ | 2.55           | 2.31 – 2.74        |
|  | 2.43           | 2.21 – 2.64        |
| $\sin^2 \theta_{12}$                     | 0.320          | 0.27–0.37          |
| $\sin^2 \theta_{23}$                     | 0.613          | 0.36–0.68          |
|  | 0.600          | 0.37–0.67          |
| $\sin^2 \theta_{13}$                     | 0.0246         | 0.017–0.033        |
|  | 0.0250         |                    |
| $\delta$                                 | $0.80\pi$      | $0 - 2\pi$         |
|  | $-0.03\pi$     |                    |

Table 5.1: Globalna prilagodba [24] parametara neutrinjskih oscilacija.  $\Delta m_{ij}^2 = m_i^2 - m_j^2$  je razlika kvadrata masa, pri čemu gornji (donji) redci za  $\Delta m_{31}^2$ ,  $\sin^2 \theta_{23}$ ,  $\sin^2 \theta_{13}$  i  $\delta$  odgovaraju normalnoj (invertiranoj) hijerarhiji neutrinjskih masa.

### 5.1.1 Mehanizmi njihalice

Neisčezavajuće neutrinjske mase predstavljaju prvo opipljivo odstupanje od standardnog modela. Da bi objasnili male mase neutrina treba proširiti čestični sastav standardnog modela novim stupnjevima slobode. Neutrinjske mase se mogu realizirati efektivnim operatorom dimenzije pet

$$\mathcal{L} = \frac{\bar{l}_L \tilde{H} \tilde{H}^T l_L^c}{\Lambda}, \quad (5.3)$$

kojeg je uveo Weinberg [25]. To je jedini efektivni operator dimenzije pet u standardnom modelu i vodi na neutrinjske mase potisnute visokom masenom skalom  $\Lambda$ . Weinbergov operator se može generirati na granastom nivou i na nivou kvantnih petlji. Na granastom nivou postoje samo tri realizacije efektivnog operatora dimenzije pet [26]: mehanizam njihalice tipa I [27, 28, 29, 30, 31], tipa II [32, 33, 34, 35, 36, 37] i tipa III [38], prenošene teškim fermionskim singletom  $N_R$ , skalarnim tripletom  $\Delta$  i fermionskim tripletom  $\Sigma_R$ . U uobičajenoj slici mehanizma njihalice mase novih stupnjeva slobode su povezane sa skalom teorija velikog ujedinjenja. Kao posljedica, mogućnost direktnog testiranja tih mehanizama njihalice čini se praktično nemoguća. Iz

tog razloga predložen je niz modela u kojima se skala njihalice spušta na skalu TeV-a kako bi ti modeli mogli biti eksperimentalno provjereni.

### 5.1.2 Mehanizmi njihalice na niskoj skali

Mehanizam njihalice na niskoj skali može se ostvariti kraćenjem doprinosa neutrinjskim masama u mehanizmu njihalice tipa I [39, 40, 41]. Izučena je i mogućnost kraćenja između doprinosa neutrinjskim masama od tipa I i od tipa II [42, 43]. U modelu inverzne njihalice [44, 45] skala TeV-a se pojavljuje po konstrukciji.

Mehanizam njihalice na niskoj skali se može ostvariti i generiranjem masa neutrina na razini petlje. Takav model je prvo uveden na razini jedne petlje u [46]. Ova ideja je kasnije primjenjena u mehanizmima na razini jedne [47], dvije [49, 48, 50] i tri petlje [51, 52].

U modelu višestruke njihalice predložene u [53] i primjenjene u [54] uvode se diskretne simetrije i dodatna polja bitna za spuštanje skale njihalice na skalu TeV-a [55].

### 5.1.3 Reprezentacije viših dimenzija

Svi fermioni i skalari standardnog modela transformiraju se u odnosu na faktore grupe standardnog modela  $SU(3)_C \times SU(2)_L \times U(1)_Y$  bilo kao singleti, bilo kao fundamentalne reprezentacije. Multiplieti koji se transformiraju kao reprezentacije viših dimenzija grupe slabog izospina  $SU(2)_L$  izučavani su u modelima neutrinjskih masa i tamne tvari.

Između multiplleta uvedenih u modelu minimalne tamne tvari (MDM) [56], fermionski kvintuplet  $\Sigma \sim (1, 5, 0)$  identificiran je kao najbolji kandidat za MDM. Fenomenologija tog fermionskog kvintupleta proučavana je u nizu publikacija [57, 58, 59]. Drugi kandidat za MDM, skalarni septuplet  $\Phi \sim (1, 7, 0)$ , proučavan je u [60].

Najpoznatiji izučavan višedimenzionalni multiplet je fermionski triplet hipernaboja nula iz mehanizma njihalice tipa III [38]. Triplet neisčezavajućeg hipernaboja  $\Sigma_{L,R} \sim (1, 3, 2)$  upotrebljen je, u sprezi sa skalarnih kvadrupletom  $\Phi \sim (1, 4, -3)$ , za generiranje neutrinskih masa na granastom nivou od operatora dimenzije sedam [61].

Pokušaj povezivanja radijacijskog generiranja neutrinskih masa i MDM bez dodatnih simetrija izvan standardnog modela ( $R\nu$ MDM) učinjen je u [62] i potom primjenjen na izučavanje barionske asimetrije [63]. U [64] su nađeni dodatni renormalizabilni operatori koji narušavaju stabilnost tako predložene MDM.

## § 5.2 Model s Majoraninim leptonskim kvintupletom

Model s Majoraninim leptonskim kvintupletom koji ovdje prikazujemo naličuje na poopćenje modela njihalice tipa III s tripletnih na kvintupletne medijatore. Pritom, da bi ostvarili njihalicu na granastoj razini moramo fermionskom medijatoru slabog izospina većeg od jedinice pridružiti skalarni multiplet koji je višeg izospina od Higgsovog dubleta SM-a. Pri konstrukciji modela njihalice moramo poštivati simetriju baždarne grupe standardnog modela,  $SU(3)_C \times SU(2)_L \times U(1)_Y$ . Fermionima standardnog modela dodajemo tri generacije leptonskih kvintupleta isčezavajućeg hipernaboja  $\Sigma_R = (\Sigma_R^{++}, \Sigma_R^+, \Sigma_R^0, \Sigma_R^-, \Sigma_R^{--})$ , koji se transformiraju s obzirom na baždarnu grupu kao  $(1, 5, 0)$ . Uz Higgsov dublet  $H = (H^+, H^0)$  uvodimo i skalarni kvadruplet  $\Phi = (\Phi^+, \Phi^0, \Phi^-, \Phi^{--})$  koji se transformira kao  $(1, 4, -1)$ .

Baždarno invarijantni, renormalizabilni langranžijan koji sadržava nova polja je

$$\mathcal{L} = \overline{\Sigma_R} i \gamma^\mu D_\mu \Sigma_R + (D_\mu \Phi)^\dagger (D_\mu \Phi) - (\overline{L}_L Y \Phi \Sigma_R + \frac{1}{2} \overline{(\Sigma_R)^C} M \Sigma_R + \text{H.c.}) - V(H, \Phi). \quad (5.4)$$

Ovdje je  $D_\mu$  kovarijantna baždarna derivacija,  $Y$  je matrica Yukawinog vezanja, a  $M$  je masena matrica teških leptona koju odabiremo da bude realna i dijagonalna. Indeksi okusa su ispušteni zbog jednostavnosti.



Raspisivanjem masenog člana po komponentama kvintupleta  $\Sigma_R$  dobivamo članove

$$\begin{aligned} \overline{(\Sigma_R)^C} M \Sigma_R &= \overline{(\Sigma_R^{++})^C} M \Sigma_R^{--} - \overline{(\Sigma_R^+)^C} M \Sigma_R^- + \overline{(\Sigma_R^0)^C} M \Sigma_R^0 \\ &- \overline{(\Sigma_R^-)^C} M \Sigma_R^+ + \overline{(\Sigma_R^{--})^C} M \Sigma_R^{++} , \end{aligned} \quad (5.5)$$

koji sadrže dva nabijena Diracova fermiona i jedan neutralni Majoranin fermion.

$$\Sigma^{++} = \Sigma_R^{++} + \Sigma_R^{--C} , \quad \Sigma^+ = \Sigma_R^+ - \Sigma_R^{-C} , \quad \Sigma^0 = \Sigma_R^0 + \Sigma_R^{0C} . \quad (5.6)$$

### 5.2.1 Skalarni potencijal

Baždarno invarijanti skalarni potencijal dan je s

$$\begin{aligned} V(H, \Phi) &= -\mu_H^2 H^{*i} H_i + \mu_\Phi^2 \Phi^{*ijk} \Phi_{ijk} + \lambda_1 (H^{*i} H_i)^2 \\ &+ \lambda_2 (H^* H \Phi^* \Phi)_1 + \lambda_3 (H^* H \Phi^* \Phi)_2 \\ &+ (\lambda_4 e^{i\alpha} H^* H H \Phi + \text{H.c.}) + (\lambda_5 e^{i\beta} H H \Phi \Phi + \text{H.c.}) \\ &+ (\lambda_6 e^{i\gamma} H \Phi^* \Phi \Phi + \text{H.c.}) + \lambda_7 (\Phi^{*ijk} \Phi_{ijk})^2 + \lambda_8 \Phi^* \Phi \Phi^* \Phi , \end{aligned} \quad (5.7)$$

gdje su svi parametri realni, a zbog jednostavnosti uzimamo da su sva kvartična vezanja realna.

Lomljenje elektroslabe simetrije (EWSB) dolazi uobičajenom vakuumskom očekivanom vrijednošću (vev)  $v_H$  Higgsovog dubleta, što odgovara negativnom predznaku člana  $\mu_H^2$  u jedn. (5.7). Elektroslabi parametar  $\rho$  diktira malu vrijednost za vev  $v_\Phi$  skalarnog kvadrupleta, a time i pozitivni predznak člana  $\mu_\Phi^2$ . Ipak, prisutnost člana  $\lambda_4$  u jedn. (5.7) vodi na inducirani vev  $v_\Phi$  polja  $\Phi^0$ . Budući da se time mijenja parametar  $\rho$  od jedinice na  $\rho \simeq 1 + 6v_\Phi^2/v_H^2$ , usporedba s eksperimentalnom vrijednošću  $\rho = 1.0004_{-0.0004}^{+0.0003}$  [66] postavlja gornju granicu  $v_\Phi \lesssim 3.2$  GeV i time postavlja granicu  $v_\Phi/v_H < 0.01$ .

Nakon EWSB neutralne komponente skalarnih polja poprimaju vakuumske vrijednosti tako da je njihov oblik

$$H^0 = \frac{1}{\sqrt{2}}(v_H + h^0 + i\chi) , \quad \Phi^0 = \frac{1}{\sqrt{2}}(v_\Phi + \varphi^0 + i\eta) . \quad (5.8)$$

Budući da su sva kvartična vezanja u skalarnom potencijalu realna, uvjet minimuma potencijala

$$\frac{\partial V_0(v_H, v_\Phi)}{\partial v_H} = 0, \quad \frac{\partial V_0(v_H, v_\Phi)}{\partial v_\Phi} = 0 \quad (5.9)$$

daje

$$\mu_H^2 = \lambda_1 v_H^2 + \left(\frac{1}{2}\lambda_2 + \frac{1}{6}\lambda_3 - \frac{2}{3}\lambda_5\right)v_\Phi^2 + \frac{\sqrt{3}}{2}\lambda_4 v_H v_\Phi - \frac{\sqrt{3}}{9}\lambda_6 \frac{v_\Phi^3}{v_H}, \quad (5.10)$$

$$\mu_\Phi^2 = -\left(\frac{1}{2}\lambda_2 + \frac{1}{6}\lambda_3 - \frac{2}{3}\lambda_5\right)v_H^2 - \frac{\sqrt{3}}{6}\lambda_4 \frac{v_H^3}{v_\Phi} + \frac{\sqrt{3}}{3}\lambda_6 v_H v_\Phi - \left(\lambda_7 + \frac{5}{9}\lambda_8\right)v_\Phi^2. \quad (5.11)$$

U vodećem redu u omjeru  $v_\Phi/v_H$ , vev  $v_\Phi$  skalarnog kvadrupleta je

$$v_\Phi \simeq -\frac{1}{2\sqrt{3}}\lambda_4 \frac{v_H^3}{\mu_\Phi^2}. \quad (5.12)$$

## 5.2.2 Mase neutrina

Vakuumska očekivana vrijednost  $v_\Phi$  generira putem jedn. (5.4) Diracov mase-ni član koji povezuje  $\nu_L$  i  $\Sigma_R^0$  i daje nedijagonalne članove u masenoj matrici neutralnih leptona

$$\mathcal{L}_{\nu\Sigma^0} = -\frac{1}{2} \left( \overline{\nu_L} \overline{(\Sigma_R^0)^C} \right) \begin{pmatrix} 0 & \frac{1}{2}Y v_\Phi \\ \frac{1}{2}Y^T v_\Phi & M \end{pmatrix} \begin{pmatrix} (\nu_L)^c \\ \Sigma_R^0 \end{pmatrix} + \text{H.c.} \quad (5.13)$$

Nakon dijagonalizacije masene matrice neutralnih leptona, neutriini dobivaju Majoraninu masenu matricu

$$(m_\nu)_{ij}^{tree} = -\frac{1}{4}v_\Phi^2 \sum_k \frac{Y_{ik}Y_{jk}}{M_k}. \quad (5.14)$$

Zajedno s induciranom vev iz jednadžbe (5.12), dobivamo

$$(m_\nu)_{ij}^{tree} = -\frac{1}{48}\lambda_4^2 \frac{v_H^6}{\mu_\Phi^4} \sum_k \frac{Y_{ik}Y_{jk}}{M_k}, \quad (5.15)$$

doprinos masi neutrina generiran operatorom dimenzije devet koji odgovara mehanizmu njihalice na granastoj razini prikazanom na slici 5.1.

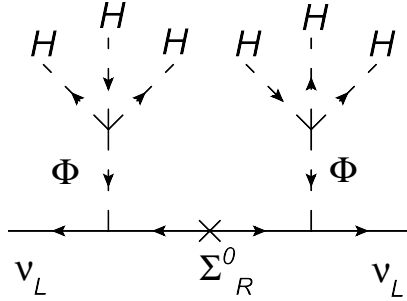


Figure 5.1: Granasti dijagram za operator dimenzije devet u jedn. (5.15). Fermionski tok odgovara Majoraninoj prirodi medijatora njihovice.

Osim na granstoj razini, mase neutrina se generiraju i na razini kvantne petlje prikazane na slici 5.2. Ako zanemarimo razlike masa unutar multipleta  $\Sigma$  i  $\Phi$ , doprinos masenoj matrici neutrina je

$$(m_\nu)_{ij}^{loop} = \frac{-5\lambda_5 v_H^2}{48\pi^2} \sum_k \frac{Y_{ik} Y_{jk} M_k}{m_\Phi^2 - M_k^2} \left[ 1 - \frac{M_k^2}{m_\Phi^2 - M_k^2} \ln \frac{m_\Phi^2}{M_k^2} \right]. \quad (5.16)$$

Zbrajanjem dvaju doprinosa dobivamo masenu matricu neutrina

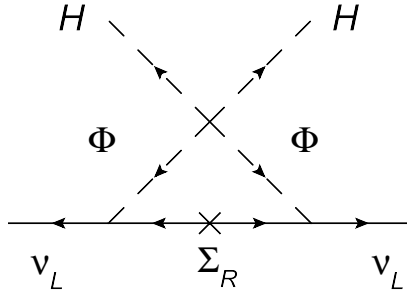


Figure 5.2: Doprinos masi lakog neutrina na razini jedne petlje.

$$\begin{aligned} (m_\nu)_{ij} &= (m_\nu)_{ij}^{tree} + (m_\nu)_{ij}^{loop} \\ &= \frac{-1}{48} \lambda_4^2 \frac{v_H^6}{\mu_\Phi^4} \sum_k \frac{Y_{ik} Y_{jk}}{M_k} + \frac{-5\lambda_5 v_H^2}{48\pi^2} \sum_k \frac{Y_{ik} Y_{jk} M_k}{m_\Phi^2 - M_k^2} \left[ 1 - \frac{M_k^2}{m_\Phi^2 - M_k^2} \ln \frac{m_\Phi^2}{M_k^2} \right]. \end{aligned} \quad (5.17)$$

U slučaju da su mase novih leptona i novih skalara približno jednake, masena matrica neutrina je

$$(m_\nu)_{ij} = \left[ \frac{-1}{48} \lambda_4^2 \frac{v_H^6}{\mu_\Phi^4} + \frac{-5\lambda_5 v_H^2}{96\pi^2} \right] \sum_k \frac{Y_{ik} Y_{jk}}{M_k}. \quad (5.18)$$

Pomoću tog izraza možemo procijeniti skalu visokih energija u našem modelu. Ilustracije radi, uzimamo iste vrijednosti za masene parametre ( $\mu_\Phi = M_\Sigma = \Lambda_{NP}$ ) i empirijske vrijednosti  $v_H = 246$  GeV i  $m_\nu \sim 0.1$  eV. Za umjerene vrijednosti parametara  $Y \sim 10^{-3}$ ,  $\lambda_4 \sim 10^{-2}$  i  $\lambda_5 \sim 10^{-4}$  dobivamo  $\Lambda_{NP} \simeq 440$  GeV. Nova stanja tih masa mogu se testirati na LHC-u.

Na slici 5.3 je prikazana razdijelnica dvaju sektora u kojima dominira granasti doprinos ili doprinos kvantne petlje.

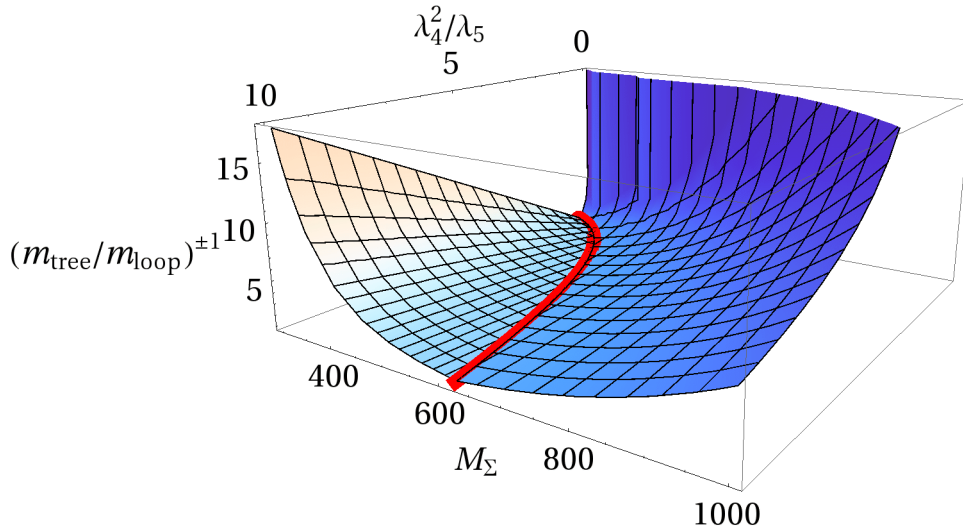


Figure 5.3: Lijevo od razdijelnice, gdje dominira granasti doprinos neutrinjskoj masi, prikazan je omjer  $m_{tree}/m_{loop}$ . Desno od razdijelnice, gdje dominira doprinos kvantne petlje, prikazan je omjer  $m_{loop}/m_{tree}$ .

### 5.2.3 Produkcija stanja Majoraninog kvintupleta na LHC-u

Produkcija teških leptona iz kvintupleta odvija se na LHC-u putem anihilacija kvarka i antikvarka u neutralne i nabijene baždarne bozone

$$q + \bar{q} \rightarrow A \rightarrow \Sigma + \bar{\Sigma}, \quad A = \gamma, Z, W^\pm,$$

i određena je langranžijanom

$$\begin{aligned} \mathcal{L}_{gauge}^{\Sigma\bar{\Sigma}} = & + e(2\bar{\Sigma}^{++}\gamma^\mu\Sigma^{++} + \bar{\Sigma}^+\gamma^\mu\Sigma^+)A_\mu \\ & + g \cos \theta_W(2\bar{\Sigma}^{++}\gamma^\mu\Sigma^{++} + \bar{\Sigma}^+\gamma^\mu\Sigma^+)Z_\mu \\ & + g(\sqrt{2}\bar{\Sigma}^+\gamma^\mu\Sigma^{++} + \sqrt{3}\bar{\Sigma}^0\gamma^\mu\Sigma^+)W_\mu^- + \text{H.c.} . \end{aligned} \quad (5.19)$$

Udarni presjek partonskog procesa je

$$\hat{\sigma}(q\bar{q} \rightarrow \Sigma\bar{\Sigma}) = \frac{\beta(3 - \beta^2)}{48\pi} \hat{s}(V_L^2 + V_R^2) , \quad (5.20)$$

gdje je  $\hat{s} \equiv (p_q + p_{\bar{q}})^2$  Mandelstamova varijabla sustava kvarka i antikvarka, parametar  $\beta \equiv \sqrt{1 - 4M_\Sigma^2/\hat{s}}$  označava brzinu teškog leptona, a lijeva i desna vezanja su dana izrazima

$$V_{L,R}^{(\gamma+Z)} = \frac{Q_\Sigma Q_q e^2}{\hat{s}} + \frac{g^{Z\Sigma} g_{L,R}^q g^2}{c_W^2(\hat{s} - M_Z^2)} , \quad (5.21)$$

$$V_L^{(W^-)} = \frac{g^{W\Sigma} g^2 V_{ud}}{\sqrt{2}(\hat{s} - M_W^2)} = V_L^{(W^+)*} , \quad (5.22)$$

$$V_R^{(W^\pm)} = 0 . \quad (5.23)$$

Kvarkovska vezanja na  $Z$  bozon su  $g_L^q = T_3 - s_W^2 Q_q$  i  $g_R^q = -s_W^2 Q_q$ , a vektorska vezanja teških leptona na baždarne bozone su

$$g^{Z\Sigma} = T_3 - s_W^2 Q_\Sigma \text{ and } g^{W\Sigma} = \sqrt{2} \text{ or } \sqrt{3} , \quad (5.24)$$

gdje se  $g^{W\Sigma}$  može očitati iz zadnjeg retka jedn. (5.19), relevantnog za produkciju parova  $\Sigma^{++}\bar{\Sigma}^+$  i  $\Sigma^+\bar{\Sigma}^0$ .

Da bi dobili udarne presjeke za hadrone partonski izrazi iz jedn. (5.20) moraju se prointegrirati preko odgovarajućih partonskih distribucijskih funkcija (PDFs od engl. parton distribution functions),  $q(x, \mu^2)$ . Pri izračunu udarnih presjeka rabimo CTEQ6.6 PDFs [68] putem LHAPDF-a [69] uz odabir faktorizacijske skale  $\mu = M_\Sigma$ .

Na slici 5.4 prikazujemo očekivani broj proizvedenih dvostruko nabijenih čestica  $\Sigma^{++}$  i  $\bar{\Sigma}^{++}$  za tri tipične postavke sudarivača. Specifično, za  $M_\Sigma = 400$  GeV i  $5 \text{ fb}^{-1}$  integriranog luminoziteta na LHC-u tijekom 2011. pri  $\sqrt{s} = 7$  TeV i  $21 \text{ fb}^{-1}$  integriranog luminoziteta na LHC-u tijekom 2012. pri  $\sqrt{s} = 8$  TeV, proizvelo bi se oko 3200 dvostruko nabijenih fermiona. Ukupno bi se proizvelo 4000 svih parova  $\Sigma - \bar{\Sigma}$ .

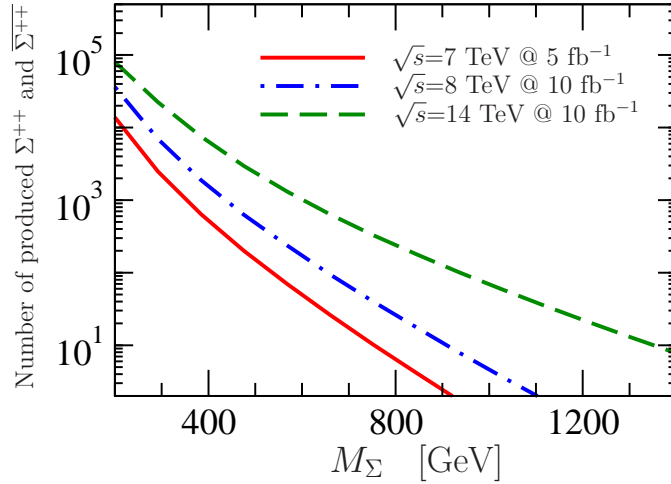


Figure 5.4: Broj proizvedenih dvostruko nabijenih čestica  $\Sigma^{++}$  i  $\overline{\Sigma}^{++}$  za tri tipične postavke sudarivača, u ovisnosti o masi teškog leptona  $M_\Sigma$ .

Eksperimentalnom provjerom proizvodnje teških leptona mogli bi identificirati kvantne brojeve čestica iz kvintupleta, ali da bi potvrdili njihovu ulogu u generiranju neutrinjskih masa treba također proučiti njihove raspade.

### 5.2.4 Raspadi leptona iz Majoraninog kvintupleta

Uz pretpostavku da su egzotični skalari nešto teži od naših egozičnih leptona, ti se skalari neće pojavljivati u konačnim stanjima ovdje izučavanih raspada teških leptona. Jakosti vezanja odgovornih za raspade pojavljuju se u nedijagonalnim članovima masenih matrica. Diagonalizacijom tih matrica dobiva se lagranžijan u masenoj bazi

$$\begin{aligned} \mathcal{L}_{NCZ} = & \frac{g}{c_W} \left[ \bar{\nu} \left( \frac{1}{2\sqrt{2}} U_{PMNS}^\dagger V \gamma^\mu P_L - \frac{1}{2\sqrt{2}} U_{PMNS}^T V^* \gamma^\mu P_R \right) \Sigma^0 \right. \\ & \left. + \bar{l}^c \left( \frac{\sqrt{3}}{4} V^* \gamma^\mu P_R \right) \Sigma^+ + \text{H.c.} \right] Z_\mu^0, \end{aligned} \quad (5.25)$$

|  | $\Sigma^{++} \rightarrow \ell^- W^-$<br>(0.66) | $\Sigma^+ \rightarrow \ell^- Z^0$<br>(0.06) | $\Sigma^0 \rightarrow \ell^+ W^-$<br>(0.30) | $\Sigma^0 \rightarrow \ell^- W^+$<br>(0.30) |
|--|--|---|---|---|
| $\Sigma^{++} \rightarrow \ell^+ W^+$<br>(0.66) | $\ell^+ \ell^- W^+ W^-$<br>(0.44)              | $\ell^+ \ell^- W^+ Z^0$<br>(0.04)           | -<br>-                                      | -<br>-                                      |
| $\Sigma^+ \rightarrow \ell^+ Z^0$<br>(0.06)    | $\ell^+ \ell^- Z^0 W^-$<br>(0.04)              | $\ell^+ \ell^- Z^0 Z^0$<br>(0.004)          | $\ell^+ \ell^+ Z^0 W^-$<br>(0.02)           | $\ell^+ \ell^- Z^0 W^+$<br>(0.02)           |
| $\Sigma^0 \rightarrow \ell^- W^+$<br>(0.30)    | -<br>-   | $\ell^- \ell^- W^+ Z^0$<br>(0.02)           | -<br>-                                      | -<br>-                                      |
| $\Sigma^0 \rightarrow \ell^+ W^-$<br>(0.30)    | -<br>-   | $\ell^+ \ell^- W^- Z^0$<br>(0.02)           | -<br>-                                      | -<br>-                                      |

Table 5.2: Raspadi egzotičnih leptona na leptone SM-a, uključujući multileptonske događaje i događaje s dileptonima istog naboja. U zagradama su prikazani omjeri grananja za leptone ( $l = e, \mu$ ) i  $M_\Sigma = 400$  GeV.

za interakciju neutralne struje i lagranžijan

$$\begin{aligned}
\mathcal{L}_{CC} = & g \left[ \bar{\nu} \left( -\sqrt{\frac{3}{2}} U_{PMNS}^\dagger V \gamma^\mu P_L + \frac{-\sqrt{3}}{2\sqrt{2}} U_{PMNS}^T V^* \gamma^\mu P_R \right) \Sigma^+ \right. \\
& + \bar{l} (-V \gamma^\mu P_L) \Sigma^0 \\
& \left. + \bar{l}^c \left( \sqrt{\frac{3}{2}} V^* \gamma^\mu P_R \right) \Sigma^{++} \right] W_\mu^- + \text{H.c.} , \tag{5.26}
\end{aligned}$$

za interakciju nabijene struje, gdje je matrica  $V$  dana s

$$(V)_{l\Sigma} = \left( \frac{v_\Phi}{\sqrt{2}} Y M^{-1} \right)_{l\Sigma} . \tag{5.27}$$

Neutralni lepton  $\Sigma^0$  se raspada kao  $\Sigma^0 \rightarrow \ell^\mp W^\pm$  i  $\Sigma^0 \rightarrow \nu_m Z^0$ . Jednostruko nabijeni  $\Sigma^+$  se raspada kao  $\Sigma^+ \rightarrow \ell^+ Z^0$  i  $\Sigma^+ \rightarrow \nu_m W^+$ , dok se dvostruko nabijeni  $\Sigma^{++}$  raspada isključivo putem nabijene struje,  $\Sigma^{++} \rightarrow \ell^+ W^+$ . Ipak, razlika masa inducirana kvantnom petljom baždarnih bozona i kvintupleta [56] omogućuje dodatni, potisnuti kanal raspada  $\Sigma^{++} \rightarrow \pi^+ \Sigma^+$  i  $\Sigma^+ \rightarrow \pi^+ \Sigma^0$ . Za ilustraciju na slici 5.5 prikazujemo širine raspada jednostruko nabijenog  $\Sigma^+$  leptona. U tablici 5.2 prikazana su konačna stanja tih raspada, pri čemu posebnu ulogu imaju stanja s dileptonima istog naboja, kao istaknuti potpis na LHC-u.

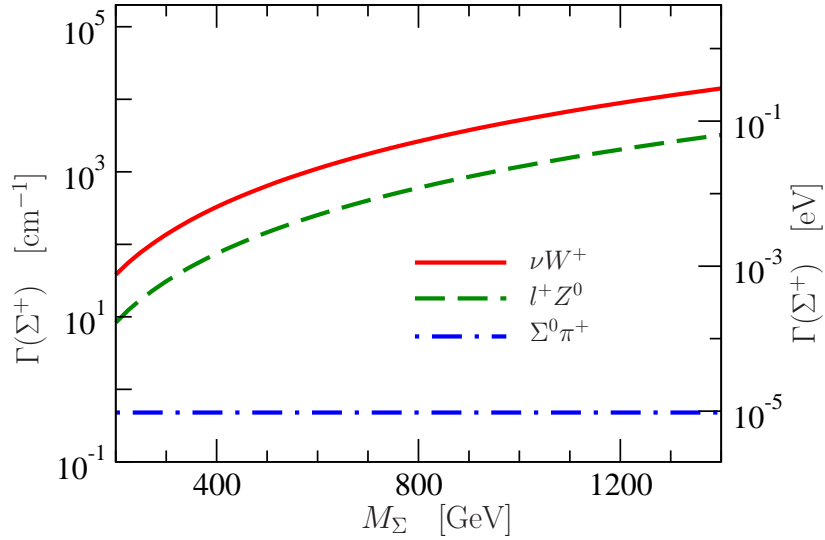


Figure 5.5: Parcijalne širine raspada teškog leptona  $\Sigma^+$  za odabranu jakost vezanja  $|V_{l\Sigma}| = 3.5 \cdot 10^{-7}$ , u ovisnosti o masi kvintupleta  $M_\Sigma$ .

### 5.2.5 Kvinuplet kao tamna tvar

Fermionski kvintuplet koji je originalno predložen za minimalnu tamnu tvar [56] u uloji medijatora njihalice je sparen sa skalarnim multipletom, što ga čini nestabilnim. Nametne li se dodatna  $Z_2$  pod kojom su teška stanja neparna ( $\Sigma \rightarrow -\Sigma$ ,  $\Phi \rightarrow -\Phi$ ) najlakše komponente tih multiplata ponovno mogu biti kandidati tamne tvari. Budući da kvartično vezanje  $\lambda_5$  nije zabranjeno dodatnom simetrijom prežive radijativno generirane mase neutrina (5.16).

Ukoliko je  $\Sigma^0$  čestica tamne tvari njena je masa određena reliktnim obiljem na vrijednost  $M_\Sigma \approx 10$  TeV [56]. Uz izbor  $\lambda_5 = 10^{-7}$  dobiva se dovoljno potisnuće neutrinških masa i za velika Yukawina vezanja,  $Y \sim 0.1$ . U tom dijelu parametarskog prostora model bi mogao voditi na zanimljive efekte narušenja leptonskog okusa [62].



## 5.2.6 Raspadi higgsa inducirani kvantnom petljom

Zanimljivo je izučiti učinke egotičnik skalarnih polja putem kvantnih petlji. Osim u već opisanom radijacijskom generiranju masa neutrina, petlje sa skalarima se pojavljuju i u rijetkim raspadim higgsa SM-a. Nedavno otkrivena rezonancija mase  $m_h \simeq 125 - 126$  GeV [74, 75] ima karakteristike higgsa, no to se još mora potvrditi. Postoje i naznake da broj događaja raspada  $h \rightarrow \gamma\gamma$  [76, 77], do na kromodinamičke neodređenosti [78], odstupaju za faktor 1.5 - 2 [79, 80] od broja očekivanog u SM-u,

$$\frac{[\sigma(gg \rightarrow h) \times \text{BR}(h \rightarrow \gamma\gamma)]_{\text{LHC}}}{[\sigma(gg \rightarrow h) \times \text{BR}(h \rightarrow \gamma\gamma)]_{\text{SM}}} = 1.71 \pm 0.33 . \quad (5.28)$$

To ukazuje na mogućnost postojanja dodatnih nabijenih čestica, poput nabijenih komponenti našeg skalarnog kvadrupleta.

Vezanja higgsa na nabijene skalare relevantna za raspad  $h \rightarrow \gamma\gamma$  su

$$-\mathcal{L} = c_{\Phi^+} v_H h^0 \Phi^{+*} \Phi^+ + c_{\Phi^-} v_H h^0 \Phi^{-*} \Phi^- + c_{\Phi^{--}} v_H h^0 \Phi^{--*} \Phi^{--} , \quad (5.29)$$

gdje su uvedena vezanja

$$c_{\Phi^+} = \lambda_2 , \quad c_{\Phi^-} = \lambda_2 + \frac{2}{3}\lambda_3 , \quad c_{\Phi^{--}} = \lambda_2 + \lambda_3 , \quad (5.30)$$

izražena kvartičnim vezanjima  $\lambda_2$  i  $\lambda_3$  u potencijalu (5.7). Time se uz dominantne doprinose od  $W$  bosona i top kvarka u SM-u, u izrazu za parcijalnu širinu raspada  $h \rightarrow \gamma\gamma$  pojavljuje doprinos nabijenih skalara [81, 94, 95, 96]

$$\Gamma(h \rightarrow \gamma\gamma) = \frac{\alpha^2 m_h^3}{256\pi^3 v_H^2} \left| A_1(\tau_W) + N_c Q_t^2 A_{1/2}(\tau_t) + N_{c,S} Q_S^2 \frac{c_S}{2} \frac{v_H^2}{m_S^2} A_0(\tau_S) \right|^2 . \quad (5.31)$$

U tim članovima  $\tau_i \equiv 4m_i^2/m_h^2$  ( $i = W, t, S$ ) odnose se na  $W$  boson spina 1, top kvark spina 1/2 i nabijene skalare spina 0 u petlji s pridruženim integralima preko petlje  $A_1(x)$ ,  $A_{1/2}(x)$ ,  $A_0(x)$ . Moguće pojačanje u odnosu na doprinose u SM-u definiran je kao u [81]

$$R_{\gamma\gamma} = \left| 1 + \sum_{S=\Phi^+, \Phi^-, \Phi^{--}} Q_S^2 \frac{c_S}{2} \frac{v_H^2}{m_S^2} \frac{A_0(\tau_S)}{A_1(\tau_W) + N_c Q_t^2 A_{1/2}(\tau_t)} \right|^2 . \quad (5.32)$$

Pojačanje će se dobiti ako doprinos nabijenih skalara interferira konstruktivno s doprinosom  $W$  bozona. Budući da to zahtjeva negativnu vrijednost

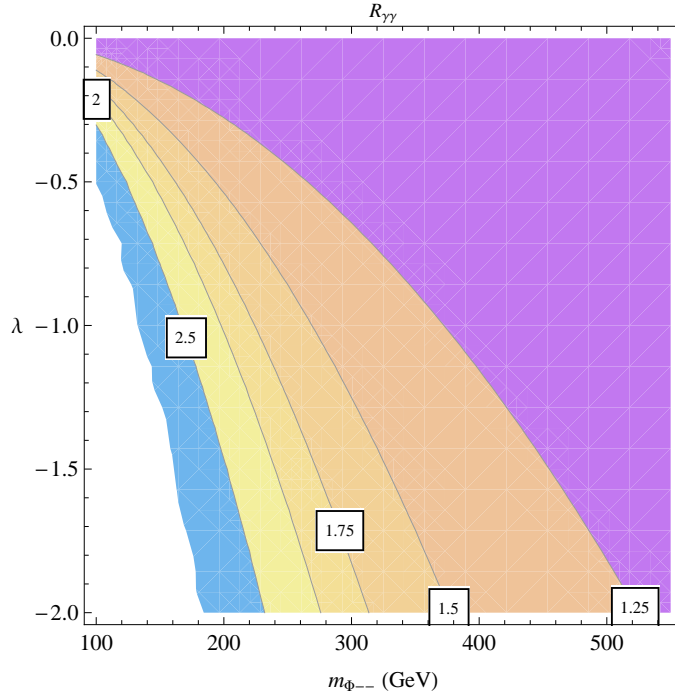


Figure 5.6: Faktor pojaćanje  $R_{\gamma\gamma} = (2.5, 2, 1.75, 1.5, 1.25)$  za širinu raspada  $h \rightarrow \gamma\gamma$  u ovisnosti o skalarnim veznjima  $\lambda = \lambda_2 = \lambda_3$  i masi  $\Phi$  multiplet,  $m(\Phi^{--})$ .

za vezanje u jedn. (5.31), promatramo  $\lambda_{2,3} < 0$ . Najveći doprinos vjerojatnosti raspada  $h \rightarrow \gamma\gamma$  dolazi od dvostruko nabijenog  $\Phi^{--}$ .

Na slici 5.6 je prikazan faktor pojaćanja  $R_{\gamma\gamma}$  kao funkcija skalarnih veznaja, gdje zbog jednostavnosti uzimamo  $\lambda_2 = \lambda_3 = \lambda$ , i mase najlakšeg nabijenog skalara  $m(\Phi^{--})$ .

Napomenimo da iste čestice u kvantnim petljama modificiraju i širinu raspada  $h \rightarrow Z\gamma$ . Pri tom opažamo antikorelaciju dva procesa. U dijelu parametarskog prostora gdje je raspada  $h \rightarrow \gamma\gamma$  znatno pojaćan, raspad  $h \rightarrow Z\gamma$  je u manjoj mjeri potisnut [93].

### 5.2.7 Mogućnost provjere na LHC-u

Velika očekivana količina produciranih teških leptona obećava mogućnost provjere modela na LHC-u. Među njima, proizvelo bi se  $\sim 3000$  dvostruko nabijenih  $\Sigma^{++}$  i  $\overline{\Sigma}^{++}$  tijekom 2011 ( $5 \text{ fb}^{-1}$ ) i 2012 ( $21 \text{ fb}^{-1}$ ), ako je njihova masa  $M_\Sigma = 400 \text{ GeV}$ . Raspadi tih stanja u dileptone istog naboja imaju zanemarivu pozadinu od SM-a [97, 98, 99, 100].

Za odabir parametara u tablici 5.2 razlikujemo četiri klase obećavajućih događaja raspada  $\Sigma^+$  na  $e^+$  ili  $\mu^+$  i  $Z^0 \rightarrow (\ell^+ \ell^-, q\bar{q})$ :

$$(i) \quad pp \rightarrow \Sigma^+ \bar{\Sigma}^+ \rightarrow (\ell^+ Z^0) (\ell^- Z^0),$$

koji ima mali udarni presjek 0.03 fb u odnosu na 0.6 fb pozadine SM-a, pri  $\sqrt{s} = 7 \text{ TeV}$  na LHC-u;

$$(ii) \quad pp \rightarrow \Sigma^+ \bar{\Sigma}^0 \rightarrow (\ell^+ Z^0) (\ell^- W^+),$$

udarnog presjeka 0.7 fb usporedivog s pozadinskim 0.8 fb;

$$(iii) \quad pp \rightarrow \Sigma^+ \bar{\Sigma}^0 \rightarrow (\ell^+ Z^0) (\ell^+ W^-),$$

događaj s narušenjem leptonskog broja, udarnog presjeka 0.7 fb, koji ne postoji u SM-u;

$$(iv) \quad pp \rightarrow \Sigma^{++} \bar{\Sigma}^+ \rightarrow (\ell^+ W^+) (\ell^- Z^0),$$

relativno velikog udarnog presjeka od 1.1 fb u odnosu na pozadinskih 0.8 fb. Posljednje dvije klase vode na signale iscrpno proučene u [73, 97, 98].

### § 5.3 Model s Diracovim leptonskim kvintupletom

Model s Diracovim leptonskim kvintupletom kojeg ovdje prikazujemo potaknut je poopćenjima SM-a koja daju prednost vektorskim fermionima u odnosu na kiralne fermione četvrte generacije. Tako je u radu [102] izučavan vektorski partner top kvarka koji mehanizmom Diracove njihalice povećava masu top kvarka [103]. Ovdje se u leptonskom sektoru ispituje mogućnost da Diracovi fermioni vektorskog tipa budu medijatori mehanizma njihalice. Oslanjanjem samo na baždarnu simetriju i renormalizabilnost SM-a uveden je novi mehanizam njihalice koji se oslanja na Diracove fermione višeg izospina. Pod tim uvjetima nađene su dvije mogućnosti realizacije njihalice prikazane u tablici 5.3: Diracov triplet uveden u [61] i Diracov kvintuplet uveden u [104], koji je predmet ovog poglavlja.

Model koji izučavamo vodi na operator  $(LLHH)(H^\dagger H)^2$  dimenzije devet i time je dostupan testovima na LHC-u. Uz leptone SM-a  $L_L$  and  $l_R$  uvodi

| Njihalica           | Novi fermion          | Novi skalar                   | Skalarno vezanje             | $m_\nu$ na   |
|---------------------|-----------------------|-------------------------------|------------------------------|--------------|
| Tip I               | $N_R \sim (1, 0)$     | -                             | -                            | dim 5        |
| Tip II              | -                     | $\Delta \sim (3, 2)$          | $\mu\Delta HH$               | dim 5        |
| Tip III             | $N_R \sim (3, 0)$     | -                             | -                            | dim 5        |
| Spregnuti medijator | Novi fermioni         | Novi skalari $\Phi_1, \Phi_2$ | Skalar - higgs vezanje       | $m_\nu$ at   |
| dublet              | $\Sigma_{L,R} (2, 1)$ | $(3, -2), (3, 0)$             | $\mu_{1,2}\Phi_{1,2}HH$      | dim 5        |
| <b>triplet</b>      | $\Sigma_{L,R} (3, 2)$ | $(4, -3), (2, -1)$            | $\lambda_1\Phi_1HHH$         | <b>dim 7</b> |
| kvadruplet          | $\Sigma_{L,R} (4, 1)$ | $(3, -2), (3, 0)$             | $\mu_{1,2}\Phi_{1,2}HH$      | dim 5        |
| <b>kvintuplet</b>   | $\Sigma_{L,R} (5, 2)$ | $(4, -3), (4, -1)$            | $\lambda_{1,2}\Phi_{1,2}HHH$ | <b>dim 9</b> |

Table 5.3: Pridruživanje elektroslabih naboja novim česticama koje vode granasti operator njihalice do dimenzije devet.

se  $n_\Sigma$  vektorskih leptonskih kvintupleta hipernaboja dva, gdje se i lijeve i desne komponente transformiraju na grupu SM-a kao  $(1, 5, 2)$ ,

$$\Sigma_{L,R} = \begin{pmatrix} \Sigma^{+++} \\ \Sigma^{++} \\ \Sigma^+ \\ \Sigma^0 \\ \Sigma^- \end{pmatrix}_{L,R} \sim (1, 5, 2) . \quad (5.33)$$

Skalarni sketor uz Higgsov dublet  $H$ , sadrži i dva skalarna kvadrupleta  $\Phi_1$  and  $\Phi_2$  koji se transformiraju kao  $(1, 4, -3)$  i  $(1, 4, -1)$ :

$$\Phi_1 = \begin{pmatrix} \phi_1^0 \\ \phi_1^- \\ \phi_1^{--} \\ \phi_1^{---} \end{pmatrix} \sim (4, -3), \quad \Phi_2 = \begin{pmatrix} \phi_2^+ \\ \phi_2^0 \\ \phi_2^- \\ \phi_2^{--} \end{pmatrix} \sim (4, -1). \quad (5.34)$$

Baždarno invarijantna Yukawina vezanja dana su lagranžijanom

$$\begin{aligned} \mathcal{L} = & \overline{\Sigma}_L i \not{D} \Sigma_L + \overline{\Sigma}_R i \not{D} \Sigma_R - \overline{\Sigma}_R M_\Sigma \Sigma_L - \overline{\Sigma}_L M_\Sigma^\dagger \Sigma_R \\ & + \left( \overline{\Sigma}_R Y_1 L_L \Phi_1^* + \overline{(\Sigma}_L)^c Y_2 L_L \Phi_2 + \text{H.c.} \right) , \end{aligned} \quad (5.35)$$

koji vodi na Diracove masene članove vektorskih polja kvintupleta

$$\begin{aligned} -\mathcal{L}_D = & \overline{\Sigma}_R^{+++} M_\Sigma \Sigma_L^{+++} + \overline{\Sigma}_R^{++} M_\Sigma \Sigma_L^{++} \\ & + \overline{\Sigma}_R^+ M_\Sigma \Sigma_L^+ + \overline{\Sigma}_R^0 M_\Sigma \Sigma_L^0 + \overline{\Sigma}_R^- M_\Sigma \Sigma_L^- + \text{H.c.} . \end{aligned} \quad (5.36)$$

U skalarnom potencijalu istaknimo renormalizabilne članove koji su relevantni za naš mehanizam

$$\begin{aligned}
V(H, \Phi_1, \Phi_2) &\sim -\mu_H^2 H^\dagger H + \mu_{\Phi_1}^2 \Phi_1^\dagger \Phi_1 + \mu_{\Phi_2}^2 \Phi_2^\dagger \Phi_2 + \lambda_H (H^\dagger H)^2 \\
&+ \{\lambda_1 \Phi_1^* H^* H^* H^* + \text{H.c.}\} + \{\lambda_2 \Phi_2^* H H^* H^* + \text{H.c.}\} \\
&+ \{\lambda_3 \Phi_1^* \Phi_2 H^* H^* + \text{H.c.}\} .
\end{aligned} \tag{5.37}$$

Uobičajeni EWSB vodi na vakuumsku vrijednost  $v_H = 246$  GeV Higgsovog dubleta i inducirane vakuumske vrijednosti

$$v_{\Phi_1} \simeq -\lambda_1 \frac{v_H^3}{\mu_{\Phi_1}^2}, \quad v_{\Phi_2} \simeq -\lambda_2 \frac{v_H^3}{\mu_{\Phi_2}^2} . \tag{5.38}$$

### 5.3.1 Mase neutrina

Tri neutralna kiralna stanja  $\nu_L$ ,  $\Sigma_L^0$  and  $(\Sigma_R^0)^c$  razapinju simetričnu masenu matricu neutralnih stanja

$$\mathcal{L}_{\nu\Sigma^0} = -\frac{1}{2} \left( \overline{(\nu_L)^c} \overline{(\Sigma_L^0)^c} \overline{\Sigma_R^0} \right) \begin{pmatrix} 0 & m_2^T & m_1^T \\ m_2 & 0 & M_\Sigma^T \\ m_1 & M_\Sigma & 0 \end{pmatrix} \begin{pmatrix} \nu_L \\ \Sigma_L^0 \\ (\Sigma_R^0)^c \end{pmatrix} + \text{H.c.} \tag{5.39}$$

Za jednostruko nabijene fermione dobivamo nesimetričnu masenu matricu

$$\mathcal{L}_{l\Sigma} = - \left( \overline{l_R} \overline{\Sigma_R^-} \overline{(\Sigma_L^+)^c} \right) \begin{pmatrix} m_l & 0 & 0 \\ m_3 & M_\Sigma & 0 \\ m_4 & 0 & M_\Sigma^T \end{pmatrix} \begin{pmatrix} l_L \\ \Sigma_L^- \\ (\Sigma_R^+)^c \end{pmatrix} + \text{H.c.} , \tag{5.40}$$

gdje su  $m_1$ ,  $m_2$ ,  $m_3$  i  $m_4$  dobiveni iz Yukawinih interakcija u jedn. (5.35):

$$\begin{aligned}
m_1 &= \sqrt{\frac{1}{10}} Y_1 v_{\Phi_1}^* , & m_2 &= -\sqrt{\frac{3}{20}} Y_2 v_{\Phi_2} , \\
m_3 &= \sqrt{\frac{2}{5}} Y_1 v_{\Phi_1}^* , & m_4 &= \sqrt{\frac{1}{10}} Y_2 v_{\Phi_2} .
\end{aligned} \tag{5.41}$$

Blok diagonalizacijom neutralne masene matrice dobiva se u vodećem redu u  $M_\Sigma^{-1}$

$$\tilde{m}_\nu \simeq -m_2^T M_\Sigma^{-1} m_1 - m_1^T M_\Sigma^{-1} m_2, \quad (5.42)$$

gdje poznata  $U_{PMNS}$  matrica dijagonalizira efektivnu masenu matricu lakih neutrina

$$U_{PMNS}^T \tilde{m}_\nu U_{PMNS} = m_\nu. \quad (5.43)$$

Korištenjem jedn. (5.41), (5.42) i (5.38) dobiva se masa lakog neutrina

$$m_\nu^{tree} \sim \frac{Y_1 Y_2 \lambda_1 \lambda_2 v_H^6}{M_\Sigma \mu_{\Phi_1}^2 \mu_{\Phi_2}^2}, \quad (5.44)$$

koja odgovara granastom operatoru dimenzije devet prikazanom na slici 5.7.

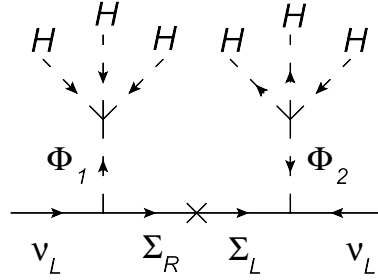


Figure 5.7: Granasti dijagram operatora dimenzije devet. Tok na fermionskoj liniji označava Diracov medijator.

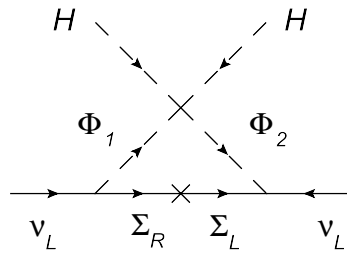


Figure 5.8: Operator dimenzije pet na razini kvantne petlje određen vezanjem  $\lambda_3$  iz jedn. (5.37).

Doprinos masi neutrina se pojavljuje na razini kvantne petlje kroz operator dimenzije pet

$$m_\nu^{loop} \sim \frac{Y_1 Y_2 \lambda_3 v_H^2}{16\pi^2 M_\Sigma}, \quad (5.45)$$

prikazan na slici 5.8.

### 5.3.2 Produkcija stanja Diracovog kvintupleta na LHC-u

Produkcija stanja Diracovog kvintupleta na LHC-u odvija se putem anihilacije kvarka i antikvarka u neutralne i nabijene baždarnе bozone

$$q + \bar{q} \rightarrow A \rightarrow \Sigma + \bar{\Sigma}, \quad A = \gamma, Z, W^\pm,$$

određene baždarnim langranžijanom

$$\begin{aligned} \mathcal{L}_{gauge}^{\Sigma\bar{\Sigma}} = & + e(3\bar{\Sigma}^{+++}\gamma^\mu\Sigma^{+++} + 2\bar{\Sigma}^{++}\gamma^\mu\Sigma^{++} + \bar{\Sigma}^+\gamma^\mu\Sigma^+ - \bar{\Sigma}^-\gamma^\mu\Sigma^-)A_\mu \\ & + \frac{g}{c_W}((2 - 3s_W^2)\bar{\Sigma}^{+++}\gamma^\mu\Sigma^{+++} + (1 - 2s_W^2)\bar{\Sigma}^{++}\gamma^\mu\Sigma^{++})Z_\mu \\ & + \frac{g}{c_W}((-s_W^2)\bar{\Sigma}^+\gamma^\mu\Sigma^+ + (-1)\bar{\Sigma}^0\gamma^\mu\Sigma^0 + (-2 + s_W^2)\bar{\Sigma}^-\gamma^\mu\Sigma^-)Z_\mu \\ & + g(\sqrt{2}\bar{\Sigma}^{++}\gamma^\mu\Sigma^{+++} + \sqrt{3}\bar{\Sigma}^+\gamma^\mu\Sigma^{++} \\ & + \sqrt{3}\bar{\Sigma}^0\gamma^\mu\Sigma^+ + \sqrt{2}\bar{\Sigma}^-\gamma^\mu\Sigma^0)W_\mu^- + \text{H.c.} . \end{aligned} \quad (5.46)$$

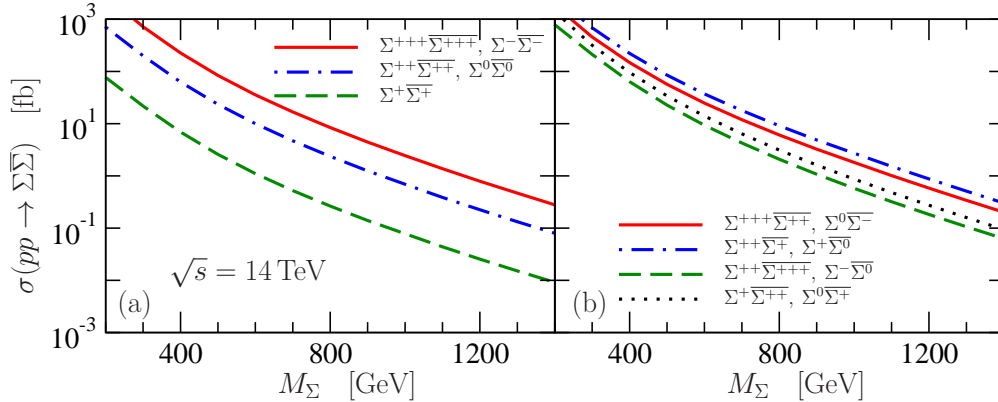


Figure 5.9: Udarni presjek produkcije para komponenti Diracovog kvintupleta putem neutralnih (a)  $\gamma, Z$  i nabijenih baždarnih bozona (b)  $W^\pm$  u ovisnosti o masi quintupleta  $M_\Sigma$  za predviđenih  $\sqrt{s} = 14$  TeV na LHC-u.

Udarni presjeci za produkciju para komponenti Diracovog kvintupleta za predviđenih  $\sqrt{s} = 14$  TeV na LHC-u prikazani su na slici 5.9. Na primjer za prikupljenih  $5 \text{ fb}^{-1}$  tijekom 2011 i  $21 \text{ fb}^{-1}$  tijekom 2012 na LHC-u

proizvelo bi se 8000 parova  $\Sigma\text{-}\bar{\Sigma}$  ako je njihova masa  $M_\Sigma = 400$  GeV. Među njima bilo bi 3300 trostruko nabijenih  $\Sigma^{+++}$  i  $\bar{\Sigma}^{+++}$  fermiona. Eksperimentalnom provjerom proizvodnje teških leptona mogli bi identificirati kvantne brojeve čestica iz kvintupleta, ali da bi potvrdili njihovu ulogu u generiranju neutrinskih masa treba također proučiti njihove raspade.

### 5.3.3 Raspadi leptona iz Diracovog kvintupleta

Uz pretpostavku da su Diracovi fermioni lakši od egzotičnih skalara oni se neće pojavljivati u konačnim stanjima raspada teških leptona. Za moguće raspade relevantne su i elektroslabe razlike masa među komponentama kvintupleta eksplicitno izračunate u [56], koje su primjerice za  $M_\Sigma = 400$  GeV

$$\begin{aligned} M_{\Sigma^{+++}} - M_{\Sigma^{++}} &\simeq 1130 \text{ MeV}, \quad M_{\Sigma^{++}} - M_{\Sigma^+} \simeq 804 \text{ MeV}, \\ M_{\Sigma^+} - M_{\Sigma^0} &\simeq 477 \text{ MeV}, \quad M_{\Sigma^0} - M_{\Sigma^-} \simeq 150 \text{ MeV}. \end{aligned} \quad (5.47)$$

#### • TOČKASTI RASPADI

Lagranžijan u masenoj bazi relevantan za raspade putem neutralnih struja ima oblik

$$\begin{aligned} \mathcal{L}_{NCZ} &= \frac{g}{c_W} \left[ \bar{\nu} \left( \frac{3}{2} U_{PMNS}^\dagger V_1 \gamma^\mu P_L - \frac{\sqrt{3}}{2\sqrt{2}} U_{PMNS}^T V_2^* \gamma^\mu P_R \right) \Sigma^0 \right. \\ &\quad \left. + \bar{l} (3V_1 \gamma^\mu P_L) \Sigma^- + \bar{l}^c \left( \frac{1}{2} V_2^* \gamma^\mu P_R \right) \Sigma^+ \right] Z_\mu^0 + \text{H.c.}, \end{aligned} \quad (5.48)$$

a putem nabijenih struja

$$\begin{aligned} \mathcal{L}_{CC} &= g \left[ \bar{\nu} \left( -\sqrt{3} U_{PMNS}^\dagger V_1 \gamma^\mu P_L + \sqrt{2} U_{PMNS}^T V_2^* \gamma^\mu P_R \right) \Sigma^+ \right. \\ &\quad \left. + \bar{\Sigma}^- \left( \sqrt{3} V_2^T U_{PMNS}^* \gamma^\mu P_R \right) \nu + \bar{l} \left( -\frac{3}{\sqrt{2}} V_1 \gamma^\mu P_L \right) \Sigma^0 \right. \\ &\quad \left. + \bar{\Sigma}^0 \left( -\frac{\sqrt{3}}{2} V_2^T \gamma^\mu P_R \right) l^c + \bar{l}^c \left( -\sqrt{3} V_2^* \gamma^\mu P_R \right) \Sigma^{++} \right] W_\mu^- + \text{H.c.}, \end{aligned} \quad (5.49)$$

gdje su matrice vezanja  $V_1$  and  $V_2$  dane izrazima

$$V_1 = \sqrt{\frac{1}{10}} Y_1^\dagger v_{\Phi_1} M_\Sigma^{-1}, \quad V_2 = \sqrt{\frac{1}{10}} Y_2^\dagger v_{\Phi_2}^* M_\Sigma^{-1}. \quad (5.50)$$



Raspadi neutralnih i jednostruko nabijenih  $\Sigma$  leptona prikazani su u tablici 5.4. Za ilustraciju prikazujemo parcijalne širine raspada neutralnih leptona na slici 5.10.

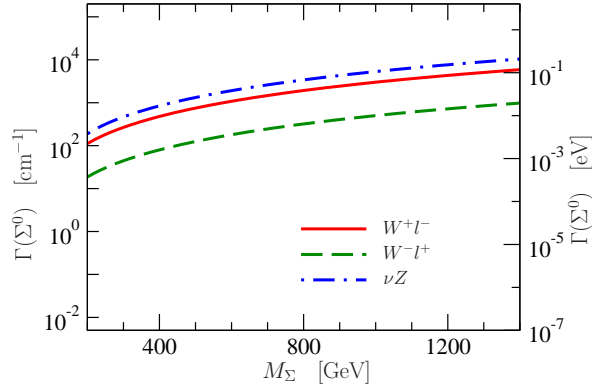


Figure 5.10: Parcijalna širina raspada neutralnog  $\Sigma^0$  leptona za  $|V_1^{\ell\Sigma}| = |V_2^{\ell\Sigma}| = 10^{-6} \sqrt{\frac{20}{M_\Sigma(\text{GeV})}}$ , u ovisnosti o masi  $M_\Sigma$ .

|                                   | $\overline{\Sigma^+} \rightarrow \ell^- Z^0$ | $\overline{\Sigma^0} \rightarrow \ell^+ W^-$ | $\overline{\Sigma^0} \rightarrow \ell^- W^+$ | $\overline{\Sigma^-} \rightarrow \ell^+ Z^0$ |
|-----------------------------------|--|--|--|--|
| $\Sigma^+ \rightarrow \ell^+ Z^0$ | $\ell^+ \ell^- Z^0 Z^0$                      | $\ell^+ \ell^+ Z^0 W^-$                      | $\ell^+ \ell^- Z^0 W^+$                      | -  |
| $\Sigma^0 \rightarrow \ell^- W^+$ | $\ell^- \ell^- W^+ Z^0$                      | $\ell^- \ell^+ W^+ W^-$                      | $\ell^- \ell^- W^+ W^+$                      | $\ell^- \ell^+ W^+ Z^0$                      |
| $\Sigma^0 \rightarrow \ell^+ W^-$ | $\ell^+ \ell^- W^- Z^0$                      | $\ell^+ \ell^+ W^- W^-$                      | $\ell^+ \ell^- W^- W^+$                      | $\ell^+ \ell^+ W^- Z^0$                      |
| $\Sigma^- \rightarrow \ell^- Z^0$ | -  | $\ell^- \ell^+ Z^0 W^-$                      | $\ell^- \ell^- Z^0 W^+$                      | $\ell^- \ell^+ Z^0 Z^0$                      |

Table 5.4: Raspadi egzotičnih leptona na čestice SM-a, uključujući događaje s narušenjem leptonskog broja.

Dvostruko nabijeno stanje  $\Sigma^{++}$  raspada se isključivo nabijenom strujom i ima parcijalnu širinu

$$\Gamma(\Sigma^{++} \rightarrow \ell^+ W^+) = \frac{g^2}{32\pi} \left| \sqrt{3} V_2^{\ell\Sigma} \right|^2 \frac{M_\Sigma^3}{M_W^2} \left( 1 - \frac{M_W^2}{M_\Sigma^2} \right)^2 \left( 1 + 2 \frac{M_W^2}{M_\Sigma^2} \right). \quad (5.51)$$

Napomenimo da takvi točkasti raspadi ne postoje za  $\Sigma^{+++}$ , na čijim raspadima ćemo se posebno zadržati.

- **KASKADNI RASPADI**

Tipični kaskadni raspad  $\Sigma^i$  na lakše stanje  $\Sigma^j$  dan izrazom

$$\Gamma(\Sigma^i \rightarrow \Sigma^j \pi^+) = (g^{W\Sigma})_{ij}^2 \frac{2}{\pi} G_F^2 |V_{ud}|^2 f_\pi^2 (\Delta M_{ij})^3 \sqrt{1 - \frac{m_\pi^2}{(\Delta M_{ij})^2}}, \quad (5.52)$$

potisnut je malom razlikom masa  $\Delta M_{ij} = M_i - M_j$  iz jedn. (5.47). Izuzetak je raspad  $\Sigma^{+++}$  gdje je razlika masa  $\Delta M_{32}$  između  $\Sigma^{+++}$  i  $\Sigma^{++}$  dovoljno velika da omogući dvopionski raspad. Ukupni tročestični raspad dominiran je rezonancijom  $\rho(770)$  i dan je izrazom

$$\Gamma(\Sigma^{+++} \rightarrow \Sigma^{++} \pi^+ \pi^0) \simeq \Gamma(\Sigma^{+++} \rightarrow \Sigma^{++} \rho^+) = \frac{24}{\pi} G_F^2 V_{ud}^2 f_\rho^2 (\Delta M_{32})^3 \left(1 - \frac{4m_\pi^2}{m_\rho^2}\right)^{-1} \sqrt{1 - \frac{m_\rho^2}{(\Delta M_{32})^2}}, \quad (5.53)$$

gdje su mezonske konstante raspada  $f_\pi \simeq 130$  MeV i  $f_\rho \simeq 150$  MeV.

- **ZLATNI RASPAD  $\Sigma^{+++} \rightarrow W^+ W^+ l^+$**

Najspektakularniji raspad Diracovog teškog leptona je  $\Sigma^{+++} \rightarrow W^+ W^+ l^+$  u  $W$  bozone na ljusci mase, prikazan Feynmanovim dijagramom na slici 5.11.

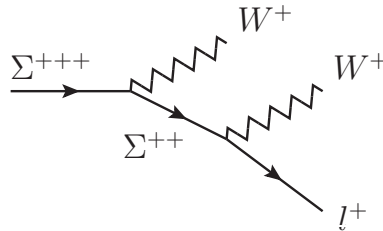


Figure 5.11: Feynmanov dijagram zlatnog raspada trostruko nabijenog leptona

Širina raspada u granici  $M_\Sigma \gg M_W$  ima prikaz

$$\Gamma(\Sigma^{+++} \rightarrow W^+ W^+ l^+) \Big|_{M_\Sigma \gg M_W} = \frac{g^2}{384 \pi^2 s_W^2} \left| \sqrt{3} V_2^{\ell\Sigma} \right|^2 \frac{M_\Sigma^5}{M_W^4}. \quad (5.54)$$

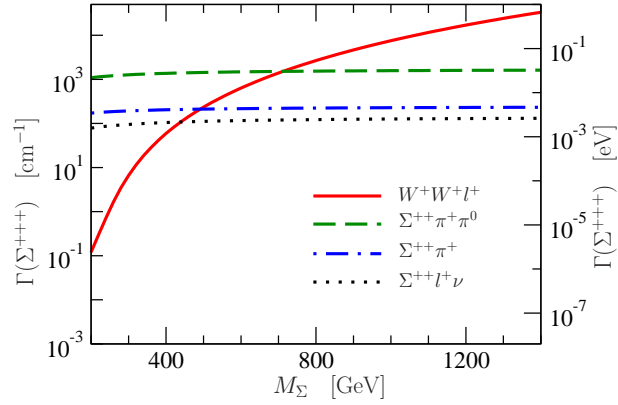


Figure 5.12: Odabrane parcijalne širine raspada leptona  $\Sigma^{+++}$  za  $|V_2^{l\Sigma}| = 10^{-6} \sqrt{\frac{800}{M_\Sigma(\text{GeV})}}$  u ovisnosti o njegovoj masi  $M_\Sigma$ .

i određen je istom jakošću kao i raspad  $\Sigma^{++}$  u jedn. (5.51). Taj raspad s preostalim raspadima  $\Sigma^{+++}$  je prikazan na slici 5.12.

Za diskutiranih prikupljenih  $5 \text{ fb}^{-1}$  tijekom 2011. i  $21 \text{ fb}^{-1}$  tijekom 2012. na LHC-u proizvelo bi se 3300 trostruko nabijenih  $\Sigma^{+++}$  i  $\overline{\Sigma}^{+++}$  fermiona, što bi rezultiralo s  $\sim 300$  raspada  $\Sigma^{+++}(\overline{\Sigma}^{+++}) \rightarrow W^\pm W^\pm l^\pm$  za  $M_\Sigma = 400 \text{ GeV}$  i  $|V_2^{l\Sigma}| = 10^{-6} \sqrt{\frac{800}{M_\Sigma(\text{GeV})}}$ .

## § 5.4 Zaključak

Puštanje u rad LHC-a omogućuje otkrića novih čestica. Budući da mase neutrina daju najopipljivije odstupanje od SM-a, za potragu su najbolje motivirane čestice koje se pojavljuju u TeV skalnim modelima njihalice za objašnjenje masa neutrina. Konvencionalni modeli njihalice zaustavljaju se na tripletima slabog izospina i pritom vode na visoku skalu njihalice. Ako takva stanja nisu ostvarena u prirodi, postoji mogućnost objašnjenja neutri-nskih masa s višim izomultipletima na nižoj skali njihalice reda TeV-a. Ova disertacija iznosi dva takva modela koja se temelje na fermionskim kvintupletima. U prvom modelu pojavljuje se Majoranin kvintuplet čija je neutralna komponenta potencijalni kandidat za tamnu tvar. U drugom modelu se pojavljuje Diracov kvintuplet koji posjeduje trostruko nabijenu komponentu provjerljivu na LHC-u.

Oba predložena modela se temelje na baždarnoj simetriji i renormalizabilnosti standardnog modela. U njima se mase neutrina pojavljuju na granastoj razini od operatora dimenzije devet i od petljom potisnutog operatora dimenzije pet. Ti kvintupleti posjeduju netrivialne baždarne naboje pa njihove komponente mogu biti obilno proizvedene i testirane na LHC-u. Pri tome se one raspadaju na višeleptonska konačna stanja uključujući dileptone istog naboja. Postavlja se pitanje mogućnosti razlikovanja Majoraninih i Diracovih kvintupleta. Zahvaljujući njegovoj trostruko nabijenoj komponenti, Diracov kvintuplet vodi na spektakularne provjerljive zapise. Već samo neopažanja trostruko nabijenih fermiona stavit će u prvi plan izučavanje Majoraninih kvintupleta. U slučaju da su kvintupleti kinematički izvan izravnog dosega LHC-a oni još uvijek mogu radijacijski generirati mase neutrina, a neutralna komponenta Majoraninog kvintupleta može biti kandidat za tamnu tvar.



# Bibliography

- [1] B. Pontecorvo, *Mesonium and anti-mesonium*, Sov. Phys. JETP **6** (1957) 429 [Zh. Eksp. Teor. Fiz. **33** (1957) 549].
- [2] B. Pontecorvo, *Inverse beta processes and nonconservation of lepton charge*, Sov. Phys. JETP **7** (1958) 172 [Zh. Eksp. Teor. Fiz. **34** (1957) 247].
- [3] Z. Maki, M. Nakagawa and S. Sakata, *Remarks on the unified model of elementary particles*, Prog. Theor. Phys. **28** (1962) 870.
- [4] B. T. Cleveland, T. Daily, R. Davis, Jr., J. R. Distel, K. Lande, C. K. Lee, P. S. Wildenhain and J. Ullman, *Measurement of the solar electron neutrino flux with the Homestake chlorine detector*, Astrophys. J. **496** (1998) 505.
- [5] Y. Fukuda *et al.* [Kamiokande Collaboration], *Solar neutrino data covering solar cycle 22*, Phys. Rev. Lett. **77** (1996) 1683.
- [6] J. N. Abdurashitov *et al.* [SAGE Collaboration], *Measurement of the solar neutrino capture rate with gallium metal. III: Results for the 2002–2007 data-taking period*, Phys. Rev. C **80** (2009) 015807 [arXiv:0901.2200 [nucl-ex]].
- [7] P. Anselmann *et al.* [GALLEX Collaboration], *Solar neutrinos observed by GALLEX at Gran Sasso*, Phys. Lett. B **285** (1992) 376.
- [8] W. Hampel *et al.* [GALLEX Collaboration], *GALLEX solar neutrino observations: Results for GALLEX IV*, Phys. Lett. B **447** (1999) 127.
- [9] M. Altmann *et al.* [GNO Collaboration], *Complete results for five years of GNO solar neutrino observations*, Phys. Lett. B **616** (2005) 174 [hep-ex/0504037].

- [10] S. Fukuda *et al.* [Super-Kamiokande Collaboration], *Determination of solar neutrino oscillation parameters using 1496 days of Super-Kamiokande I data*, Phys. Lett. B **539** (2002) 179 [hep-ex/0205075].
- [11] Q. R. Ahmad *et al.* [SNO Collaboration], *Measurement of the rate of  $\nu_e + d \rightarrow p + p + e^-$  interactions produced by B-8 solar neutrinos at the Sudbury Neutrino Observatory*, Phys. Rev. Lett. **87** (2001) 071301 [nucl-ex/0106015].
- [12] Q. R. Ahmad *et al.* [SNO Collaboration], *Direct evidence for neutrino flavor transformation from neutral current interactions in the Sudbury Neutrino Observatory*, Phys. Rev. Lett. **89** (2002) 011301 [nucl-ex/0204008].
- [13] Y. Fukuda *et al.* [Super-Kamiokande Collaboration], *Evidence for oscillation of atmospheric neutrinos*, Phys. Rev. Lett. **81** (1998) 1562 [hep-ex/9807003].
- [14] Y. Ashie *et al.* [Super-Kamiokande Collaboration], *Evidence for an oscillatory signature in atmospheric neutrino oscillation*, Phys. Rev. Lett. **93** (2004) 101801 [hep-ex/0404034].
- [15] K. Eguchi *et al.* [KamLAND Collaboration], *First results from KamLAND: Evidence for reactor anti-neutrino disappearance*, Phys. Rev. Lett. **90** (2003) 021802 [hep-ex/0212021].
- [16] T. Araki *et al.* [KamLAND Collaboration], *Measurement of neutrino oscillation with KamLAND: Evidence of spectral distortion*, Phys. Rev. Lett. **94** (2005) 081801 [hep-ex/0406035].
- [17] M. H. Ahn *et al.* [K2K Collaboration], *Measurement of Neutrino Oscillation by the K2K Experiment*, Phys. Rev. D **74** (2006) 072003 [hep-ex/0606032].
- [18] D. G. Michael *et al.* [MINOS Collaboration], *Observation of muon neutrino disappearance with the MINOS detectors and the NuMI neutrino beam*, Phys. Rev. Lett. **97** (2006) 191801 [hep-ex/0607088].
- [19] P. Adamson *et al.* [MINOS Collaboration], *Measurement of Neutrino Oscillations with the MINOS Detectors in the NuMI Beam*, Phys. Rev. Lett. **101** (2008) 131802 [arXiv:0806.2237 [hep-ex]].
- [20] K. Abe *et al.* [T2K Collaboration], *Indication of Electron Neutrino Appearance from an Accelerator-produced Off-axis Muon Neutrino Beam*, Phys. Rev. Lett. **107** (2011) 041801 [arXiv:1106.2822 [hep-ex]].

- 
- [21] P. Adamson *et al.* [MINOS Collaboration], *Improved search for muon-neutrino to electron-neutrino oscillations in MINOS*, Phys. Rev. Lett. **107** (2011) 181802 [arXiv:1108.0015 [hep-ex]].
- [22] F. P. An *et al.* [DAYA-BAY Collaboration], *Observation of electron-antineutrino disappearance at Daya Bay*, Phys. Rev. Lett. **108** (2012) 171803 [arXiv:1203.1669 [hep-ex]].
- [23] J. K. Ahn *et al.* [RENO Collaboration], *Observation of Reactor Electron Antineutrino Disappearance in the RENO Experiment*, Phys. Rev. Lett. **108** (2012) 191802 [arXiv:1204.0626 [hep-ex]].
- [24] D. V. Forero, M. Tortola and J. W. F. Valle, *Global status of neutrino oscillation parameters after Neutrino-2012*, Phys. Rev. D **86** (2012) 073012 [arXiv:1205.4018 [hep-ph]].
- [25] S. Weinberg, *Baryon and Lepton Nonconserving Processes*, Phys. Rev. Lett. **43** (1979) 1566.
- [26] E. Ma, *Pathways to naturally small neutrino masses*, Phys. Rev. Lett. **81** (1998) 1171 [hep-ph/9805219].
- [27] P. Minkowski,  *$\mu \rightarrow e\gamma$  at a Rate of One Out of 1-Billion Muon Decays?*, Phys. Lett. B **67** (1977) 421.
- [28] T. Yanagida, *Horizontal symmetry and masses of neutrinos*, in the *Proceedings of the Workshop on Unified Theory and the Baryon Number of the Universe*, O. Sawada and A. Sugamoto eds., KEK, Tsukuba Japan (1979) 95.
- [29] M. Gell-Mann, P. Ramond and R. Slansky, *Complex spinors and unified theories*, in *Supergravity*, P. van Nieuwenhuizen and D. Freedman eds., North Holland, Amsterdam The Netherlands (1979) 315.
- [30] S. L. Glashow, *The future of elementary particle physics*, in *Quarks and Leptons*, M. Lévy *et al.* eds., Plenum, New York U.S.A. (1980) 707.
- [31] R. N. Mohapatra and G. Senjanović, *Neutrino Mass and Spontaneous Parity Violation*, Phys. Rev. Lett. **44** (1980) 912.
- [32] W. Konetschny and W. Kummer, *Nonconservation of Total Lepton Number with Scalar Bosons*, Phys. Lett. B **70** (1977) 433.
- [33] M. Magg and C. Wetterich, *Neutrino Mass Problem And Gauge Hierarchy*, Phys. Lett. B **94** (1980) 61.



- 
- [34] J. Schechter and J. W. F. Valle, *Neutrino Masses in  $SU(2) \times U(1)$  Theories*, Phys. Rev. D **22** (1980) 2227.
- [35] T. P. Cheng and L.-F. Li, *Neutrino Masses, Mixings and Oscillations in  $SU(2) \times U(1)$  Models of Electroweak Interactions*, Phys. Rev. D **22** (1980) 2860.
- [36] G. Lazarides, Q. Shafi and C. Wetterich, *Proton Lifetime and Fermion Masses in an  $SO(10)$  Model*, Nucl. Phys. B **181** (1981) 287.
- [37] R. N. Mohapatra and G. Senjanović, *Neutrino Masses and Mixings in Gauge Models with Spontaneous Parity Violation*, Phys. Rev. D **23** (1981) 165.
- [38] R. Foot, H. Lew, X. G. He and G. C. Joshi, *Seesaw Neutrino Masses Induced By A Triplet Of Leptons*, Z. Phys. C **44** (1989) 441.
- [39] A. Pilaftsis, *Resonant tau-leptogenesis with observable lepton number violation*, Phys. Rev. Lett. **95** (2005) 081602 [hep-ph/0408103].
- [40] A. de Gouvea, *GeV seesaw, accidentally small neutrino masses, and Higgs decays to neutrinos*, [arXiv:0706.1732 [hep-ph]].
- [41] J. Kersten and A. Y. Smirnov, *Right-Handed Neutrinos at CERN LHC and the Mechanism of Neutrino Mass Generation*, Phys. Rev. D **76** (2007) 073005 [arXiv:0705.3221 [hep-ph]].
- [42] W. Chao, S. Luo, Z.-z. Xing and S. Zhou, *A Compromise between Neutrino Masses and Collider Signatures in the Type-II Seesaw Model*, Phys. Rev. D **77** (2008) 016001 [arXiv:0709.1069 [hep-ph]].
- [43] M. J. Luo and Q. Y. Liu, *Small Neutrino Masses From Structural cancellation In Left-Right Symmetric Model*, JHEP **0812** (2008) 061 [arXiv:0812.3453 [hep-ph]].
- [44] M. C. Gonzalez-Garcia and J. W. F. Valle, *Fast Decaying Neutrinos And Observable Flavor Violation In A New Class Of Majoron Models*, Phys. Lett. B **216** (1989) 360.
- [45] F. Deppisch and J. W. F. Valle, *Enhanced lepton flavor violation in the supersymmetric inverse seesaw model*, Phys. Rev. D **72** (2005) 036001 [hep-ph/0406040].

- 
- [46] A. Zee, *A Theory of Lepton Number Violation, Neutrino Majorana Mass, and Oscillation*, Phys. Lett. B **93** (1980) 389 [Erratum-ibid. B **95** (1980) 461].
- [47] E. Ma, *Verifiable radiative seesaw mechanism of neutrino mass and dark matter*, Phys. Rev. D **73** (2006) 077301 [hep-ph/0601225].
- [48] A. Zee, *Charged Scalar Field and Quantum Number Violations*, Phys. Lett. B **161** (1985) 141.
- [49] A. Zee, *Quantum Numbers Of Majorana Neutrino Masses*, Nucl. Phys. B **264** (1986) 99.
- [50] K. S. Babu, *Model of 'Calculable' Majorana Neutrino Masses*, Phys. Lett. B **203** (1988) 132.
- [51] L. M. Krauss, S. Nasri and M. Trodden, *A Model for neutrino masses and dark matter*, Phys. Rev. D **67** (2003) 085002 [hep-ph/0210389].
- [52] M. Aoki, S. Kanemura and O. Seto, *Neutrino mass, Dark Matter and Baryon Asymmetry via TeV-Scale Physics without Fine-Tuning*, Phys. Rev. Lett. **102** (2009) 051805 [arXiv:0807.0361 [hep-ph]].
- [53] E. Ma, *Naturally small seesaw neutrino mass with no new physics beyond the TeV scale*, Phys. Rev. Lett. **86** (2001) 2502 [hep-ph/0011121].
- [54] W. Grimus, L. Lavoura and B. Radovčić, *Type II seesaw mechanism for Higgs doublets and the scale of new physics*, Phys. Lett. B **674** (2009) 117 [arXiv:0902.2325 [hep-ph]].
- [55] Z.-z. Xing and S. Zhou, *Multiple seesaw mechanisms of neutrino masses at the TeV scale*, Phys. Lett. B **679** (2009) 249 [arXiv:0906.1757 [hep-ph]].
- [56] M. Cirelli, N. Fornengo and A. Strumia, *Minimal dark matter*, Nucl. Phys. B **753** (2006) 178 [hep-ph/0512090].
- [57] M. Cirelli, A. Strumia and M. Tamburini, *Cosmology and Astrophysics of Minimal Dark Matter*, Nucl. Phys. B **787** (2007) 152 [arXiv:0706.4071 [hep-ph]].
- [58] M. Cirelli, R. Franceschini and A. Strumia, *Minimal Dark Matter predictions for galactic positrons, anti-protons, photons*, Nucl. Phys. B **800** (2008) 204 [arXiv:0802.3378 [hep-ph]].

- [59] M. Cirelli and A. Strumia, *Minimal Dark Matter: Model and results*, New J. Phys. **11** (2009) 105005 [arXiv:0903.3381 [hep-ph]].
- [60] T. Hambye, F.-S. Ling, L. Lopez Honorez and J. Rocher, *Scalar Multiplet Dark Matter*, JHEP **0907** (2009) 090 [Erratum-ibid. **1005** (2010) 066] [arXiv:0903.4010 [hep-ph]].
- [61] K. S. Babu, S. Nandi and Z. Tavartkiladze, *New Mechanism for Neutrino Mass Generation and Triply Charged Higgs Bosons at the LHC*, Phys. Rev. D **80** (2009) 071702 [arXiv:0905.2710 [hep-ph]].
- [62] Y. Cai, X.-G. He, M. Ramsey-Musolf and L.-H. Tsai,  *$R\nu$ MDM and Lepton Flavor Violation*, JHEP **1112** (2011) 054 [arXiv:1108.0969 [hep-ph]].
- [63] C.-H. Chen and S. S. C. Law, *Exotic fermion multiplets as a solution to baryon asymmetry, dark matter and neutrino masses*, Phys. Rev. D **85** (2012) 055012 [arXiv:1111.5462 [hep-ph]].
- [64] K. Kumerički, I. Picek and B. Radovčić, *Critique of Fermionic  $R\nu$ MDM and its Scalar Variants*, JHEP **1207** (2012) 039 [arXiv:1204.6597 [hep-ph]].
- [65] K. Kumerički, I. Picek and B. Radovčić, *TeV-scale Seesaw with Quintuplet Fermions*, Phys. Rev. D **86** (2012) 013006 [arXiv:1204.6599 [hep-ph]].
- [66] J. Beringer *et al.* [Particle Data Group Collaboration], *Review of Particle Physics (RPP)*, Phys. Rev. D **86** (2012) 010001 [http://pdg.lbl.gov/].
- [67] E. Ma, *Radiative Scaling Neutrino Mass and Warm Dark Matter*, Phys. Lett. B **717** (2012) 235 [arXiv:1206.1812 [hep-ph]].
- [68] P. M. Nadolsky, H.-L. Lai, Q.-H. Cao, J. Huston, J. Pumplin, D. Stump, W.-K. Tung and C.-P. Yuan, *Implications of CTEQ global analysis for collider observables*, Phys. Rev. D **78** (2008) 013004 [arXiv:0802.0007 [hep-ph]].
- [69] M. R. Whalley, D. Bourilkov and R. C. Group, *The Les Houches accord PDFs (LHAPDF) and LHAGLUE*, (2005) [hep-ph/0508110].
- [70] B. Ren, K. Tsumura and X.-G. He, *A Higgs Quadruplet for Type III Seesaw and Implications for  $\mu \rightarrow e\gamma$  and  $\mu - e$  Conversion*, Phys. Rev. D **84** (2011) 073004 [arXiv:1107.5879 [hep-ph]].

- 
- [71] K. Kumerički, I. Picek and B. Radovčić, *Exotic Seesaw-Motivated Heavy Leptons at the LHC*, Phys. Rev. D **84** (2011) 093002 [arXiv:1106.1069 [hep-ph]].
- [72] W. Grimus and L. Lavoura, *The Seesaw mechanism at arbitrary order: Disentangling the small scale from the large scale*, JHEP **0011** (2000) 042 [hep-ph/0008179].
- [73] T. Li and X.-G. He, *Neutrino Masses and Heavy Triplet Leptons at the LHC: Testability of Type III Seesaw*, Phys. Rev. D **80** (2009) 093003 [arXiv:0907.4193 [hep-ph]].
- [74] G. Aad *et al.* [ATLAS Collaboration], *Observation of a new particle in the search for the Standard Model Higgs boson with the ATLAS detector at the LHC*, Phys. Lett. B **716** (2012) 1 [arXiv:1207.7214 [hep-ex]].
- [75] S. Chatrchyan *et al.* [CMS Collaboration], *Observation of a new boson at a mass of 125 GeV with the CMS experiment at the LHC*, Phys. Lett. B **716** (2012) 30 [arXiv:1207.7235 [hep-ex]].
- [76] S. Chatrchyan *et al.* [CMS Collaboration], *Search for the standard model Higgs boson decaying into two photons in pp collisions at  $\sqrt{s} = 7$  TeV*, Phys. Lett. B **710** (2012) 403 [arXiv:1202.1487 [hep-ex]].
- [77] G. Aad *et al.* [ATLAS Collaboration], *Search for the Standard Model Higgs boson in the diphoton decay channel with  $4.9 \text{ fb}^{-1}$  of pp collisions at  $\sqrt{s} = 7$  TeV with ATLAS*, Phys. Rev. Lett. **108** (2012) 111803 [arXiv:1202.1414 [hep-ex]].
- [78] J. Baglio, A. Djouadi and R. M. Godbole, *The apparent excess in the Higgs to di-photon rate at the LHC: New Physics or QCD uncertainties?*, Phys. Lett. B **716** (2012) 203 [arXiv:1207.1451 [hep-ph]].
- [79] P. P. Giardino, K. Kannike, M. Raidal and A. Strumia, *Is the resonance at 125 GeV the Higgs boson?*, Phys. Lett. B **718** (2012) 469 [arXiv:1207.1347 [hep-ph]].
- [80] T. Corbett, O. J. P. Eboli, J. Gonzalez-Fraile and M. C. Gonzalez-Garcia, *Constraining anomalous Higgs interactions*, Phys. Rev. D **86** (2012) 075013 [arXiv:1207.1344 [hep-ph]].
- [81] M. Carena, I. Low and C. E. M. Wagner, *Implications of a Modified Higgs to Diphoton Decay Width*, JHEP **1208** (2012) 060 [arXiv:1206.1082 [hep-ph]].

- 
- [82] W.-F. Chang, J. N. Ng and J. M. S. Wu, *Constraints on New Scalars from the LHC 125 GeV Higgs Signal*, Phys. Rev. D **86** (2012) 033003 [arXiv:1206.5047 [hep-ph]].
- [83] C.-W. Chiang and K. Yagyu, *Higgs boson decays to  $\gamma\gamma$  and  $Z\gamma$  in models with Higgs extensions*, [arXiv:1207.1065 [hep-ph]].
- [84] I. Dorsner, S. Fajfer, A. Greljo and J. F. Kamenik, *Higgs Uncovering Light Scalar Remnants of High Scale Matter Unification*, JHEP **1211** (2012) 130 [arXiv:1208.1266 [hep-ph]].
- [85] S. Chatrchyan *et al.* [CMS Collaboration], *A search for a doubly-charged Higgs boson in  $pp$  collisions at  $\sqrt{s} = 7$  TeV*, Eur. Phys. J. C **72** (2012) 2189 [arXiv:1207.2666 [hep-ex]].
- [86] G. Aad *et al.* [ATLAS Collaboration], *Search for anomalous production of prompt like-sign muon pairs and constraints on physics beyond the Standard Model with the ATLAS detector*, Phys. Rev. D **85** (2012) 032004 [arXiv:1201.1091 [hep-ex]].
- [87] G. Aad *et al.* [ATLAS Collaboration], *Search for doubly-charged Higgs bosons in like-sign dilepton final states at  $\sqrt{s} = 7$  TeV with the ATLAS detector*, [arXiv:1210.5070 [hep-ex]].
- [88] A. Melfo, M. Nemevsek, F. Nesti, G. Senjanovic and Y. Zhang, *Type II Seesaw at LHC: The Roadmap*, Phys. Rev. D **85** (2012) 055018 [arXiv:1108.4416 [hep-ph]].
- [89] A. Arhrib, R. Benbrik, M. Chabab, G. Moulhaka and L. Rahili, *Higgs boson decay into 2 photons in the type II Seesaw Model*, JHEP **1204** (2012) 136 [arXiv:1112.5453 [hep-ph]].
- [90] S. Kanemura and K. Yagyu, *Radiative corrections to electroweak parameters in the Higgs triplet model and implication with the recent Higgs boson searches*, Phys. Rev. D **85** (2012) 115009 [arXiv:1201.6287 [hep-ph]].
- [91] A. G. Akeroyd and S. Moretti, *Enhancement of  $H$  to gamma gamma from doubly charged scalars in the Higgs Triplet Model*, Phys. Rev. D **86** (2012) 035015 [arXiv:1206.0535 [hep-ph]].
- [92] E. J. Chun, H. M. Lee and P. Sharma, *Vacuum Stability, Perturbativity, EWPD and Higgs-to-diphoton rate in Type II Seesaw Models*, JHEP **1211** (2012) 106 [arXiv:1209.1303 [hep-ph]].

- 
- [93] I. Picek and B. Radovčić, *Enhancement of  $h \rightarrow \gamma\gamma$  by seesaw-motivated exotic scalars*, Phys. Lett. B **719** (2013) 404 [arXiv:1210.6449 [hep-ph]].
- [94] J. R. Ellis, M. K. Gaillard and D. V. Nanopoulos, *A Phenomenological Profile of the Higgs Boson*, Nucl. Phys. B **106** (1976) 292.
- [95] M. A. Shifman, A. I. Vainshtein, M. B. Voloshin and V. I. Zakharov, *Low-Energy Theorems for Higgs Boson Couplings to Photons*, Sov. J. Nucl. Phys. **30** (1979) 711 [Yad. Fiz. **30** (1979) 1368].
- [96] A. Djouadi, *The Anatomy of electro-weak symmetry breaking. I: The Higgs boson in the standard model*, Phys. Rept. **457** (2008) 1 [hep-ph/0503172].
- [97] F. del Aguila and J. A. Aguilar-Saavedra, *Electroweak scale seesaw and heavy Dirac neutrino signals at LHC*, Phys. Lett. B **672** (2009) 158 [arXiv:0809.2096 [hep-ph]].
- [98] J. A. Aguilar-Saavedra, *Heavy lepton pair production at LHC: Model discrimination with multi-lepton signals*, Nucl. Phys. B **828** (2010) 289 [arXiv:0905.2221 [hep-ph]].
- [99] B. Mukhopadhyaya and S. Mukhopadhyay, *Same-sign trileptons and four-leptons as signatures of new physics at the CERN Large Hadron Collider*, Phys. Rev. D **82** (2010) 031501 [arXiv:1005.3051 [hep-ph]].
- [100] S. Mukhopadhyay and B. Mukhopadhyaya, *Same-sign trileptons at the LHC: A Window to lepton-number violating supersymmetry*, Phys. Rev. D **84** (2011) 095001 [arXiv:1108.4921 [hep-ph]].
- [101] J. Alwall, M. Herquet, F. Maltoni, O. Mattelaer and T. Stelzer, *MadGraph 5 : Going Beyond*, JHEP **1106** (2011) 128 [arXiv:1106.0522 [hep-ph]].
- [102] I. Picek and B. Radovčić, *Nondecoupling of terascale isosinglet quark and rare  $K$ - and  $B$ -decays*, Phys. Rev. D **78** (2008) 015014 [arXiv:0804.2216 [hep-ph]].
- [103] M. I. Vysotsky, *New (virtual) physics in the era of the LHC*, Phys. Lett. B **644** (2007) 352 [hep-ph/0610368].
- [104] I. Picek and B. Radovčić, *Novel TeV-scale seesaw mechanism with Dirac mediators*, Phys. Lett. B **687** (2010) 338 [arXiv:0911.1374 [hep-ph]].

- 
- [105] A. de Gouvea and J. Jenkins, A Survey of Lepton Number Violation Via Effective Operators, *Phys. Rev. D* **77** (2008) 013008 [arXiv:0708.1344 [hep-ph]].
- [106] F. Bonnet, D. Hernandez, T. Ota and W. Winter, *Neutrino masses from higher than  $d=5$  effective operators*, *JHEP* **0910** (2009) 076 [arXiv:0907.3143 [hep-ph]].
- [107] Y. Liao, *Unique Neutrino Mass Operator at any Mass Dimension*, *Phys. Lett. B* **694** (2011) 346 [arXiv:1009.1692 [hep-ph]].
- [108] C. -K. Chua and S. S. C. Law, *Phenomenological constraints on minimally coupled exotic lepton triplets*, *Phys. Rev. D* **83** (2011) 055010 [arXiv:1011.4730 [hep-ph]].
- [109] A. Delgado, C. Garcia Cely, T. Han and Z. Wang, *Phenomenology of a lepton triplet*, *Phys. Rev. D* **84** (2011) 073007 [arXiv:1105.5417 [hep-ph]].
- [110] H. Hettmansperger, M. Lindner and W. Rodejohann, *Phenomenological Consequences of sub-leading Terms in See-Saw Formulas*, *JHEP* **1104** (2011) 123 [arXiv:1102.3432 [hep-ph]].
- [111] T. Hahn and M. Perez-Victoria, *Automatized one loop calculations in four-dimensions and  $D$ -dimensions*, *Comput. Phys. Commun.* **118** (1999) 153 [hep-ph/9807565].

# Curriculum Vitae

**First name | Surname :** Branimir Radovčić

## Address

Physics Department  
Faculty of Science  
University of Zagreb  
Bijenička cesta 32, P.O.B. 331  
HR-10002 Zagreb, Croatia

e-mail: bradov@phy.hr | telephone: +385 1 460 5599 | fax: +385 1  
460 5606

**Born** 1 September 1983, Split, Croatia

## Education

1990-1998 Elementary school (*Split 3*, Split)  
1998-2001 High school (*III. Gimnazija*, Split)  
2001-2007 Faculty of Science, University of Zagreb

23 Mar 2007 **dipl. ing.**, Diploma thesis: *Rare decays  $K \rightarrow \pi \bar{\nu} \nu$  as golden rare decays of flavour physics*, advisor: Prof. Ivica Picek

2007-2013 PhD student, University of Zagreb

Jan 2013 **PhD** thesis completed and submitted



## Research interests

Beyond standard model physics; Neutrino masses; Dark matter

## Position

Since 2007 research and teaching assistant at Faculty of Science, University of Zagreb.

## Research stay

From October 2008 to February 2009, one semester research stay at the University of Vienna.

## Teaching experience

Teaching assistant in courses:

- Elementary particle physics (4th year courses)
- Group theory (3rd year course)
- Symmetries in physics (3rd year course)
- Symbolic programming (2nd year course)
- Chosen topics in nuclear and particle physics (4nd year course)

## List of publications

1. I. Picek and B. Radovčić, *Nondecoupling of terascale isosinglet quark and rare  $K$ - and  $B$ -decays*, Phys. Rev. D **78** (2008) 015014 [arXiv:0804.2216 [hep-ph]].
2. W. Grimus, L. Lavoura and B. Radovčić, *Type II seesaw mechanism for Higgs doublets and the scale of new physics*, Phys. Lett. B **674** (2009) 117 [arXiv:0902.2325 [hep-ph]].
3. I. Picek and B. Radovčić, *Novel  $TeV$ -scale seesaw mechanism with Dirac mediators*, Phys. Lett. B **687** (2010) 338 [arXiv:0911.1374 [hep-ph]].
4. K. Kumerički, I. Picek and B. Radovčić, *Exotic Seesaw-Motivated Heavy Leptons at the LHC*, Phys. Rev. D **84** (2011) 093002 [arXiv:1106.1069 [hep-ph]].
5. K. Kumerički, I. Picek and B. Radovčić, *Critique of Fermionic  $R\nu$ MDM and its Scalar Variants*, JHEP **1207** (2012) 039 [arXiv:1204.6597 [hep-ph]].
6. K. Kumerički, I. Picek and B. Radovčić,  *$TeV$ -scale Seesaw with Quintuplet Fermions*, Phys. Rev. D **86** (2012) 013006 [arXiv:1204.6599 [hep-ph]].
7. I. Picek and B. Radovčić, *Enhancement of  $h \rightarrow \gamma\gamma$  by seesaw-motivated exotic scalars*, Phys. Lett. B **719** (2013) 404 [arXiv:1210.6449 [hep-ph]].

## Conference proceedings

1. I. Picek and B. Radovčić, *Testing new  $TeV$ -scale seesaw mediators at the LHC*, PoS ICHEP **2010** (2010) 329 [arXiv:1105.5561 [hep-ph]].